Optimal Sizing and Control of Renewable Energy Based Hybrid Power Generating System

A thesis Submitted to the
Delhi Technological University
for the Award of Doctor of Philosophy
In
Electrical Engineering

Submitted By:

BANDANA

(2K18/PhD/EE/11)

Under the Supervision of

Prof. M. Rizwan
Professor
Department of Electrical Engineering
Delhi Technological University,
Delhi

Dr. Priyanka
Associate Professor
Department of ECE
BPS Mahila Vishwavidyalaya,
Khanpur Kalan, Sonipat, Haryana

DEPARTMENT OF ELECTRICAL ENGINEERING

DELHI TECHNOLOGICAL UNIVERSITY

(Formerly Delhi College of Engineering)

DELHI-110042, INDIA

2023

Table of Contents

DECLARATION

I Bandana a Scholar of Ph.D. hereby declare that the thesis titled **Optimal Sizing and Control of Renewable Energy based Hybrid Power Generating System** which is submitted by me to the Department of Electrical Engineering, Delhi Technological University, Delhi in partial fulfillment of the requirement for the award of the degree of Doctor of Philosophy has not previously formed the basis for the award of any Degree, Diploma, fellowship or other similar title or recognition.

Place: Delhi (**Bandana)**

Date:

CERTIFICATE

On the basis of the declaration submitted by Ms. Bandana, Scholar of Ph.D., We hereby certify that the thesis titled **Optimal Sizing and Control of Renewable Energy Based Hybrid Power Generating System** which is submitted to the Department of Electrical Engineering, Delhi Technological University, Delhi in partial fulfillment of the requirement for the award of the degree of Doctor of Philosophy is an original contribution with existing knowledge and faithful record of research carried out by her under our guidance and supervision.

To the best of our knowledge this work has not been submitted in part or full for any Degree or Diploma to this University or elsewhere.

Date:

(Prof. M. Rizwan)
Supervisor
Professor
Department of Electrical Engineering
Delhi Technological University
Delhi, India

(Dr. Priyanka)
Supervisor
Associate Professor
Department of ECE
BPS Mahila Vishwavidyalaya,
Khanpur Kalan, Sonipat, Haryana,
India

ACKNOWLEDGEMENT

First and foremost, I sincerely acknowledge my most sincere gratitude to my supervisors Prof. M. Rizwan and Dr. Priyanka for their valuable guidance, support, and motivation throughout this research work. They have been outstanding mentors and working with them has been a remarkable experience. The valuable hours of discussion that I had with them undoubtedly helped in supplementing my thoughts in the right direction for attaining the desired objectives. I consider it my proud privilege to have worked with them, ever ready to lend a helping hand. I am forever thankful to them for all their wise words and inspiring thoughts.

I am also thankful to HOD, Prof. Rachana Garg and all faculty members of the Department of Electrical Engineering, Delhi Technological University, Delhi, for their encouragement and moral support for the completion of this thesis.

I would like to extend my special thanks to SRC members mainly Prof. Salman Hameed, Professor, Department of Electrical Engineering AMU, Aligarh who have given me valuable guidance and advice to improve the quality of my research work.

I extend my thanks to my friends and colleagues especially, Dr. Rashid Ali, Dr. Bilal, Dr. Astitva, Dr. Isaka, Ms. Rahma Aman, Ms. Lipika Datta, Mr. Ganesh Jaiswal, Mr. Deepak, Ms. Urmila, Ms. Arpana, Ms. Upma Singh, Ms. Apoorva, Ms. Neelam Verma, Ms. Ashima Taneja, Mr. Satyajeet for their constant motivation and support for reminding me to complete my work at the earliest.

The assistance of the valuable staff in the Renewable Energy Research Facility of Delhi Technological University is gratefully acknowledged. I am especially thankful to

Mr. Vickey Kumar Prasad, Mr. Ankit Kumar, and Mr. Manoj Kumar for their substantial assistance during my research.

I want to take this opportunity to thank my parents, from the bottom of my heart for everything that they have done for me. I also want to thank to my other family members for being a constant source of support.

This acknowledgment would not be complete without mentioning my husband and my daughter Nishtha. They both are my core support system and words cannot articulate my admiration for them. They gave me unconditional support and continues to be a source of inspiration during my research.

I am thankful to God for all resources, opportunities and inspirations that led to this moment.

Date: **Bandana**

Place: Delhi

LIST OF FIGURES

LIST OF TABLES

LIST OF SYMBOLS AND ABBREVIATION

List of Symbols

PV_p^o	SPV output power
D_f	Derating factor
PV_p^r	Rated power
S_i	Solar irradiance
S_r^i	Solar irradiance at reference
k_t	Temperature coefficient
t_c	Cell temperature
t_{ref}	Cell temperature at reference conditions
t_{amb}	Ambient temperature
E_{pv}	Energy produced by the SPV
W_o^p	Output power of WT
u	Wind speed
u_{ci}	Cut in speed of WT
u_{co}	Cut out speed of WT
a, b, c	Elements of quadratic function
E_W	Energy produced by the WT
N_W	Number of WT
BMG_p^o	Output power of BMG
Q_{BMG}	Biomass available in tons/year
C_{BMG}	Calorific value of biomass
H_{BMG}	Operational hours of BMG
η_{BMG}	Conversion efficiency of a BMG
E_{BMG}	Energy output of BMG
BGG_p^o	Output power of BGG
Q_{BGG}	Biogas available per day
C_{BGG}	Calorific value of biogas
H_{BGG}	Operational hours of BGG
η_{BGG}	Conversion efficiency of a BGG

E_{BGG}	Energy output of BGG
E_b	Energy stored in the battery
γ	Battery discharge rate
e_{xpv}	Extra energy generated by the SPV
e_{xpv}	Extra energy generated by the BMG
e_{xpv}	Extra energy generated by the BGG
$\eta_{charging}$	Charging efficiency of battery
e_{df}	Unmet ED
$\eta_{discharging}$	Discharging efficiency of battery
$\eta_{inverter}$	inverter efficiency
$e_{gp}(t)$	Energy purchased from grid
$e_d(t)$	Hourly ED
E_{bmn}	Minimum capacity of battery
$e_{gs}(t)$	Energy sold to grid
E_{bmx}	Maximum capacity of battery
npc_{pv}	NPC of SPV
pv_{CC}	CC of SPV
pv_{OMC}	OMC of SPV
pv_{SV}	SV of SPV
N_{pv}	Number of SPV panels
ψ_{pv}	Initial cost of the SPV system expressed in $/kW
ω_{pv}	OMC of SPV panel in $/kW/year
ζ_{pv}	Escalation rate of SPV
μ	Lifetime of Project
r	Interest rate
ε_{pv}	Resale value of SPV panel in $/kW
λ	Annual inflation rate
npc_{wt}	NPC of WT
WT_{CC}	CC of WT
WT_{OMC}	Total OMC of WT
WT_{SV}	SV of WT
ψ_w	Initial cost of the WT system expressed in $/kW

ω_w	OMC of WT in \$/kW/year
ζ_w	Escalation rate of WT
ε_W	Resale value of WT in \$/kW
npc_{bmg}	NPC of BMG
bmg_{CC}	CC of BMG
bmg_{OMC}	OMC of BMG
bmg_{FC}	FC of BMG
bmg_{SV}	SV of BMG
ψ_{BMG}	Initial cost of the BMG system expressed in \$/kW
ω_{f_bmg}	Fixed OMC of the BMG system
ω_{v_bmg}	Variable OMC of the BMG system
$p^w_{a\_bmg}$	Annual operating power of the BMG system in kWh/year
ζ_{bmg}	Escalation rate of BMG
ε_{bmg}	Resale value of BMG in \$/kW
φ_{bmg}	Biomass fuel cost in \$/tons
npc_{bgg}	NPC of BGG
bgg_{CC}	CC of BGG
bgg_{OMC}	OMC of BGG
bgg_{SV}	SV of BGG
bgg_{FC}	FC of BGG
ψ_{bg}	Initial cost of the BGG system expressed in \$/kW
ω_{f_bgg}	Fixed OMC of the BGG system
ω_{v_bgg}	Variable OMC of the BGG system
ζ_{bgg}	Escalation rate of BGG
$p^w_{a\_bgg}$	Annual operating power of the BGG system
ε_{bgg}	Resale value of BGG in \$/kW
φ_{bgg}	Annual biogas FC in \$/m^3
bgg_{yearly}	Amount of biogas required annually
re_{bg}	Revenue generated by the organic manure in BGG system
d_{bgg}	Manure produced annually
M_{bgg}	Cost of generated manure in \$/tons
npc_B	NPC of battery

B_{CC}	CC of battery
B_{OMC}	OMC of battery
B_{RC}	RC of battery
B_{SV}	SV of battery
N_B	Number of batteries
ψ_B	Initial cost of the battery expressed in $/kW
ω_B	Annual OMC of batteries in $/year
ζ_B	Escalation rate of battery
ε_B	Resale price of battery
n_{rb}	Number of instances a battery has to be replaced
μ_B	Life of battery
$npc_{inverter}$	NPC of inverter
I_{CC}	CC of inverter
I_{OMC}	OMC of inverter
I_{RC}	RC of inverter
I_{SV}	SV of inverter
N_I	Number of inverters
ψ_I	Initial cost of the inverter expressed in $/kW
φ_I	Cost of one inverter
ζ_I	Escalation rate of inverter
$\in_G^S$	NPC of GS
$\in_G^P$	NPC of GP
$\emptyset_G^S$	Unit costs of selling power to grid
$\emptyset_G^P$	Unit costs of purchasing power from grid
e_{gs}	Excess energy sold to grid in kWh
e_{gp}	Deficit energy to be purchased from grid in kWh
C_r^f	Capital recovery factor
E_a^d	Annual ED in kWh/year
Q_{PV}	Annual average solar daily radiation
N_{CR}	Gross crop residue available in kg/year
S_{CR}	Surplus crop residue fraction
C_{IA}	Crop irrigated area in hectare

C_Y	Crop yield in kg/hectare
C_{RR}	Crop residue ratio
P_{BG}	Biogas potential
C_D	Availability of cattle dung in kg/day
Y_{BG}	Biogas yield in m^3/kg
E_W	Annual energy potential of WT in kWh/m^2/year
P_D	Wind power density in kW/m^2
H_L	Land required for installation of HRES
L_j	Land requirement for each RES in m^2/kW
S_j	Optimal size of each RES
N_{res}	Total number of RES considered in the proposed HRES.
$Y_b(\varphi)$	Best position of Aquila
$Y_m(\varphi)$	Average location of all aquilas in the current iteration
φ	Current iteration
T	Maximum iteration
n	Population size
r_1	Arbitrary numeral between 0-1
$Y_r(\varphi)$	Arbitrary location of aquila
d	Dimension size
r_2	Random value within the range (0, 1)
$lf(d)$	Levy Flight Function
α, δ	Exploitation adjustment parameters
lb	Lower bound
ub	Upper bound
qf	Quality function
g_1	Movement parameter during tracking prey
L_{c1}	Learning coefficient
L_{c2}	Learning coefficient
w_f	Weight factor of inertia
Y_b	Position of food
P_s	Strength of prey
$P_{nearest}$	Location of the nearest predator

$\vec{H}$	Gravity force
$\vec{E}$	Deep ocean advection
$\vec{N}$	Social forces among SA
Q_{min}	Initial speeds to make social interaction
Q_{max}	Subordinate speeds to make social interaction
$\overrightarrow{P_D}$	Distance between the food source and SA
$\overrightarrow{F_S}$	Position of optimum food source
$\overrightarrow{Q_p}$	Position of tunicate

List of Abbreviations

AI	Artificial Intelligence
ANN	Artificial Neural Network
BBO	Biogeography-based Optimization
BESS	Battery Energy Storage Systems
BGG	Biogas Generator
BMG	Biomass Generator
CB	Circuit Breakers
CC	Capital Cost
CEED	Combined Economic Emission Dispatch
COE	Cost of Energy
CPA	Colony Predation Algorithm
CS	Chaotic Search
CT	Current Transformers
DCHSSA	Discrete Chaotic Harmony Search based Simulated Annealing
DG	Diesel Generator
DHS	Discrete HS
DR	Demand Response
DSG	Distributed Generators
DSM	Demand Side Management
DT	Decision Tree
ED	Energy Demand
FC	Fuel Cost
FM	Forecasting Model
GA	Genetic Algorithm

GHG	Greenhouse Gases
GHI	Global Horizontal Irradiation
GP	Grid Purchase
GPR	Gaussian Process Regression
GS	Grid Sale
GW	Giga Watt
GWO	Grey Wolf Optimization
hHHO-AOA	Hybrid Harris Hawks Optimizer Arithmetic Optimization Algorithm
HMM	Harmony Memory Matrix
HMS	Harmony Memory Size
HOGA	Hybrid Optimization by Genetic Algorithm
HOMER	Hybrid optimization of Multiple Energy Resources
HRES	Hybrid Renewable Energy Systems
HS	Harmony Search
HYBRID2	Hybrid System Simulation Model
KUSUM	Kisan Urja Suraksha evam Utthaan Mahabhiyan
kW	Kilo Watt
LCOE	Levelized Cost of Energy
LPSP	Loss of Power Supply Probability
LSTM	Long Short term Memory
LV	Low Voltage
MCS	Monte Carlo Simulations
ML	Machine Learning
MW	Mega Watt
NASA	National Aeronautics and Space Administration

NDC	Nationally Determined Contributions
NPC	Net Present Cost
OFG	Off-Grid
OMC	Operational and Maintenance Cost
OT	Optimization Technique
PCC	Point of Common Coupling
ppm	part per million
PSO	Particle Swarm Optimization
RC	Replacement Cost
RES	Renewable Energy Sources
RN	Random Number
RWOA	Refraction-based whale Optimization Algorithm
SA	Simulated Annealing
SPV	Solar Photovoltaic
SV	Salvage Value
SVR	Support Vector Regression
TAC	Total Annual Cost
TS	Tabu Search
TSA	Tunicate Swarm Algorithm
TV	Television
TWh	Terawatt-hour
UN	United Nations
WEO	World Energy Outlook
WF	Weight Factor
WOA	Whale Optimization Algorithm

WT	Wind turbine
XGBT	Extreme Gradient Boosting

ABSTRACT

In India, the demand for electricity has been surging due to population growth and increased technological usage in homes, industries, and agriculture. To meet this escalating demand and align with the government's objectives of promoting green and clean energy while ensuring 24x7 availability, renewable energy sources are gaining popularity as a promising solution. India's tropical location offers excellent opportunities for biomass, solar, and wind power generation. Leveraging the country's vast agricultural capacity, substantial amounts of agricultural waste can be harnessed to generate electricity, particularly benefiting communities facing frequent power outages. However, relying solely on renewable energy sources poses challenges due to their sporadic and variable supply. To overcome these issues, the concept of hybrid renewable energy systems (HRES) has emerged as a viable approach to integrate and optimize multiple renewable sources for a more stable and reliable power generation.

HRES involves the combination of multiple renewable energy sources like solar, wind, hydro, biomass, or geothermal, alongside energy storage technologies. The primary goal of HRES is to fulfill the energy requirements of a specific system or community while ensuring reliability and sustainability. By harnessing the potential of various renewable sources and mitigating their intermittency challenges, HRES offers a reliable energy supply. If one energy source experiences fluctuations or downtime, other sources can step in to compensate and maintain a continuous and uninterrupted power output. As a result, the overall energy system becomes more reliable, minimizing the risk of power outages.

The optimal sizing of a HRES is a crucial aspect of its design, involving the determination of appropriate capacities for each renewable energy source, energy storage system, and other components. This process revolves around matching the system's capabilities with the community's energy demand. Over sizing the components can lead to unnecessary costs and resource underutilization, while under sizing may result in inadequate energy production, compromising the system's reliability. Therefore, the present work focuses on optimizing the sizing of grid-connected HRES, combining renewable energy sources with storage devices and the grid. Initially, the feasibility studies, techno-economic analyses, and develops HRES models for two remote sites in the Indian provinces of Haryana and Uttar Pradesh has been conducted . To aid in this analysis, the Hybrid Optimization Model for Electrical Renewable Pro (HOMER Pro) software has been utilized, which effectively assesses feasibility and designs hybrid models based on renewable energy source availability.

Given the unpredictable nature of most renewable energy sources in their generation, integrating them into the electricity grid can be challenging and time-consuming. This approach presents various technical and non-technical difficulties. The thesis also covers the benefits, challenges, and suggested solutions arising from the process of integrating diverse renewable energy sources into the grid.

In recent years, researchers have extensively explored intelligent techniques inspired by natural phenomena to optimize various engineering and technological fields. Therefore, this research utilizes three recently developed optimization algorithms: Aquila Optimization (AO), Colony Prediation Algorithm (CPA), and Tunicate Swarm Algorithm (TSA) for sizing and optimizing HRES.

Further, to enhance the accuracy of size optimization in HRES, precise weather data obtained through forecasting plays a crucial role. In this study, four machine learning (ML) techniques Gaussian Process Regression (GPR), Support Vector Regression (SVR), Extreme Gradient Boosting (XGBT), and Decision Tree (DT) are employed for hourly forecasting of solar radiation, temperature, and wind speed in selected areas. Comparing the results of these forecasting models (FM) reveals that GPR outperforms the other techniques for both sites.

The forecasted data from GPR for solar, wind, and temperature are then utilized for sizing the HRES, catering to the energy needs of remote sites in the Indian provinces of Haryana and Uttar Pradesh. Afterward, the study proceeds with a thorough comparison of the three optimization algorithms: CPA, AO, and TSA. Among these algorithms, TSA stands out as the most promising option, offering superior results and better outcomes in the optimization process.

CHAPTER 1

INTRODUCTION

1.1 GENERAL

Energy is an essential factor for economic growth since it is a necessary input in various production and utilization activities. The energy consumption keeps on growing with increase in the world population as well as living standards of people. In accordance with the World Energy Outlook (WEO) 2022, the global community continues to be on track to realize its objectives of providing everyone with access to electricity that is both inexpensive and sustainable by the year 2030. Approximately 76% of the world's population lives in the twenty least-electrified nations. There are currently 733 million population throughout the world who do not have access to electricity, and 2.4 billion individuals still prepare their food by utilizing harmful fuels, which is both hazardous to their health as well as the environment [1]. Moreover, the combustion of these fuels emits greenhouse gases (GHG), which contribute to global warming. Thus, to achieve the United Nations (UN) Sustainable Development Goal 7, which is about ensuring access to clean and cheap energy, the globe is rapidly moving towards the maximum use of renewable energy sources (RES) for power generation. These RES offer numerous benefits, including the fact that they are environmentally friendly, readily available, inexpensive, and abundant [2].

In India, the demand of electricity is skyrocketing due to population growth and greater technological use in homes and industrial sectors, as well as in agriculture. In order

to fulfill the above increased demand and the Indian Government's missions like "Power to All" and "Green and Clean energy" with its availability 24x7, the RES are becoming more popular for generating green and clean energy. Due to its tropical location, India has an excellent climate for biomass, solar and wind power generation opportunities. The country's vast agricultural capacity generates vast quantities of agricultural waste, which can eventually be used to create electricity. It might be a boon for communities with regular power outages. However, when RES are used alone to generate power, there are significant issues because of their sporadic and variable supply. The idea of hybrid renewable energy systems (HRES) has emerged to address these issues [3].

Before initiating the design and development of any HRES, a comprehensive investigation and assessment of various RES and their energy generation capabilities, including their financial aspects, are of utmost importance. Hence, conducting a techno-economic feasibility analysis of HRES tailored to specific regions becomes a primary objective. Furthermore, it is crucial to explore and create multiple potential configurations suitable for different scenarios. To guarantee cost-effectiveness and reliability, the most optimal configuration is chosen from the available options. This holistic approach ensures efficient utilization of RES and ensures the implementation of a dependable and economically viable HRES customized to meet the unique requirements of the targeted region [3].

Sizing is also an essential aspect of designing an effective HRES. It involves determining the appropriate capacities of each RES, energy storage system, and other components based on the load demand of the community. The proper sizing ensures that

RES are appropriately scaled to meet theenergy demand (ED). Over sizing can lead to unnecessary costs and underutilization of resources, while under sizing may result in insufficient energy production, compromising the reliability of the system. Consequently, recent research has concentrated on employing intelligent approaches to optimize the sizing of HRES. These intelligent methods aim to determine the most suitable capacities of RES and storage systems, maximizing energy utilization, and guaranteeing a well-balanced and effective HRES that meets the specific energy requirements of the community [3].

1.2 GLOBAL ENERGY SCENARIO

Global energy consumption has been steadily increasing over the years due to several factors such as population growth, technological advancements, and improved living standards. The energy consumption all over the globe can be seen in Fig. 1.1.

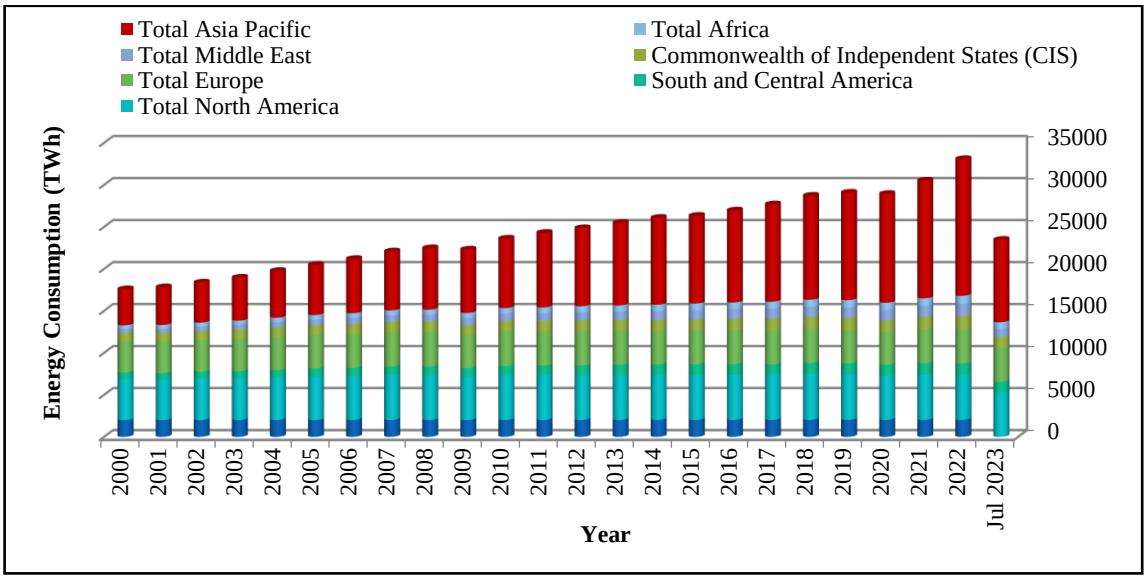

Fig. 1. 1 Global Energy Consumption [4]

As of 2022, total power consumption of the world is almost 30000 terawatt-hour (TWh). It is worth noting that a major share of this demand is coming from the Asia Pacific region,

which accounts for around 50% followed by North America, Europe. The share of demands for south and central America, Africa and the middle east is almost the same. However, supply has been unable to keep pace with demand, and many parts of the world are seeing power outages due to inadequate power supply. Also, several parts of the world have not yet been electrified [4-5]

1.2.1. Fossil and Nuclear Fuel in Power Generation

The share of various sources of world electricity generation is presented in Fig. 1.2. Currently, a significant proportion of power is derived from fossil fuels such as coal, diesel, and natural gas, accounting for 61% of total power generation, while nuclear fuels contribute 10%. Combining both sources, they account for 71% of the total [4]. However, both fossil and nuclear fuels pose hazards due to emissions of smoke and GHG from fossil fuel-fired power plants and the risk of radiation from nuclear plants. Besides their environmental problems, these fuels are limited and unsustainable in the long term. Therefore, there is a critical need for a sustainable energy source that is everlasting and

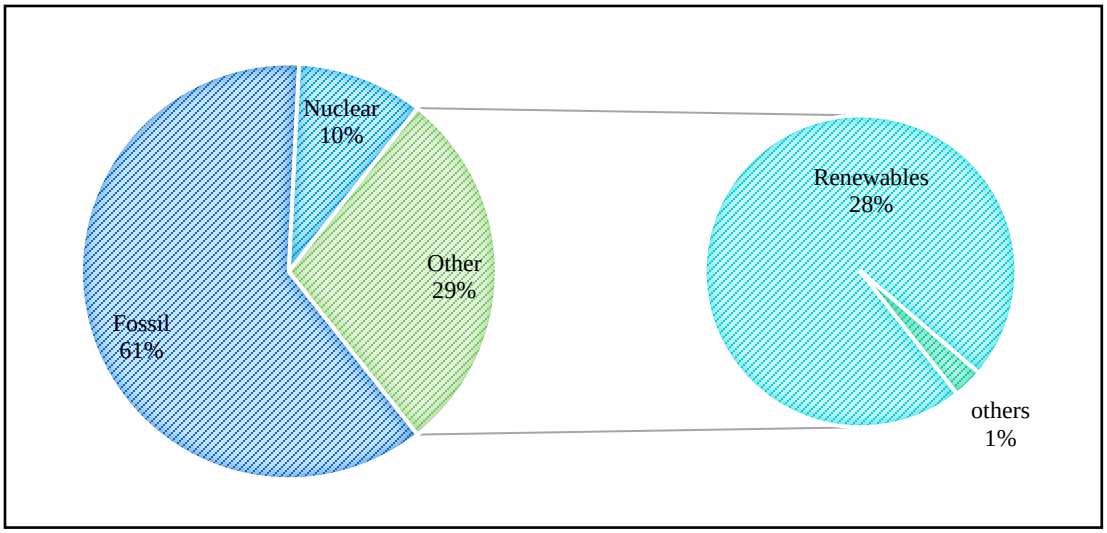

Fig. 1. 2 Share of Fossil Fuel and Nuclear Fuel in Global Energy Generation [4]

clean. Consequently, it is evident that adopting RES is essential, and the sooner this transition occurs, the better it will be for the environment and future generations [4].

1.2.2. GHG Emissions

Studies have shown that in pre-industrial times, CO_2 share in the atmosphere was 280 parts per million (ppm) which accounts for 0.028%. This had been consistent for six thousand years of human civilization. After that, an estimated 1.5 trillion tons of CO_2 has increased. Now, the share has increased to more than four hundred twenty ppm (0.042%) which will keep warming the environment for a long time. Fig.1.3 represents the share of CO_2 in the atmosphere from 1963 to 2023 [5-6].

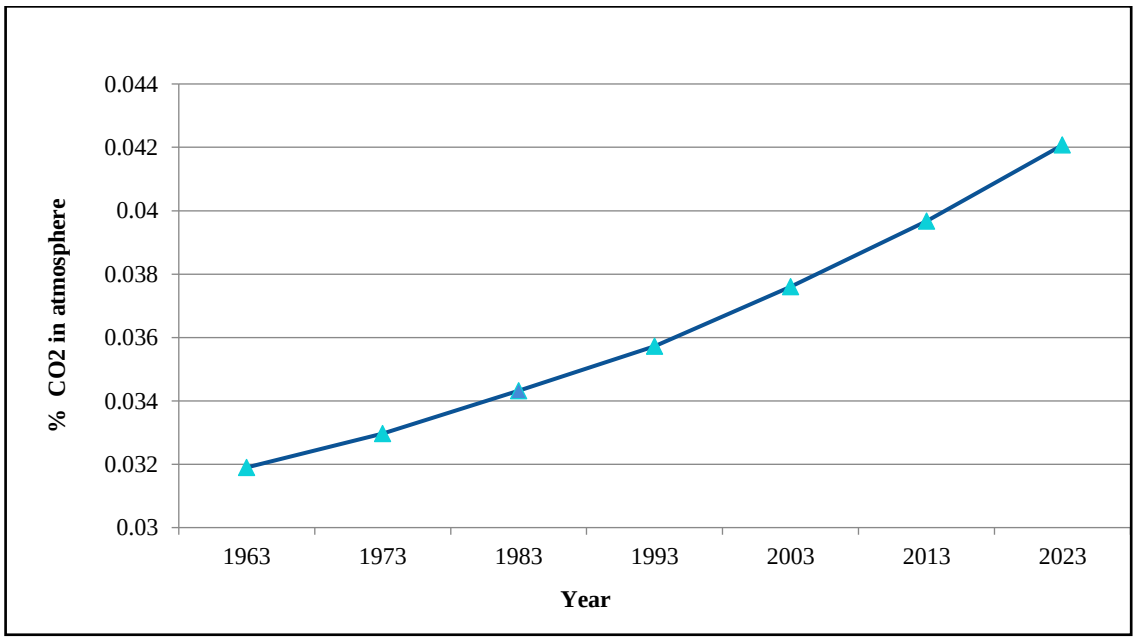

Fig. 1. 3 Global CO_2 Emissions [5]

Presently, the CO_2 levels are comparable to that millions of years ago. In comparison to pre-industrial periods, the temperature at that time was 7^o Fahrenheit higher. Sea levels were 5 to 25 meter (m) higher than today. It will be sufficient to submerge several of the biggest cities of present times. As the CO_2 is increasing at a rate higher than ever,

the situation is very much alarming. Governments across the world have their targets to reduce GHG emissions in the desired time limit. Over two hundred nations pledged to work together under the Paris Agreement to cut GHG emissions and prevent climate changes. As compared to pre-industrial levels, the treaty aims to keep global warming to far below 2°C, possibly below 1.5°C [5-6].

1.2.3 Growth of RES

Major RES include small hydro, solar photovoltaic (SPV), wind and biomass. Large hydro is also renewable, but it is usually considered as a conventional source and not accounted for along with other RES. Gradually, RES power has also been increasing, and there is impetus to increase them fast due to the reasons discussed in above section [2]. Fig. 1.4

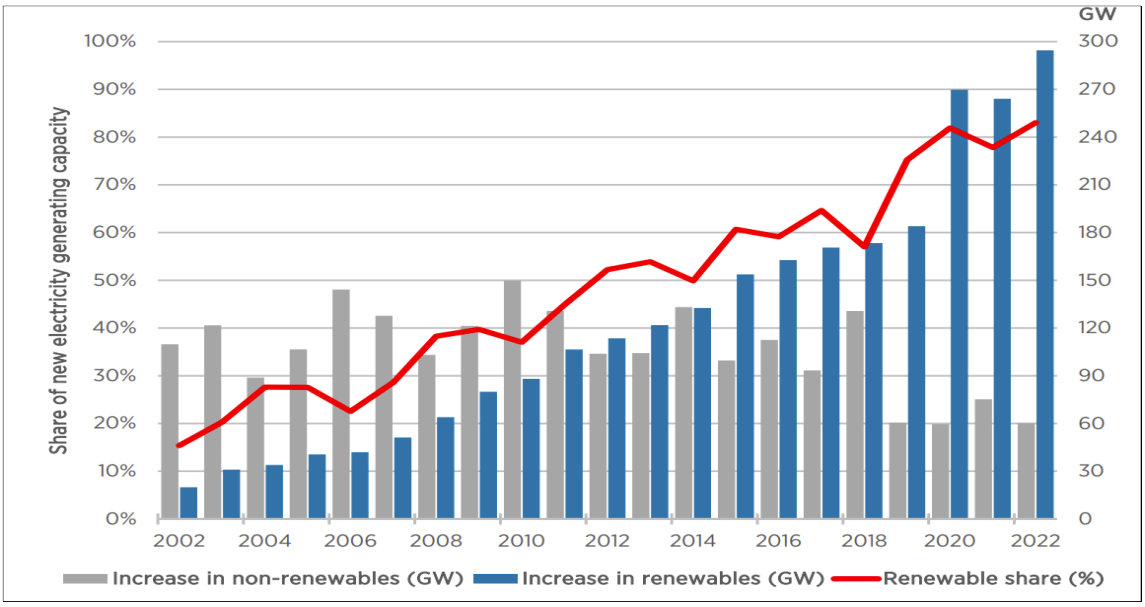

Fig. 1. 4 Growth of RES in World Electricity Generation [2]

illustrates the global trends in RES. Clear from the figure is the remarkable surge in the proportion of RES within the global energy generation landscape. In 2002, RES accounted for a modest share of approximately 15%. However, by the conclusion of 2022, the

contribution of RES to the energy mix had surged significantly, nearly quadrupling to reach an impressive 80% [2].

1.3 INDIAN ENERGY SCENARIO

The total installed capacity of India's national electric grid is 421.9 Gigawatts (GW) as on 30th June 2023 [7]. Fig. 1.5 shows the share of different energy sources in the installed capacity of India. The highest share in installed capacity is thermal power plants which is 237.93 GW followed by RES based power plants, 129.64 GW, hydro power plants 46.85 GW, and nuclear power plants 7.48 GW.

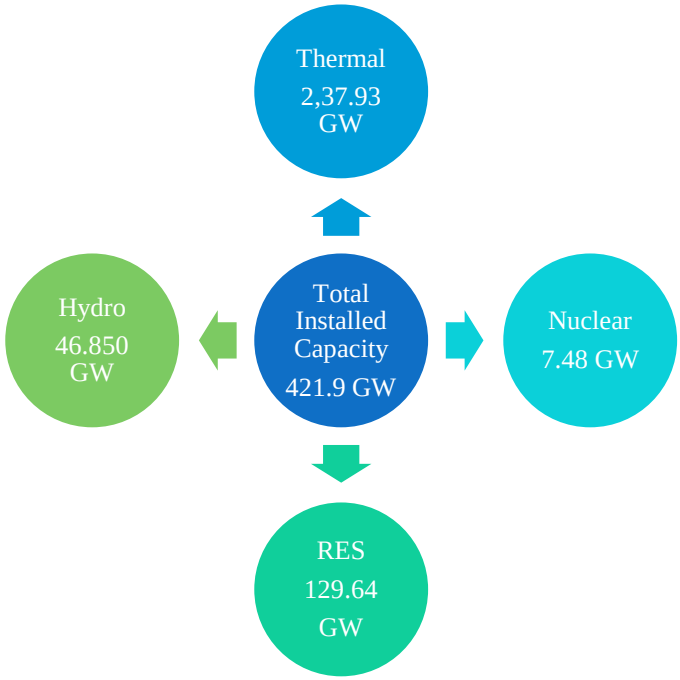

Fig. 1. 5 Share of Various Sources in Total Installed Capacity [7]

The electrical industry in India is dominated by fossil fuels, particularly coal, which provided around three-fourth of the total energy generation [8-9]. To get green and clean energy, the government of India is making efforts to increase investment in renewable

energy. The government's draft National Electricity Plan of 2022 which states that the country does not need any more fossil fuel power plants in the utility sector until 2027 besides those currently under construction [10-11]. It is expected that non-fossil fuel generation contribution is likely to be around 44.7% of the total gross energy generation by 2029–30 [12]. India is the third largest producer of electricity in the world. During 2022–23, the total generation in the country was 1624 TWh which shows an increase in generation by 8.87% from previous year [4].

1.3.1. Trends in Energy Consumption

The demand for energy is continuously increasing in India at an extremely fast pace. Within 13 years from 2010 to 2023, demand has increased from 800 to 1503 billion units, which a is whopping 50% rise. In recent times, supply has been catching fast to meet the demand. Major share of addition in present times is coming from RES and now the renewable energy installed capacity has increased 286% in last 7.5 years [13].

1.3.2. Why Energy Crisis is more Profound in India

Power situation in India is particularly more complicated due to several factors as discussed below.

- **Population-** Population of India is huge. As per current census it is around 1400 million, equal to that of Entire North America, South America, Russia, UK, France, and Germany put together. Everyday population of India increases by forty thousand. Power demand also increases proportionately.
- **Living standard-** Presently, India is a developing country, and there are many places that does not receive power regularly due to demand supply gap. Due to

improvement in living standard, per capita consumption of electricity is also increasing. India is also undergoing rapid industrialization and industry consumes power at much larger scale. Railways are also undergoing electrification. Electric vehicles have started appearing on the roads and are fast replacing fueled vehicles.

- **Technological advancement-** Apart from present usage of electricity, technological developments are opening newer means of power consumption like computers, phones, robots, drones etc. So, in future per capita power consumption will increase further.
- **Climatic challenges-** Being in a tropical region, India's power consumption will also increase for cooling due to the effect of global warming.

To summarize, not only India has to fill up the demand supply gap to present level, but also has to take care of future demand which is going to increase substantially. This increased demand cannot be fulfilled by fossil fuels only, but large capacity of RES generation is required.

1.3.3. Present Sources of Power Generation

The breakup of power sources of the Indian nation are shown in the Fig. 1.6. In the year 2023, the primary sources of power generation in India predominantly consist of fossil fuels and nuclear energy, accounting for 56% and 2% respectively. On the other hand, Renewable Energy Sources (RES) and large hydro contribute to 31% and 11% of the total power generation [7].

1.4 RENEWABLE ENERGY OVERVIEW

The source of renewable energy is provenance, which is fundamentally unlimited. The main benefits of RES are that they may be used without emitting hazardous pollutants

into the environment. India, which has a population of 1.4 billion, has a huge power demand to support its quickly expanding economy. The nation has been working for more than 70

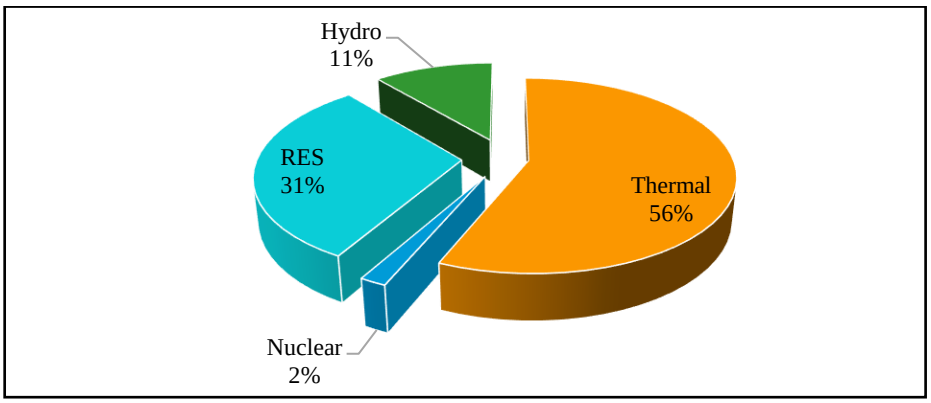

Fig. 1. 6 Proportion of Sources in Power Generation [14]

years to become energy independent, being a country with an electricity deficit at the moment of independence. Now a days India's renewable business is flourishing. The country is expected to add 35 to 40 GW of renewable energy yearly through 2030, which may supply up to thirty million additional households [14].

1.4.1. Contribution of RES

The initial source of power generation in India was hydroelectric power, which commenced with the establishment of the Sidrapong plant near Darjeeling in 1897, boasting a capacity of 130 kW. From 1920 onward, the generation of thermal power also commenced and gradually surpassed hydroelectric power generation in terms of capacity.

As of year 2023, solar power is largest source of renewable energy, and its installation capacity is increasing fast. Fig.1.7 shows the share of different RES as on 30th June 2023 [15]. The highest contribution is from solar (54%), followed by wind (34%) biomass (8%) and small hydro (4%). In near future, lot of capacity expansion in SPV has been planned. In 2012, installed capacity for solar power was 1205 Mega watt (MW), which

has increased to 70096.83 MW by 2023, which is 50 times in 11 years. Bhadla Solar Park in Rajasthan is planned to produce 2245 MW of power, and shall be world's largest solar park. Pavagarh Solar Park in Karnataka at 2050 MW is world's second largest Solar Park. In wind power also, remarkable progress has been made. In 2012, installed capacity for wind power was 20149 MW, which doubled to 43773 MW in 11years by 2023 [15].

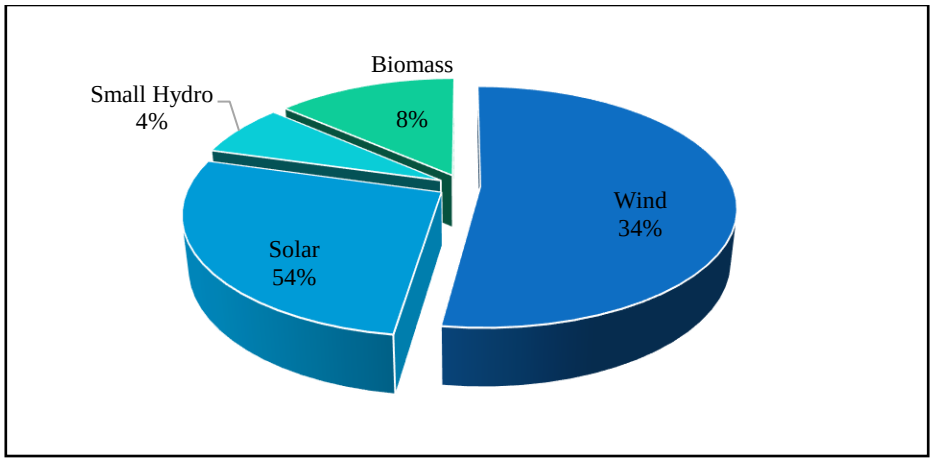

Fig. 1. 7 Share of Various RES in Energy Generation [15]

1.4.2. Renewable Energy and its Current Scenario

India is ranked fourth in the world for wind energy capacity and fifth for solar energy capacity. In accordance with the report of Indian renewable energy market forecast, 2027-28, the renewable energy industry in India is expected to develop at a compound annual growth rate of more than 13% in cumulative volume capacity over the projected period [14]. With a market share of more than 40% in renewable energy, solar energy is now the industry leader. Comparing market shares by region, the south has the largest market share while the north has the lowest market share in the domestic marketplace. With a market dominance of more than 16% at the state level, Tamil Nadu is the industry leader in terms of cumulative capacity. The importance of RES in the energy and power mix is becoming increasingly important as the country deals with the increasingly

devastating effects of climate change, which are mostly produced by humanistic rising actions.

For India's renewable energy industry, 2021 was a breakthrough year in which important milestones were achieved even as the country recovered from the Covid-19 epidemic. By surpassing the 40% installed capacity goal from RES in November 2021 by itself, India met one of its Paris 2030 Nationally Determined Contributions commitments nine years earlier. On August 20th , 2021, the nation crossed the benchmark of 100 GW installed renewable energy capacity (excluding large hydro). India is now ranked fourth globally in terms of installedrenewable energy capacity. At the UN's 26th conference of Parties in Glasgow in November 2021, India made a number of bold climate change announcements that focused heavily on renewable energy. In addition to reducing its economy's carbon intensity by more than 45%, India also announced its plans to reach the goal of "Net Zero" emissions by 2070. Together with developing a framework, India is also working on a path to accomplish a 500 GW RES capacity goal by 2030 [14].

1.4.3. Renewable Energy Initiatives

The main goals of renewable energy deployment in India are to promote economic growth, enhance energy security, increase access to electricity, and slow down global warming. By utilizing sustainable energy and guaranteeing that all individuals have access to cost-effective, reliable, sustainable, and contemporary energy, sustainable development is made feasible. India is already a prominent player in the most lucrative markets for renewable energy due to the country's strong backing from the government and the increasingly favorable economic environment. The government has created liberal rules, programs, and an atmosphere to attract international investment and quickly advance the

nation in the renewable energy sector. In the coming years, it is projected that the domestic employment situation in the renewable energy sector would improve significantly [9].

The Government of India have been implementing numerous initiatives, programs, renewable energy schemes, and incentives to boost the growth of the renewable energy sector in order to meet optimistic renewable energy targets and the commitment to the entire world in the fight against climate change. These incentives and activities are aimed at accelerating widespread adoption in tier 3 and rural areas. State government incentives and subsidies are essential to the expansion of renewable energy in small-scale power generation, including solar rooftop SPV systems. Solar pump subsidies are also becoming more common, which makes it easier to connect RES into the electrical grid [14].

The Kisan Urja Suraksha evam Utthaan Mahabhiyan (KUSUM) Scheme was introduced in 2019 and consists of several parts, including the construction of more than 17 lakh stand-alone solar agriculture pumps and more than 10 lakh grid-connected agriculture pumps, as well as the establishment of 10 GW of distributed grid-tied solar or other renewable energy power plants on unused land. The obstacles that the renewable energy sector is now facing are being solved by all of these initiatives, incentives, and programs [14-15].

1.5 OVERVIEW OF HRES

Worldwide energy consumption has grown as a result of the population expansion and industrialization that is happening so quickly. Due to their inherent restrictions including limited supply and GHG emissions, existing fossil fuel supplies are running out and cannot keep up with the rising demand for energy. As a result of the rising need for

electricity, research is now focused on finding more affordable and environmentally friendly alternatives to conventional energy sources. The best alternatives to fossil fuels that can meet the rising demand without having a significant adverse effect on the environment are the RES. HRES is produced by combining these RES with backup and storage systems. Both off-grid (OFG) and grid-tied designs for these HRES are possible. There are several combinations of HRES to suit the load requirement based on the site and resource availability [3].

1.5.1. Motivation for HRES

RES are quite erratic and reliant on climate factors. For instance, although solar energy is accessible throughout the day, different energy sources or stored energy are needed at night. As a result, RES alone might not be sufficient to satisfy the energy needs of the particular location. In this situation, combining RES can lessen the effect of any uncertainties already present in RES and increase their predictability. A HRES combines RES with storage technologies [16].

When contrasted to a system that is based on a single source, HRES improves overall benefits by combining several generating, storage, and utilization techniques into a single design. Initially intended to combine traditional, non-renewable power, such as diesel generator (DG) with battery energy storage system (BESS), its definition has now been modified to encompass systems that are primarily based on renewable energy, including SPV and wind, with storage systems. HRES have also expanded in size, moving from modest OFG systems of a few kW, normally made for low voltage DC and AC, to enormous MW systems that may now be linked to grids [17].

1.5.2. Types of HRES

There are primarily two modes of HRES, which are known as the stand-alone HRES, and the grid connected HRES [16]. In grid connected mode, HRESs are capable of being connected to electrical grids in either a grid-connected or parallel application, giving them the ability to purchase or sell power at a set price anytime whenever there is either a surplus of energy or a shortage of energy. The stand-alone HRES is suitable for meeting the energy requirements of isolated locations that either do not have access to a power grid or where the installation of an electricity infrastructure would be prohibitively expensive. HRES are becoming increasingly popular for electricity generating purposes in distant areas, since these are usually one of most cost effective and sustainable method of producing electricity for the rural application [16].

1.5.3. Optimal Design of HRES

It might be difficult to determine location where RES could be deployed and what mix, or matching capacity of RES are required [18]. These issues have prompted researchers to create models for optimum HRES design. The design challenge entails determining the optimum mix of RES as well as evaluating their optimum capacities necessary to produce the necessary power. It has the potential to make HRES to provide more affordable and reliable energy. Many studies have been undertaken in recent times to optimize the design of an HRES, but it remains a challenging topic due to fluctuating energy costs, variations in energy consumption, and uncertainty in RES supplies. Furthermore, environmental concerns have become more significant in the HRES design [19]. As a

result, numerous factors must be considered during the design phase of these systems, like net present cost (NPC), environmental issues, and reliability of power supply.

1.6 ORGANIZATION OF THE THESIS

This study is focused on designing an optimal hybrid system by leveraging the locally available renewable energy sources for specific sites. The research work is structured and organized in the following manner:

Chapter 1: In this chapter, an analysis of global and Indian energy consumption, GHG emissions, and renewable energy production is presented. Further, an overview of HRES is provided, along with an exploration of the reasons and necessity for implementing HRES.

Chapter 2: This chapter offers a comprehensive literature survey, covering various aspects related to HRES. The literature review entails an extensive analysis of various aspects related to HRES. It covers the feasibility assessment of HRES, exploration of conventional optimization techniques (OT), investigation of new-generation OT, examination of hybrid OT, and scrutiny of size OT employed for HRES. The final section of the chapter introduces a research gap analysis, paving the way for the research objectives.

Chapter 3: This chapter focuses on the mathematical modeling of HRES components, including SPV,WT, BMG, biogas generator (BGG), and battery. It also covers system reliability modeling and energy cost modeling. These models aid in assessing the feasibility, performance, and economic viability of the HRES, contributing to the design and optimization of the system.

Chapter 4: This chapter focuses on estimating the potential of locally available renewable energy sources and load requirements for selected sites in Uttar Pradesh and Haryana states, India, with the aim of developing hybrid models. In this connection, the feasibility analysis of potential off grid and grid-connected models using locally available renewable energy sources for fulfilling the energy demand of the selected sites has been carried out using HOMER Pro software.

Chapter 5: This chapter provides insights into various benefits, difficulties, and challenges that might arise throughout the process of integrating various renewable energy sources into the grid, as well as some viable alternatives.

Chapter 6: In this chapter, the size optimization of HRES for selected sites has been presented. The primary objective was to minimize the NPC of HRES while adhering to constraints related to component boundaries, battery storage limits, and system reliability. To achieve this, various models were analyzed in both off grid and grid-connected scenarios using novel AO algorithm. Further, the results of AO algorithms were then compared with HS and PSO algorithms.

Chapter 7: In this chapter, the size optimization of HRES has been carried out for the outlying region of Mewat, and Agra India. Grid-connected configurations were designed and presented using the forecasted data for global horizontal irradiation (GHI) and temperature for study area I and GHI, temperature and W_S for study area II. The four ML techniques: GPR, SVR, XGBT, and DT were used for forecasting. Further, the HRES was optimized using recently developed CPA, TSA, and AO algorithms using forecasted data.

Chapter 8: This chapter of the thesis outlines the key findings of the research work conducted. Additionally, it provides a concise overview of the potential areas for future exploration in the field of HRES.

CHAPTER 2

LITERATURE REVIEW

2.1 GENERAL

This chapter includes a literature overview on different aspects of HRES, such as feasibility and techno economic analysis of RES based hybrid models, the design and development of HRES, intelligent approaches for modelling and sizing of HRES, Investigation of issues in grid integration of various resources for the development of hybrid model, sizing, and control of hybrid model for rural applications. Over a hundred and ten different research articles on the topic of HRES have been read, and their findings have been reviewed. This overview of the relevant literature has been divided into a variety of sub-parts, each of which has been addressed in the subsequent sections.

2.2 FEASIBILITY ANALYSIS OF HRES

A feasibility assessment of a HRES is often performed prior to installation and operation. Essentially, this analysis entails examining the climatic conditions of the proposed location, assessing the accessibility of RES, evaluating the potential load, and understanding the demand of the targeted area. The feasibility study aids in pinpointing the optimal site for implementing an HRES. Various researchers have made significant contributions in this domain, focusing on key aspects that are discussed herein.

Researcher carried out a feasibility study of grid isolated HRES to electrify a farm and irrigation sector in Dongola, Sudan. The framework uses techno-economic analysis for HRES systems with variable RES penetrations. The study compares various configurations

to determine the solution with the lowest NPC and GHG emissions. The sensitivity analysis has also been performed to determine how design parameter uncertainty affects HRES design and cost [20].

The feasibility analysis is carried out by researchers for a grid connected HRES for a village located in Pakistan using HOMER Pro software. The potential for wind, solar, and biomass energy generation was assessed in this research. Optimization and sensitivity analysis was also done to ensure robustness and cost of the HRES. In this work, RES was properly dispersed, and surplus power was delivered to the grid [21]. Through a case study of a hamlet in West China, the authors aim to show the techno-economic viability of an OFG HRES for long-term distant rural electrification. The simulation results revealed that the SPV/ WT/biogas generator (BGG)/DG/BESS would be the most reliable and cost-effective configuration for the OFG HRES. The results revealed that this configuration can make the village independent from the main grid and can also provide electricity to the consumers at an affordable cost of $0.201/kWh [22].

Researchers examined the RES potential of an Ethiopian village for electrification using HOMER Pro software. To ascertain the impact of variations in solar radiation, wind speed (WS), and fuel price on optimum system configurations, a sensitivity analysis was also carried out. The findings indicate that the most advantageous alternative from an economical perspective is a SPV/ WT/ BESS/ DG based HRES. When the optimal HRES design is compared to DG alone to generate energy, the optimum system enables an annual decrease in GHG emissions of 37.3 tons [23].

The research carried out to power a specific load at a workshop in the Iranian industrial city of Ardabil, OFG HRES option was found to be more optimal. The findings

demonstrated that the industrial city has a sufficient potential of wind and solar energy for electricity generation. Due to the specific climate in the region, a WT produces more energy than a SPV panel. Utilizing SPV and WT was regarded as essential for the system since they significantly lower GHG emissions as well as operational and maintenance cost (OMC). Four potential energy sources: DG, SPV, wind, and batteries were chosen. The optimization findings demonstrate the feasibility and reliability of providing the workshop with energy using the suggested HRES [24].

Authors performed a techno-economic feasibility analysis of HRES in the hamlet of Fouay, Benin Republic for sustained rural electrification. According to the research, the hybrid SPV/DG/BESS was the most optimum solution among the several scenarios evaluated to electrify the hamlet in a sustainable way. Furthermore, the findings revealed that the most cost-effective HRES in each site was greatly influenced by the potential of the alternative power sources as well as the distance of the source from the load point. As an example, the hydropower potential at the site is significant, but due to the distance of the site from the settlement, an additional investment cost for grid extension makes such a system less cost-effective than the SPV/DG/BESS [25].

A techno-economic assessment of an OFG HRES to electrify a commercial-load demand was presented by the researcher. The HOMER Pro software was used to investigate the feasibility of specific RES alternatives and a DG based system. A techno-economic research and sensitivity analysis was also carried out to assess the financial feasibility and RES compliance of the various configurations. Levelized Cost of energy (LCOE) and NPC were the two key factors considered in the feasibility study. The

WT/DG/Fuel cell BESS was determined to be the most optimal configuration based on the upfront charges and replacement cost (RC) [26].

The techno-economic and environmental feasibility of seven distinct OFG hybrid configurations with and without storage unit were assessed by researcher to discover the most optimum and cost-effective HRES for a remote location in India's western Himalayan territory. The research of RES assessment found that the western Himalayan region has several extra benefits over barren locations, such as abundant unutilized forest biomass, excellent circumstances for SPV power generation with abundant solar radiation, and a moderate temperature range [27].

Authors investigated several configurations of HRES for communications applications in Punjab, India. The SPV/WT/DG/BESS was identified as the most viable with the lowest cost of energy (COE) [28]. Many authors have also conducted similar studies utilizing HOMER Pro software to undertake feasibility analysis in finding appropriate HRES for supplying power to various locations [29-32]. In addition, using case studies from diverse rural locations, researchers used multiple modelling approaches and established methodologies to investigate various forms of RES to generate electricity [33-35].

For the modelling, design, and development of HRES for specific locations, a suitable optimization approach is required. The following section includes a detailed summary of the most popular OT during the last few years.

2.3 OPTIMIZATION TECHNIQUES FOR MODELLING OF HRES

When it comes to hybrid systems, there are lot of different objectives that need to be addressed, such as the system size, modelling, management, and control [36]. This

section contains a comprehensive analysis of the optimization strategies that have been used the most frequently during the past few years Subramanian et al., classified modelling approaches for energy systems may be divided into two groups, one based on the modelling methodology, and the other on the needs of the application area [37]. Ghofrani and Hosseini used a different approach and categorized the key OT into three separate groups: classical, metaheuristics, and hybrids techniques [38]. Tina et al. and Khatod et al. separated the approaches to modelling energy systems into three distinct categories: analytical, simulation, and Monte Carlo simulations (MCS). In the last category, three different modelling sub-approaches were included, each of which was determined by the input variable management methodologies. It was also taken into consideration to look at simple time series, probabilistic techniques, and average daily or even monthly values for the energy balance [39-40]. According to a different viewpoint the various optimization strategy that have been explored may be divided into two primary categories: classic OT and next generation optimization approaches. According to the framework that most scientists working in the HRES sector use, the modelling approaches that are described in this study have been divided into three distinct groups as shown in Fig. 2.1 [37, 41].

2.3.1. Conventional Optimization Techniques

To obtain the optimum designs of HRES, many conventional approaches are used. Numerous authors used the graphical construction technique, the least square method, iterative and probabilistic approaches, linear and mixed linear integer programming. These techniques are simple to apply, comprehend, and have a broad variety of applications. The following part discusses the literature and provides a quick overview of the strategies [42].

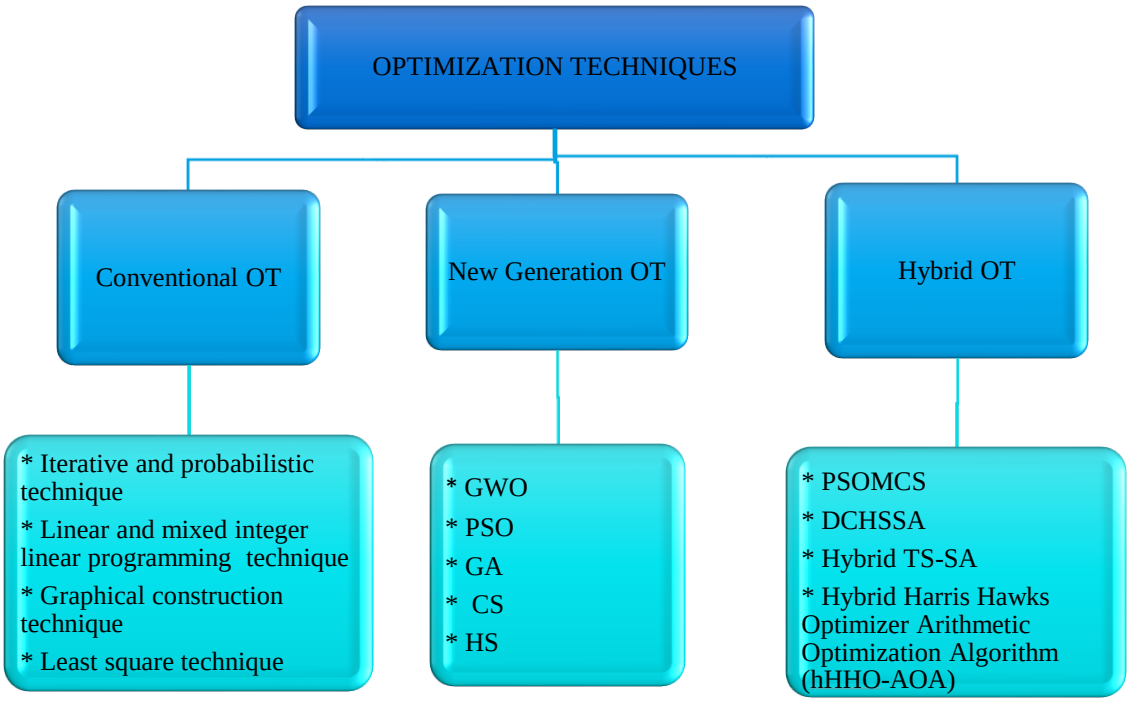

Fig. 2. 1 Optimization Techniques of HRES

The iterative approach runs a sequence of mathematical simulations to arrive at a set of outcomes that are only rough approximations of the actual results and may be utilized to solve the problem [37]. To be more explicit, iterative procedures are employed to accomplish the linear adjustment of the values that are provided to HRES decision variables, which ultimately results in a scan of all possible configurations for producing units. When viewed in this perspective, the estimation of reliability of the power may be found by analyzing each design in addition to the configuration that is optimal. The well-known iterative method inspired the creation of a new algorithm called the evolutionary algorithm, which is also frequently referred to as a heuristic approach [43]. This is despite the fact that these flaws result in a localized rather than a global optimum solution. Iterative techniques include, but are not limited to, the following: linear programming techniques

[44-45] dynamic programming techniques [46-47]. The following paragraph provides an overview of various typical optimization strategies:

The researchers used Iterative approach for design and development of HRES. The optimal system included SPV/WT/BESS. The main aim of the research was to minimize the cost of the system[48]. The probabilistic approach was used by authors for WT/ fuel cell /electrolyzer/ BESS HRES. The main objective was to minimize the total NPC of the system while fulfilling the ED [49-50]. The authors used linear programming technique to design a SPV/WT/Biomass generator (BMG) based HRES to minimize the outsourced supply [51]. Graphical construction method was also used by researchers to design SPV/WT/BESS HRES in order to minimize the COE while ensuring the reliability of power supply [52-53].

2.3.2. New Generation Optimization Techniques

For design and development of HRES lots of new generation OT like grey wolf optimization (GWO), PSO, genetic algorithm (GA), Cuckoo Search, HS etc. are available in literature. The next paragraphs will explore a couple of these techniques in more detail.

AskarZadeh et al. employed PSO to simulate HRES and estimate the sizes of HRES components for the electrification of a remote region in Iran. The HRES was developed by taking into account three variables: the area of the SPV panel, the swept area of the turbine blades, and the number of batteries [54]. PSO was also used in a study conducted by Mohamed et al. to simulate the components of the HRES. The goal of this HRES modelling was to produce a diverse load profile, reduced system costs and CO_2 emissions. Load shifting was suggested as one possible micro-grid application to do this. Moreover, a

framework for controlling and analyzing dummy load was offered. In order to predict system performance under different operating situations, sensitivity analysis was also undertaken [55]. GWO was utilized by Moghaddam et al. to provide a strategy for HRES sizing. The main objective of this study was to lower the COE of HRES while maintaining loss of power supply probability (LPSP) constraint and figuring out the adequate quantity of batteries, SPV panels, and WT [56]. A realistic evaluation framework of HRES was created by Singh et al. considering the number of SPV panels, the number of WT unit force outages, and the sporadic nature of solar and wind energy. The Cuckoo Search method was employed to create the HRES in the best possible way. The resilience of Cuckoo Search in addressing HRES design problems was validated utilizing performance evaluations with other OT such as a GA and PSO [57]. Jing et al. provided a size optimization technique for managing the demand response (DR) of domestic appliances in an island micro-grid. PSO was used to identify the optimal sizes for all critical components. Moreover, the BESS served as the control group. The results of case studies demonstrate the viability of the recommended method, and it is possible to significantly reduce island micro-grid costs by employing deferrable load and pumped hydro storage. The entire island load and water head were the subject of a sensitivity analysis [58]. At the isolated rural town of Djanet in south Algeria, Yahiaouia et al. proposed a method for optimal design and reducing the COE of HRES utilizing the GWO. An HRES including a SPV panel, a DG, battery banks, and a load was used to evaluate the recommended method. A PSO was utilized to compare the results [59]. Shahzad et al. created an OFG HRES employing solar and biomass resources to offer an excellent supply chain to Pakistan's rural areas [60]. Chauhan et al. investigated an integrated RES to satisfy

the ED for 48 communities. The use of integer linear programming was used to model a DR strategy. The size of the suggested RES with and without the DR method was optimized using the discrete HS (DHS) algorithm. The DR strategy has been demonstrated to save a significant amount of money in terms of both capacity and costs when contrasted to systems without DR [61]. Research was done by Sawle et al. on sizing of HRES component. A unique multi-objective function with several HRES objectives was provided to determine the optimal factor that determines using GA, PSO OT [62]. Using PSO, Atieh et al. conducted research to determine the optimal HRES size for a residence. The objective of this research was to reduce pollution emissions and the system's total cost. The findings demonstrate that both system costs and emissions were reduced [63]. Anand et al. used the PSO approach to perform research to determine the appropriate size of a grid tied HRES for rural areas in Haryana, India. A grid tied HRES was found to be the optimal design for the study. Hourly simulation was done to establish the appropriate size of the HRES [64]. The same researcher also investigated the best HRES component size via HS OT. In this study, a grid connected HRES was considered. The boundary constraints, battery storage limitations, and land use limits, all contribute to lowering the NPC of the HRES under consideration [65]. Ashtiani et al. conducted a study aimed at determining the optimal size of a grid-connected SPV/battery system to minimize the total NPC through the utilization of Teaching-Learning-Based Optimization (TLBO). Additionally, the researchers performed a sensitivity analysis to assess the impacts of various factors, such as equipment costs, climatic data, and load profiles, on both the NPC and COE associated with the system [66].

Das et al. conducted a study with the objective of achieving a techno-economic optimal design for an OFG hybrid SPV/BGG/pumped hydro storage/battery system. They employed the water cycle algorithm and moth-flame OT to optimize the system design specifically for a radio transmitter station located in India [67].

Mishra et al. conducted research aimed at developing an affordable and reliable grid-connected RES. They utilized DHS algorithm to optimize the NPC of the system, ensuring efficient power supply to a selected rural area. The study involved estimating the electricity and cooking demands for the chosen site, which were met by the available resources in combination with grid connectivity. The results revealed that the grid-connected system proved to be more reliable and cost-effective in comparison to a stand-alone system [68].

2.3.3. Hybrid Optimization Techniques

The majority of different evolutionary computing approaches have a drawback known as premature convergence. These methods demand a great deal of time in order to get away from the local maximum or minimum [69]. Hybrid optimization approaches like hybrid Harris Hawks Optimizer Arithmetic Optimization Algorithm (hHHO-AOA), discrete chaotic harmony search based simulated annealing (DCHSSA) algorithm, and hybrid Tabu search (TS) etc. are able to tackle a wide range of optimization challenges because they combine the best features of not just two but several approaches to optimization. Over the course of the past few years, there has been a growing interest in the study of hybrid techniques. When contrasted to use of individual approach, hybrid methods demonstrate excellent levels of strength and competitiveness.

In recent years, a number of researchers have used hybrid techniques to standalone solar, WT, and SPV-WT hybrid systems. Kalogirou, Mellit et al. used neural networks and GA to determine the optimal dimensions for solar systems[70-71]. Khatib et al. offered a case study that took place in Malaysia to determine the appropriate number of components for a hybrid system. The number of photovoltaic panels, WT, and batteries played a significant role in the decision-making process. The authors utilized a methodology that was a hybrid of iterative and GA approaches. The iterative approach was used to find a collection of alternative configurations, and the GA was used to choose the configuration that yielded the best results [72].

Askarzadeh suggested a hybrid method for obtaining the size of a SPV-WT based system by integrating three well-known algorithms, namely chaotic search (CS), HS, and SA. This was done in order to get optimal results. This algorithm was produced by combining all three methods and named DCHSS. It has been determined that the suggested algorithm is superior to each individual approach [73]. Using a mixed multiple criteria integer programming problem, Xu et al. came up with a proposal for the optimal size of the components that make up standalone hybrid wind-SPV power system. It was suggested that the GA be implemented in order to reduce the overall capital cost (CC) that was being imposed by the LPSP [74]. By investigating the significance of each particular method, Castiglioni's et al. suggested a hybrid TS and SA optimization strategy. The findings make it abundantly clear that the hybrid approach delivers a solution of sufficient quality in a shorter amount of computing time [75]. A hybrid big bang–big crunch algorithm for designing an optimal HRES was reported by Ahmadi et al. [76]. Maleki et al. presented a PSO-based MCS for an OFG hybrid system that included SPV, WTs, and batteries [77].

2.4 METHODS USED FOR SIZING OF HRES

The optimal sizing of HRES components, is one of the most significant aspects as it impacts the cost and power reliability. If the system is not adequately sized, it might be either undersized or oversized. This topic has been the subject of much investigation. There are mainly two different types of sizing techniques: software-based and conventional methods. Researchers have employed a variety of software's like HOMER Pro, RET screen etc. and conventional methods, including analytical, iterative, and probabilistic and artificial intelligence (AI) techniques that have been documented in the literature, for the size optimization of HRES. A few of these are discussed in the subsequent paragraphs.

2.4.1. Commercial Software

To perform techno economic analysis and optimal sizing of HRES, there are currently a variety of simulation software's available. Some examples of these software's include HOMER Pro, Hybrid optimization using GA (HOGA), Hybrid system simulation model (HYBRID2), RET Screen, and others. However, the HOMER Pro software is currently the most widely used of these software's. The literature has a number of publications that discuss the design of HRES employing HOMER Pro for both OFG and grid-connected applications. These HRES using HOMER Pro are covered further down in this section.

Kamel et al. performed economic comparison between hybrid power system and diesel generated power system for remote agricultural area in Egypt. It has been found that hybrid system gives favorable results in terms of NPC even though with high fuel price subsidies in case of DG [78]. In addition, Dufo-López et al. carried out a research in which

they found that SPV-DG hybrid system reduces the OMC and pollution as compared to DG alone [79]. Nouni et al. identified the various locations in India where RES based OFG power generation systems are more cost effective than grid extension. In this research it has been concluded that dual fuel biomass gasifier systems, micro-hydro, wind generators and SPV systems would be economical options in comparison to grid extension for energy supply in rural areas [80].

Abdullaha et al. employed HOMER Pro simulation software to present the cost-effectiveness of the SPV system and the hybrid SPV/hydro system for rural electrification. Results revealed that the hybrid power generation is more sustainable due to unpredictable climate conditions [81]. Rehman and Al-Hadhrami proposed a hybrid SPV, DG alongwith battery system instead of existing DG for supplying electricity to a village situated at Kingdom. HOMER Pro software was used to find the optimum hybrid system. The results revealed that existing DG is cost effective with diesel price of 0.2 $/L and hybrid system provides economic power with diesel price of 0.60 $/L or higher [82]. An analytical study for the electrification of a remote area named Kakkavayal in Kerala, India has been done by Kumaravel et al. employing HOMER Pro software. The result shows that the hybrid system comprising of SPV/pico-hydel/ biomass to meet the load demand is a better option than the existing pico-hydel/System [82]. Ioannis et al. studied four scenarios of hybrid systems i.e., SPV/DG, WT/DG, WT/Fuel cell and SPV/WT for different locations of Greece. It was found that SPV/DG system was an optimal solution for locations of an average wind speed of 3 m/s [83].

Sen and Bhattacharyya suggested the best hybrid system consisting of RES viz. SPV, WT, biodiesel, and small-scale hydropower to fulfill the electricity needs of Palari

village in Chhattisgarh state, India. The comparison was done between OFG and grid extension. The OFG hybrid system was found to be more suitable in terms of cost-effectiveness and environment sustainability [84]. Ramli et al. employed MATLAB and HOMER Pro to perform techno-economic analysis of hybrid SPV/WT energy system for electrification of west coast area of Saudi Arabia. Results indicated that SPV generates more power as compare to WT when both are of same size and are used in hybrid configuration[85]. Phuangpornpitak and Kumar developed a SPV based hybrid system for rural electrification in Thailand and they recommended that addition of DG to SPV system amends the reliability of power supply [86].

Some authors studied the sensitivity analysis of hybrid system in order to find the most sensitive parameter. Saheb-Koussa et al. employed HOMER Pro to do a comparative analysis of grid connected hybrid SPV/WT energy system with utility grid alone in terms of environmental and economical parameters. They found that there is 22% reduction in GHG with the use of HRES. Based on the sensitivity analysis, they observed that the wind speed is the most sensitive parameter which affects system cost and reliability [87]. Garrido et al. employed HOMER Pro for performance analysis of a hybrid SPV, BMG for an area located in Nampula, Mozambique by considering cashew shells as a fuel. The obtained results suggested that the proposed system offered the lesser COE of $0.33/kWh compared to SPV/DG and conventional DG [88].

Shahzad et al. proposed an OFG hybrid energy system consisting of SPV, biomass for providing electricity to residential community and agricultural farm in a village situated in Pakistan. HOMER Pro software was used for techno-economic analysis and sensitivity analysis. Results revealed that the hybrid system consisting of SPV array of 10 kilo watt

(kW), biogas of 8 kW along with 32 batteries and 12 kW converters was cost-effective with NPC of PKR4.48M. The cost of electricity of this system is 5.51 PKR/kWh in comparison to grid supply rate of 10.35 PKR/kWh. Variables such as solar radiation, biomass potential, price of biomass and hourly load were taken for sensitivity analysis. It has been found that NPC and operating cost were more sensitive to changing solar irradiance and biomass fuel [89]. Several other studies based on simulation software approach are also carried out by several researchers [90-97].

Apart from simulation software based approach for developing HRES, several other approaches available in literature are reported in the following section.

2.4.2. Conventional Methods

To perform size optimization of HRES, Researchers have employed a lot of methods like Analytical, Iterative, Probabilistic, and Artificial intelligence methods. However, the AI methods like artificial neural network (ANN), PSO, GA, GWO etc. are currently the most widely used. The literature has a number of publications that discuss the size optimization of HRES employing AI methods for both OFG and grid-connected applications. The size optimization of HRES using AI methods is covered further down in this section.

Bernal-Agustin JL et al. and Dufo-López R et al. performed a study in which they found out that the optimum size of a SPV/WT / DG HRES may be achieved using the Strength Pareto evolutionary algorithm by constructing two objective functions, namely, the reduction of system cost and the minimization of GHG emissions [98-99]. Yang H et al., Bilal BO et al., and Tafreshi SMM et al. carried out research in which GA was used to

optimize the sizing problem under a variety of objective functions, including maximizing the system's reliability under varying weather conditions, minimizing the system's annual cost, and minimizing the LPSP [100-102]. Navaeefard A et al., Bashir M et al., and Pirhaghshenasvali M et al. have utilized PSO to determine the best size of HRES [103-105]. Askarzadeh proposed a DHS based algorithm for sizing SPV and WT in HRES for a remote region of Montana State. The suggested technique was simple to use, handles discrete problems well, and finds solutions rapidly. In less than a second, the suggested technique yields encouraging findings [106]. Ismail et al. presented a hybrid system that combines solar panels and batteries to cover the energy needs of a small rural community in Palestine. The results show that the suggested solution is more advantageous than the utility grid [107].

Maleki et al. employed a HS based strategy to optimize the design of a SPV/WT based HRES for rural regions in Rafsanjan, Iran. Furthermore, the constructed device was compared to a DG in terms of overall cost and emissions[108]. In order to reduce overall NPC, Heydari et al. created a SPV system using biomass as a backup source. They discovered that the established technique for delivering energy to agricultural wells in Bardsir, Iran was more cost-effective than using solar panels or biomass alone [109]. Abak A et al. carried out research to optimize a hybrid system comprising SPV, WT, and BMG and scaled it to meet the energy needs of a faculty building. First, GA and SA were utilized. Unlike earlier research, GWO was used to optimize, and size based on reliability and economic characteristics. Then GWO findings were compared to GA and SA results [110]. Diab A et al. propose a simulation model for an HRES microgrid with battery bank storage. The suggested system's optimal size reduces the COE while boosting the HRES reliability

and efficiency. The optimized HRES was designed using various novel optimization methods and also, the suggested optimization strategies were thoroughly compared. The hybrid whale optimization algorithm (WOA) outperformed the other algorithms in simulation [111]. With the use of the PSO approach, Anand P et al. performed research to determine the optimum size of an HRES for rural areas. It was found that a grid connected HRES was the most effective architecture for the investigation. An hourly simulation was used to find the optimal size of the HRES using a grid [112]. Mwakitalima et al. performed research in which they examined both technical and non-technical aspects of solar energy generation which are essential for the growth of the industry. The authors of this article also looked at the advantages and disadvantages, possibilities and threats related to the usage of standalone SPV systems to produce electricity. The research also goes into great length on the pros and downsides of solar-powered devices [113]. Bakhshaei P carried out research to determine the best grid-purchased electricity in a grid-connected HRES. To achieve this, the system's running costs were minimized while maintaining a specified degree of stability and operating limitations. Simulation findings demonstrate that determining the best power exchange and incentive rate lowers operating costs [114]. Jamshidi S et al. conducted research to replace wind speed and solar insolation data with averaged and generally site meteorological data, such as atmospheric temperature, elevation, moisture content etc. to avoid the need for long-term and detailed HRES sizing data. A total of 105 Iranian locations have been used as training data to create and test these HRES [115]. Rezaei M et al. performed research which includes grid-independent HRES comprised of SPV, WT, and renewable hydrogen based fuel cell examined in this research to determine the optimal sizing for co-supplying electricity and heat to a tourist village, Mesr, in Iran's Isfahan

province [116]. Acharya S et al. used the Refraction-based WOA (RWOA) to solve Combined Economic Emission Dispatch (CEED) challenges by determining an optimum HRES production output. The WT might well be linked to the thermal power plant in HRES since it cannot be utilized alone to reduce economic and pollution expenses. The suggested RWOA strategy is compared to other established approaches in terms of economic cost and emission cost [117]. Das, B. K. et al. conducted research to size an HRES system, which includes SPV, WT, batteries, and converters, to meet the needs of a rural town. The power generated by this system is utilized to meet the community's thermal demand through a thermal load controller. The HRES optimized for both electric and thermal loads is compared to the identical systems optimized for just electric loads. The impacts of utilizing surplus power and not using extra electricity to meet thermal needs are also investigated. The comparative study is carried out further to look at the impact of various technical and economic characteristics of the HRES components. The GA optimization approach is also applied to optimize the HRES system [118].

2.4.3. Optimal Sizing of HRES using RES Forecasted Data

RES are becoming more appealing as ED grows and fossil fuel cost (FC) rise in remote places. The hybridization of these resources has the potential to reduce unpredictability and intermittency while increasing efficiency. The accuracy of size optimization of HRES can be improved by using accurate weather data that can be available through forecasting. Uncertainty regarding RES presents itself as one of the particular challenges faced in the design of HRES, resulting in various approaches to tackle this issue. Lei et al. provided a bibliographical assessment of current research and advancements in wind speed and power forecasting [119]. A unique hybrid technique is suggested and

compared by Catalao et al. for short-term wind forecasting employing wavelet transform [120]. The optimization approaches mentioned in the literature are often based on the previous years wind speed and solar irradiance data. However, it is well recognized that meteorological data from prior years vary dramatically from current estimates. Many models, including uncertainty for improving energy efficiency, have been developed to address this issue. In this context, Khalid et al. and Tascikarao et al. employed wind power prediction to optimize hybrid energy systems, whereas Hocaoglu et al. investigated the influence of solar irradiance forecasting on optimal system design efficiency [121-123].

To determine the optimal size of a grid connected HRES, a novel framework is put forth by Zhang et al. that comprises a new algorithm as a mix of CS, HS, and SA. Weather and load forecasts were included using ANN to increase the precision of the size-optimized design [124]. Gupta et al. suggested the biogeography-based optimization (BBO) algorithm and ANN as optimization and solar wind forecasting models (FM), respectively. The article's authors also examine the benefits of improving the small autonomous hybrid power system's optimization using forecasts rather than historical data [125]. Maleki et al. presented a HS and a hybrid of HS and CS. This study evaluated an HRES that uses iterative neural networks to anticipate the weather and meet household water needs [126]. Alfonso et al. provide a sizing methodology that utilizes long short-term memory (LSTM) cells to anticipate long-term weather conditions [127].

2.5 ISSUES IN GRID INTEGRATION OF VARIOUS RES

Decarbonization, energy security, and expanding the availability of electricity are the main reasons affecting the rise in interest in RES on a worldwide scale. The future of

clean and sustainable power generation lies in the integration of RES into already-existing electrical grids [128]. But due to RES's intermittency, there are lots of integration issues when RES are connected to the main grid. The voltage and frequency fluctuation, stability, protection, and safety will all be impacted by these uncertainties[129]. The issues, challenges, and solutions related to the integration of RES to the grid are reviewed further down in this section.

Sonali et al. highlighted the power quality concerns that have arisen as a consequence of the integration of RES into the grid, as well as the financial implications that have arisen as a result of the poor power quality. In addition, a discussion is held on the several approaches that may be utilized in conjunction with developments in technical innovation in order to overcome the difficulties associated with power quality [130]. Oyekale et al. analyze the technological issues connected with integrating RES into the electricity grid, as well as prominent methods applied. A brief but comprehensive summary of RES was presented, and the effects on the efficacy of the power system for power generation from RES were examined. They found that issue of reliable weather forecasting has a detrimental influence on market penetration for solar and wind, resulting in low system dispatch ability and dependability, as well as high prices. State-of-the-art robust weather FM are being created to limit these consequences, but additional efforts are needed in this regard, particularly by utilizing the immense potentials of AI-based forecasting and optimization methodologies. In addition, hybridization of renewable sources and deployment of energy storage devices are being investigated to boost dispatch capability [131]. Sandhu et al. carried out a study in which technical and non-technical issues and challenges of RES grid integration and potential solutions have been highlighted. Power

electronics devices are feasible choices for reducing fluctuations and intermittent difficulties. Furthermore, energy storage and the usage of dump load and maximum power point tracking might be employed to reduce power fluctuations in SPV systems [132]. Muntathir et al. conducted research on the optimal placement and penetration of SPV systems on an IEEE 30-bus system. The study was based on the optimum placement of SPV systems and the penetration levels of SPV systems [133]. Zahedi investigated the driving reasons, benefits, and barriers of RES integration into the grid, with end user perspective concerns dominating [134]. According to Soroudi et al., distribution system has been created in such a manner that they can only handle the flow of electricity in one direction. As a result, the integration of distributed generators (DSG) with the grid may cause voltage fluctuations, problems with protective device coordination, and reactive power control concerns. When solar and wind are integrated to the grid as DSG, their stochastic nature might affect power reliability. Additionally, the CC of these distributed renewable is rather high, particularly in Sub-Saharan Africa, making large-scale implementation difficult [135]. Lopes et al. classified the problems of linking DSG into three categories: technical, economic, and regulatory. Because economic and regulatory obstacles are tied to government policies, this evaluation overlooks them and focuses solely on technological issues [136]. The increasing amount of RES integration in the electricity sector will be effective only if these challenges are addressed. While undertaking grid planning and operational studies, the problems of renewable energy integration to the grid must be taken into account [137-138].

2.6 RESEARCH MOTIVATION

To fulfill the UN sustainable development goals of green energy to all and to reduce GHG emissions to mitigate climate change, the optimum utilization of RES based energy generation is essential. Several corporations and policymakers throughout the world are taking an interest in renewable energy, and it is being examined for use and electrification in many different parts of the world. The HRES are often capable of producing power for a wide range of applications including business or office space, rural regions, healthcare, network infrastructure, and a variety of other facilities. In terms of energy generation, hybrid power systems typically span from modest to big sizes. They are capable of producing energy for tiny houses as well as large-scale commercial systems that may power a whole community or island. Several years ago, HRES were created for the generation of electricity and the powering of numerous rural places and distinct commercial complexes. In India, the aforementioned RES are numerous. Wind energy and small hydro are mostly site-dependent, although solar energy and biomass are readily accessible in the majority of locations. The literature reveals that the HOMER Pro tool is commonly used for HRES feasibility analysis. In addition, the majority of efforts have been done to optimize OFG HRES. Since most researchers used fixed-size BGG, and BMG, size optimization of BGG and BMG in HRES was rarely done. The size optimization algorithms provided in the literature are based on wind speed and solar irradiance meteorological data from previous years; only a few of research incorporated forecasted data. Furthermore, seasonal fluctuation in load demand is rarely addressed during size optimization of HRES. In addition, the majority of the grid-connected different scenarios have been conducted

utilizing simulation tools such as HOMER Pro. Intelligent optimization methodologies have not been widely implemented for grid-connected systems.

Based on extensive literature review, some of research gaps are identified as follows

- Only a few studies have been reported for India especially west Uttar Pradesh.
- Only limited studies have included biomass and biogas energy sources in designing HRES.
- No attempts have been made to extend the application of HES to dairy farm.
- Very few studies have considered cluster of villages for developing hybrid power
- Limited work has been reported for grid connected hybrid systems.

2.7 RESEARCH OBJECTIVES

Based on the literature survey and growing significance of the design of hybrid system by utilizing locally available RES for power generation, the main aim of the present work is to design, optimize and analyze an effective renewable energy based hybrid system ensuring reliable and economical power supply with reduced GHG emission. The research work has been planned with following objectives:

- Feasibility and techno economic analysis of RES based hybrid model.
- Intelligent Modelling for the sizing of RES based hybrid model.
- Investigation of issues in grid integration of various resources for the development of hybrid model.
- Sizing and control of hybrid model for rural applications.

CHAPTER 3

MODELLING OF HRES COMPONENTS

3.1 INTRODUCTION

HRES have gained significant attention in recent years as a promising solution to meet the growing energy demands while reducing reliance on fossil fuels and provide a pathway towards a more sustainable and resilient energy future, driving the global transition towards cleaner and greener energy sources. Mathematical modelling plays a crucial role in understanding and optimizing HRES, which combine multiple RES to overcome the challenges of intermittency and variability [3]. These models involve the development of mathematical equations and algorithms to simulate and analyze the behavior of system components, such as renewable energy generators, storage devices, converters, and loads. By utilizing mathematical models, researchers and engineers can evaluate different operational scenarios, assess system performance, optimize system configurations, and develop effective control strategies [3].

Mathematical modelling enables the prediction of energy generation, storage requirements, and the economic viability of HRES, ultimately contributing to the design and implementation of efficient, reliable, and sustainable energy solutions [3]. In view of the above, the mathematical modelling of different RES along with energy cost models is presented in the subsequent sections in this chapter.

3.2 MODELLING OF HRES COMPONENTS

To design a HRES, mathematical modelling is a crucial step which provides the knowledge related to cost, operation, and performance of system components in various conditions. The mathematical modelling of various components for design and development of HRES are discussed in the subsequent sections.

3.2.1. Solar Photovoltaic (SPV) System

A SPV system uses modules that are linked both in series and in parallel.

The SPV power may be calculated as follows [139]:

$$PV_p^o(t) = D_f \times PV_p^r \times (s_i/s_i^r) \times [1 + k_t\,(t_c - t_{ref}) \tag{3.1}$$

$$t_c = t_{amb} + (0.0256 \times s_i) \tag{3.2}$$

Where; $PV_p^o(t)$ denotes SPV output power; D_f indicates derating factor, rated power is represented by PV_p^r, s_i is solar irradiance, solar irradiance at reference conditions is denoted by s_i^r, temperature coefficient is represented by k_t, t_c denotes cell temperature and t_{ref} is cell temperature at reference conditions,

Further, the energy produced by the SPV system ($E_{pv}\,(t)$) can be calculated as:

$$E_{pv}\,(t) = PV_p^o\,(t) \times \Delta t \tag{3.3}$$

3.2.2. Wind Energy Generator System

In order to formulate a mathematical model of a wind energy generator, curve fitting of an actual power-wind speed chart given by the manufacturer is used. These are the

equations that may be used to determine the electricity output of a particular wind energy system during the hour t [140]:

$$W_p^o(t) = \begin{cases} 0 & when\ u < u_{ci}\ and\ u > u_{co} \\ a_1u^2 + b_1u + c_1 & when\ u_{ci} \leq u < u_1 \\ a_2u^2 + b_2u + c_2 & when\ u_1 \leq u < u_2 \\ a_3u^2 + b_3u + c_3 & when\ u_2 \leq u < u_{co} \end{cases} \quad (3.4)$$

Where; $W_p^o(t)$ represents the output power of WT; u is the wind speed measured in m/second (s), u_{ci} is the speed at which the WT cuts in, and u_{co} is the speed at which WT cuts out. *a, b, c* denotes elements of quadratic function.

The electricity that is produced by a wind energy system may be calculated as follows:

$$E_W(t) = N_W \times W_p^o(t) \times \Delta t \quad (3.5)$$

Where; $E_W(t)$ indicates the energy produced by WT; the Number of WT simply represented by N_W .

3.2.3. Biomass Generator (BMG) System

The BMG system output power may be calculated using the below equation [139]:

$$BMG_p^o(t) = (Q_{BMG} \times C_{BMG} \times \eta_{BMG} \times 1000)/(365 \times 860 \times H_{BMG}) \quad (3.6)$$

Where; $BMG_p^o(t)$ indicates the output power of BMG; Q_{BMG} is the amount of biomass that is available in tons per year, and in order to convert the amount of biomass that is available from one year to one day, it is divided by 365. The calorific value of biomass is denoted by the notation C_{BMG}. The number of kilocalories must be divided by 860 in order to obtain the kWh equivalent; H_{BMG} represents the number of hours that BMG is in operation each

day; η_{BMG} refers to the total conversion efficiency of a BMG, while converting biomass to electrical energy.

Further, the BMG energy output ($E_{BMG}(t)$) may be computed as follows [3]:

$$E_{BMG}(t) = BMG_p^o(t) \times \Delta t \quad (3.7)$$

3.2.4. Biogas Generator (BGG) System

The BGG system output power is calculated as [3]:

$$BGG_p^o(t) = (Q_{BGG} \times C_{BGG} \times \eta_{BGG} \times 1000)/(365 \times 860 \times H_{BGG}) \quad (3.8)$$

Where; $BGG_p^o(t)$ denotes the power output of BGG; Q_{BGG} represents the amount of available biogas per day, C_{BGG} indicates the calorific value of biogas, and η_{BGG} indicates the efficiency with which biogas may be converted into energy. BGG daily operation hours are denoted by the H_{BGG} notation.

Electricity generated by BGG ($E_{BGG}(t)$) can be determined as follows:

$$E_{BGG}(t) = BGG_p^o(t) \times \Delta t \quad (3.9)$$

3.2.5. Battery Energy Storage System (BESS)

The battery is charged with the excess energy whenever the energy generation is greater than the ED. At the stage in which the battery is being charged, its capacity may be determined as follows [3]:

$$E_b(t) = (1 - \gamma) \times E_b(t-1) + e_{xm}(t) + e_{xg}(t) + e_{xpv}(t) \times \eta_{charging} \quad (3.10)$$

Where; γ is the rate at which the battery discharges itself, and $E_b(t)$ indicates the amount of energy that is stored in the battery. $e_{xpv}(t)$, $e_{xm}(t), e_{xg}(t)$ each represent the extra

energy generated by the SPV, BMG, and BGG systems, respectively. Charging efficiency is denoted by $\eta_{charging}$.

When ED is more than energy generation, the energy shortfall will be made up by the battery. The capacity of the battery is measured while it is being discharged as [3]:

$$E_b(t) = (1-\gamma) \times E_b(t-1) - \frac{e_{df}(t)}{\eta_{inverter} \times \eta_{discharging}} \quad (3.11)$$

Where, discharging and inverter efficiency are, symbolizes as $\eta_{discharging}$ and $\eta_{inverter}$ respectively. $e_{df}(t)$ is an unmet ED.

3.2.6. Utility Grid

When the ED is higher than the energy supply and the minimum BESS capacity the power will be drawn from the grid, and it can be determined as [140]:

$$e_{gp}(t) = e_d(t) - \Big(E_{BGG}(t) + E_{BMG}(t) + E_W(t) + E_{pv}(t) + (E_b(t) - E_{bmn})\Big) \times \eta_{inverter} \quad (3.12)$$

Where; $e_{gp}(t)$ is the power drawn from grid; $e_d(t)$ denotes hourly ED; E_{bmn} indicates the minimum capacity of battery.

When the ED is lower than the energy generation and BESS is fully charged, the power will be fed to the grid, and it can be determined as:

$$e_{gs}(t) = (E_{BGG}(t) + E_{BMG}(t) + E_W(t) + E_{pv}(t) - (E_{bmx} - E_b(t) \times \eta_{inverter}) - e_d(t) \quad (3.13)$$

Where; $e_{gs}(t)$ represents the energy sold to grid; E_{bmx} is maximum capacity of battery.

3.3 ENERGY COST MODEL

In performing an economic evaluation of the HRES, the NPC is a vital parameter under examination in the ongoing research. As a result, mathematical formulations for calculating the NPC of diverse components within the HRES have been formulated and will be expounded upon in the subsequent sections.

3.3.1. SPV Panels

For this study, the lifespan of the project was assumed to be the same as that of the SPV panels. In addition, the irradiance of the sun may be used as a fuel to create energy, which does not cost anything. As a result, there will be no expenses involved with replacement and fuel. Hence, the NPC of SPV panels (npc_{pv}) is comprised of the CC, OMC and the salvage values (SV) of SPV system. Thus, NPC for SPV system can be determined as follows [139]:

$$npc_{pv} = pv_{CC} + pv_{OMC} - pv_{SV} \tag{3.14}$$

Where, CC of SPV is denoted by pv_{CC}; pv_{OMC} represents OMC of SPV; and pv_{SV} indicates the SV of SPV.

The CC of SPV panels has been calculated as:

$$pv_{CC} = N_{pv} \times \psi_{pv} \times PV_p^o(t) \tag{3.15}$$

Where; ψ_{pv} is the startup cost of a single SPV panel expressed in dollars ($) per kW; N_{pv} denotes number of SPV panels; $PV_p^o(t)$ represents the power output of a single SPV panel expressed in kW/panel.

In addition, the OMC of SPV panels has been calculated using the following equation:

$$pv_{OMC} = \omega_{pv} \times N_{pv} \times PV_p^o(t) \times \sum_{i=1}^{\mu} \left(\frac{1+\zeta_{pv}}{1+r}\right)^i \quad (3.16)$$

The OMC of SPV panel ($/kW/year), escalation rate, and interest rate of SPV panels are denoted by ω_{pv}, ζ_{pv}, r respectively; μ denotes the total number of years in which the project will run. Further, the resale value of SPV panels after completing the project life known as SV has also been considered and determined as follows [65]:

$$pv_{SV} = \varepsilon_{pv} \times N_{pv} \times \left(\frac{1+\lambda}{1+r}\right)^{\mu} \times PV_p^o(t) \quad (3.17)$$

Where; ε_{pv} is the resale price of SPV panel measured in $/kW after the panels have reached the end of their estimated life and λ indicates the annual inflation (0.05).

3.3.2. WT

The NPC of WT (npc_{wt}) comprised mainly of CC (WT_{CC}), OMC (WT_{OMC}), SV (WT_{SV}) and can be computed as [139]:

$$npc_{wt} = WT_{CC} + WT_{OMC} - WT_{SV} \quad (3.18)$$

Furthermore, the CC of WTs, denoted by the WT_{CC} and can be determined by employing the equation below:

$$WT_{CC} = N_W \times \psi_w \times W_p^o(t) \quad (3.19)$$

Where, ψ_w is the initial cost of the WT expressed in $/kW.

The following formula has been utilized to calculate the OMC for WT [65]:

$$WT_{OMC} = \omega_w \times N_W \times W_p^o(t) \times \sum_{i=1}^{\mu} \left(\frac{1+\zeta_w}{1+r}\right)^i \quad (3.20)$$

In this, ω_w and ζ_w represent the yearly OMC of WT in \$/kW/year and the inflation rate of WT respectively.

The SV of WT also known as the resale value of components after their entire life is evaluated using the following equation.

$$WT_{SV} = \varepsilon_w \times W_p^o(t) \times \left(\frac{1+\lambda}{1+r}\right)^{\mu} \quad (3.21)$$

Where, ε_W is the resale price of the WT expressed in \$/kW.

Since the lifespan of WT is same as the project lifetime (25 years), their RC is assumed to be zero. Additionally, FC is also zero since wind is act as fuel which is available free of cost. Therefore, when analyzing NPC, these expenses are not considered.

3.3.3. BMG

The NPC of the BMG system is assessed by considering the CC, OMC, FC, and SV which are represented by $bmg_{CC}, bmg_{OMC}, bmg_{FC}, bmg_{SV}$. The NPC of the BMG system can be calculated as [3]:

$$npc_{bmg} = bmg_{CC} + bmg_{OMC} + bmg_{FC} - bmg_{SV} \quad (3.22)$$

$$bmg_{CC} = BMG_p^o(t) \times \psi_{BMG} \quad (3.23)$$

Where; npc_{bmg} denotes NPC of BMG; the ψ_{BMG} is the initial cost of the BMG system expressed in \$/kW. Further, the following formula is utilized to determine NPC of the OMC associated with the BMG:

$$bmg_{OMC} = \omega_{f\_bmg} \times BMG_p^o(t) \times \sum_{i=1}^{\mu}\left(\frac{1+\zeta_{bmg}}{1+r}\right)^i + \omega_{v\_bmg} \times p_{a\_bmg}^w \times \sum_{i=1}^{\mu}\left(\frac{1+\zeta_{bmg}}{1+r}\right)^i \quad (3.24)$$

Where, yearly fixed, and variable OMC of the BMG system is denoted by ω_{f_bmg} and ω_{v_bmg} respectively. The value represented by $p^{w}_{a\_bmg}$ is the annual power of the BMG system expressed in kWh/year. The escalating rate of the BMG system is denoted by the symbol ζ_{bmg}.

Furthermore, the following equation is utilized to calculate the SV of BMG system:

$$bmg_{SV} = \varepsilon_{bmg} \times BMG^{o}_{p}(t) \times \left(\frac{1+\lambda}{1+r}\right)^{\mu} \quad (3.25)$$

Where; ε_{bmg} is the value of reselling the BMG system expressed in $/kW.

The FC has been determined by considering the price of the biomass fuel and the amount of biomass that is required annually and is presented as:

$$bmg_{FC} = \varphi_{bmg} \times Q_{BMG} \times \sum_{i=1}^{\mu} \left(\frac{1+\zeta_{bmg}}{1+r}\right)^{i} \quad (3.26)$$

Where; φ_{bmg} represents the cost of using biomass as a fuel in $/ tons

3.3.4. BGG

By following the same methodology of the BGG system, The NPC of the BGG system abbreviated by npc_{bgg} may be estimated as follows [139]:

$$npc_{bgg} = bgg_{CC} + bgg_{OMC} - bgg_{SV} + bgg_{FC} \quad (3.27)$$

In this case, the total CC of the BGG system (bgg_{CC}) can be calculated as

$$bgg_{CC} = BGG^{o}_{p}(t) \times \psi_{bgg} \quad (3.28)$$

Where; ψ_{bg} is the initial cost of the BGG system expressed in $/kW. In addition, the following formula may be used to determine the OMC associated with the BGG system:

$$bgg_{OMC} = \omega_{f\_bgg} \times BGG_p^o(t) \times \sum_{i=1}^{\mu} \left(\frac{1+\zeta_{bgg}}{1+r}\right)^i + \omega_{v\_bgg} \times p_{a\_bgg}^w \times \sum_{i=1}^{\mu} \left(\frac{1+\zeta_{bgg}}{1+r}\right)^i \quad (3.29)$$

Where, annual fixed and variable OMC of the BGG system is denoted by ω_{f_bgg} and ω_{v_bgg} respectively. The annual operating power of the BGG system is symbolized by the acronym $p_{a\_bgg}^w$ and is expressed in kWh/year. The BGG system's escalation rate is denoted by ζ_{bgg}.

Furthermore, the NPC of the reselling of the BGG (bgg_{SV}) has been calculated as follows:

$$bgg_{SV} = \varepsilon_{bgg} \times BGG_p^o(t) \times \left(\frac{1+\lambda}{1+r}\right)^{\mu} \quad (3.30)$$

Where; ε_{bgg} is the selling price of the BGG system expressed in \$/kW.

By taking the cost of the biogas fuel and the amount of annual biogas required into the account, the FC of BGG system is obtained as:

$$bgg_{FC} = \varphi_{bgg} \times bgg_{yearly} \times \sum_{i=1}^{\mu} \left(\frac{1+\zeta_{bgg}}{1+r}\right)^i \quad (3.31)$$

Where; bgg_{FC} denotes the FC of BGG; φ_{bgg} and bgg_{yearly} stands for the annual biogas FC in \$/m^3 and annual amount of biogas that must be produced respectively.

The NPC of revenue re_{bg} generated by the organic manure in case of the BGG system has also been taken into consideration and calculated as follows:

$$re_{bgg} = M_{bgg} \times d_{bgg} \times \sum_{i=1}^{\mu} \left(\frac{1+\zeta_{bgg}}{1+r}\right)^i \quad (3.32)$$

Where; M_{bgg} and d_{bgg} represent the cost of generated manure in $/tons and the annual quantity of manure produced in tons per year respectively.

3.3.5. BESS

The NPC of the BESS includes the CC the OMC, RC, SV and it may be calculated as follows [139]:

$$npc_B = B_{CC} + B_{OMC} + B_{RC} - B_{SV} \quad (3.33)$$

$$B_{CC} = N_B \times \psi_B \quad (3.34)$$

$$B_{OMC} = \omega_B \times N_B \times \sum_{i=1}^{\mu} \left(\frac{1+\zeta_B}{1+r}\right)^i \quad (3.35)$$

$$B_{SV} = \varepsilon_B \times N_B \times \left(\frac{1+\lambda}{1+r}\right)^{\mu} \quad (3.36)$$

Where; N_B indicates the number of batteries; ψ_B represents the cost of single battery in $. ω_B and ζ_B represent the yearly OMC of batteries in $ each year and the escalation rate respectively. The resale price of single battery is represented by the symbol ε_B. Within the scope of this research, the expected lifespan of the battery (μ_B) is set at 5 years, which is much shorter than the expected lifetime of the project, which has been set at 25 years as a result, the battery has to be changed once it has been in use for five years. The number of instances a battery has to be replaced (n_{rb}) can be calculated as follows:

$$n_{rb} = \frac{\mu}{\mu_B} - 1 \quad (3.37)$$

Where, Life of battery is denoted by μ_B in years.

The following equation is used to determine the RC of battery (B_{RC}):

$$B_{RC} = N_B \times \psi_B \times \sum_{i=5,10,15,20} \left(\frac{1+\zeta_B}{1+r}\right)^i \quad (3.38)$$

3.3.6. Inverter

The NPC of the inverter $\mathrm{npc}_{\mathrm{inverter}}$ has been evaluated as [3]:

$$npc_{inverter} = I_{CC} + I_{OMC} + I_{RC} - I_{SV} \quad (3.39)$$

Where; I_{CC}, I_{OMC}, I_{RC}, and I_{SV} each indicate a CC, OMC, RC, and SV for the inverter, respectively.

$$I_{CC} = N_I \times \varphi_I \quad (3.40)$$

$$I_{OMC} = \psi_I \times N_I \times \sum_{i=1}^{\mu} \left(\frac{1+\zeta_I}{1+r}\right)^i \quad (3.41)$$

$$I_{SV} = \epsilon_I \times N_I \times \left(\frac{1+\lambda}{1+r}\right)^{\mu} \quad (3.42)$$

Where; ζ_I is the escalation rate; N_I represents number of inverters φ_I denotes cost of one inverter; ψ_I is the initial cost of the inverter expressed in $ /kW. The lifespan of the inverter, which has been estimated to be 10 years, is shorter than the duration of the project, which is 25 years. Hence, the RC of inverter can be expressed as:

$$I_{RC} = N_I \times \psi_I \times \sum_{i=10,20} \left(\frac{1+\zeta_I}{1+r}\right)^i \quad (3.43)$$

3.3.7. Grid Sale and Grid Purchase Capacity

The following formulae have been used to calculate the NPC of the grid sale (GS) and the grid purchase (GP) of power from or to the grid in the situation when the system is linked to the grid [3].

$$\in_G^S = \emptyset_G^S \times e_{gs} \times \sum_{i=1}^{\mu} I \tag{3.44}$$

$$\in_G^P = \emptyset_G^P \times e_{gp} \times \sum_{i=1}^{\mu} \left(\frac{1+\epsilon_g}{1+r}\right)^i \tag{3.45}$$

Where; $\in_G^S$ and $\in_G^P$ denotes NPC of GS and GP respectively; $\emptyset_G^S$ and $\emptyset_G^P$ are the unit costs of selling power to or purchasing power from the grid in $/kWh, respectively; e_{gs} denotes excess energy to be sold to grid (kWh); deficit energy to be purchased from grid (kWh) is represented by e_{gp}.

Finally, the *COE* of the HRES that has been suggested can be calculated as:

$$COE = \frac{NPC \times C_r^f}{E_a^d + e_{gs}} \tag{3.46}$$

Where; E_a^d is an annual ED expressed in kWh/year and e_{gs} denotes extra energy sold to grid; capital recovery factor is denoted by C_r^f and has been calculated as:

$$C_r^f = \frac{r(1+r)^{\mu}}{r(1+r)^{\mu}-1} \tag{3.47}$$

To calculate the total NPC of the HRES, the following formula has been used:

$$NPC = npc_{pv} + npc_{wt} + npc_{bmg} + npc_{bgg} + npc_B + npc_{inverter} + \in_G^P - \in_G^S \tag{3.48}$$

3.4 POWER RELIABILITY MODEL

With regard to the reliability of the electrical supply, the possibility of LPSP has been considered in this research. When the ED exceeds the energy generation, a user face

non-availability of power. The LPSP can be determined by utilizing the following expression [3].

$$\text{LPSP} = \sum_{t=1}^{t=8760} \left(\frac{\text{Unmet load for one year}}{\text{Total load for one year}} \right) \quad (3.49)$$

3.5 CONCLUSION

This chapter presents the mathematical modelling of various components including SPV, wind, BMG, BGG, BESS for design and development of HRES. In addition, the energy cost models of all the HRES components along with GP and GS. Further, the reliability model has been presented so that these can be utilized for optimization purpose in subsequent chapters.

CHAPTER 4

FEASIBILITY AND TECHNO-ECONOMIC ANALYSIS OF HRES

4.1 INTRODUCTION

In the previous chapter, the mathematical modelling of different components of HRES has been presented, which served as the basis for developing the hybrid models. However, before proceeding with the development of the HRES model, it is crucial to accurately estimate the potential of RES and assess the load demands of the selected sites. This chapter focuses on conducting a feasibility analysis based on the availability of RES and load demands of the selected sites. By conducting the feasibility analysis, the goal is to identify the most viable HRES model in terms of both technical and economic considerations. Among various combinations of RES, the model that demonstrates the highest feasibility, based on the techno-economic analysis has been selected for implementation in the considered sites. To facilitate this process, the HOMER Pro software has been utilized to develop the hybrid models. The primary objective of these HRES is to meet the electrical load requirements of the selected households, Panchayat Ghar, Gramin health care centres, schools, and other relevant facilities, etc. which have been computed considering the present and future load requirements [3].

By analyzing the feasibility of resources, load demands, and conducting techno-economic evaluations, this chapter provides valuable insights into the development of cost-effective and reliable hybrid models for the selected sites. The utilization of the HOMER

software allows for accurate optimization and assessment of the systems' NPC and COE, ensuring an effective and sustainable implementation of HRES [3].

4.2 DESCRIPTION OF SELECTED SITES

The selection of suitable sites for the implementation of a hybrid model is of paramount importance. Consequently, for this study, careful consideration was given to sites with significant potential of various RES. Two distinct locations in the Indian states of Uttar Pradesh and Haryana were chosen to develop the HRES.

4.2.1. Study Area I

Uttar Pradesh is a state located in the northern part of India. With a population of over 200 million people, it is the most populous state in India and the fourth largest in terms of land area. Geographically, it is located in between latitude 24°-31°N and longitude 77°-84°E with an area of 243290 km^2. There is an average population density of 828 persons per km^2. Uttar Pradesh has 106747 villages and is agriculturally rich, with a massive portion of its population engaged in farming. The state is known for its production of wheat, rice, sugarcane, potatoes, and fruits. It also has a growing industrial sector, particularly in cities like Kanpur, Agra, and Noida, which contribute to the state's economy [141]. The installed capacity and potential of RES based power generation in the state as per Ministry of New and Renewable Energy (MNRE) is given in Table 4.1 [142]. From Table 4.1, it has been observed that there is immense potential of RES in the state that needs to be harnessed to provide continuous supply and help in government initiatives like Power to All, Green and Clean energy, Sustainable Energy etc. Further, the Agra district in Uttar Pradesh is situated at latitude of 27.11^o latitude North and 78^o to 78.2^o longitude east.

Table 4. 1: RES Potential and Installed Capacity of Uttar Pradesh State

RES	Potential of RES (GW)	Installed capacity (GW)
Solar	2.2830	2.016
Bio Power	3.757	2.216
Small Hydro	0.522	0.049
Wind	1.260	--
Total	28.369	4.781

Its altitude is 169 m above sea level. According to Census, it is 10863 km^2 with population of 4418797. The district is divided into six tehsils and 15 blocks. It has total 906 populated villages and is agriculturally rich, with a huge portion of its population engaged in farming. Total of four villages which are in close vicinity in Etmadpur block of the Agra, district and experienced frequent power cuts and fluctuations, has been chosen as study area I with total 248 households which are still not having electricity connections [141]. Geographical representation of this area has been illustrated in Fig. 4.1 and the general information has been provided in Table 4.2 [141, 143].

Table 4. 2 Geographical and Census Data of the Study Area I [141, 143]

Description	General information			
Country, State	India, Uttar Pradesh			
District,Subdivision	Agra, Etmadpur			
Village	Sarai Jairam	Nagla Beal	Nagla Pachauri	Barhan
Latitude	27.34° N	27.36° N	27.88° N	27.33° N
Longitude	78.17° E	78.16° E	78.95° E	78.19° E
Population	2008	2881	1331	17365
Total households	332	518	213	2798

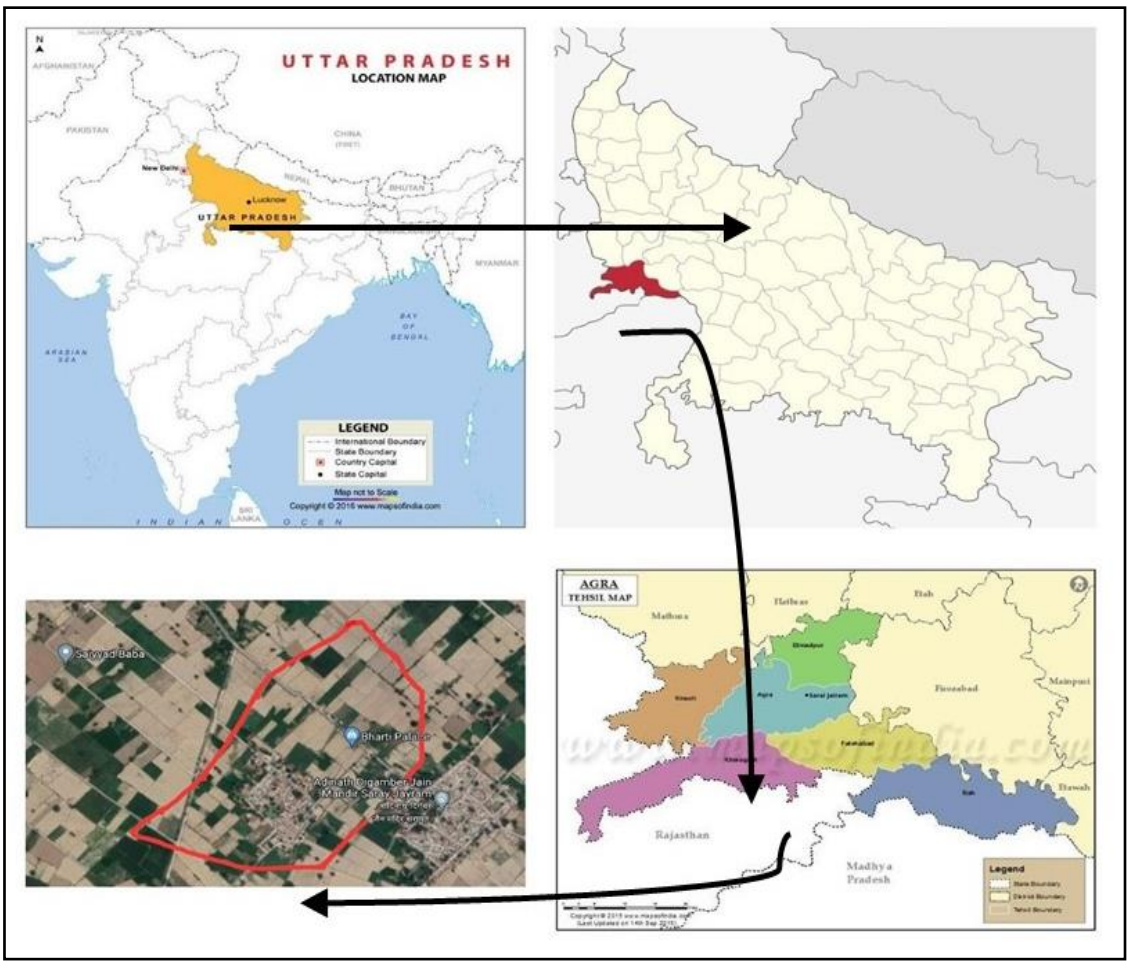

Fig. 4.1 Geographical Map of the Study Area I [143]

4.2.2. Study Area II

Haryana, a state abundant in agriculture, is geographically situated between latitudes 27.39°N-30.35°N and longitudes 74.28°E-77.36°E. Spanning an area of 44,212 square kilometers, it is divided into twenty-one districts. With a population of 25,351,462, Haryana accounts for approximately 2% of the nation's total population. The majority, around 76%, reside in rural areas. Within these rural regions, there are a total of 3,418,025 households, many of which still encounter the challenge of inadequate power supply [144].

Moreover, the electrified rural areas in Haryana face a scarcity of electricity, with availability limited to few hours only. This situation arises from a range of factors such as inadequate infrastructure, electricity theft, reluctance among local residents to pay their electricity bills, and more. It is noteworthy that a massive portion of the state's economy relies on sectors like agriculture and industries, which necessitate a stable supply of electricity. The installed capacity and RES potential for power generation in the state, as reported by the Ministry of New and Renewable Energy (MNRE), can be found in Table 4.3 [142].

Table 4. 3 RES Potential and Installed Capacity of Power Generation in Haryana

RES	**Potential of RES (GW)**	**Installed capacity (GW)**
Solar	4.560	1.362
Bio Power	1.683	0.259
Small Hydro	0.110	0.073
Wind	0.093	--
Total	6.470	1.694

Based on the results presented in Table 4.3, Haryana state possesses a substantial capacity for harnessing RES. Utilizing this potential can not only ensure a consistent and uninterrupted power supply but also align with governmental objectives such as Power to All, Green and Clean Energy, and Sustainable Energy initiatives.

Mewat district, situated within latitudes 26° N to 30° N and longitudes 76° E to 78° E, encompasses five blocks and a total of 431 villages. Geographically, it spans an area of 1507 km^2, with 1441.71 km^2 occupied by rural population and the remaining 65.29 km^2 inhabited by the urban population [144]. Data collection indicates that households in this area continue to face challenges with reliable power supply, experiencing frequent power cuts. Therefore, a group of four villages with 369 households situated in the Mewat district

has been considered as study area II. The investigation revealed that the selected area lacks a consistent power supply. During the summer season, these areas receive electricity for 6-7 hours, while in the winter season, the duration extends to 8-10 hours. Furthermore, the increasing pollution is leading to a rise in GHG emissions. Consequently, there is requirement for power generation systems that can offer uninterrupted supply to fulfill the Indian Government's objectives of "Power to All," with its availability 24 x 7, "Green and Clean Energy," and other related initiatives. Implementing such systems would not only address the power needs but also contribute to reducing pollution levels. Further, the geographical representation of the given region is depicted in Fig. 4.2, and additional general information is presented in Table 4.4 [144]

Table 4. 4 Geographical and Census Data of the Selected Area II

Description	**General information**			
Country, State, District, Block	India, Haryana, Mewat, Taoru			
Village	Population	Total households	Latitude	Longitude
Silkhoh	3467	596	28.15° N	76.96° E
Thana	786	399	28.17° N	76.95° E
Nanuka	399	110	28.16° N	76.94° E
Noorpur	514	146	28.39° N	77.04° E

4.3 ESTIMATION OF RES AT SELECTED SITES

The estimation of available RES potential and load demand was conducted by collecting data through site visits. To assess the capability of generating efficient and reliable power, a standard methodology, widely adopted by several researchers [145-146], was employed. The potential of RES for each study area has been analyzed and discussed in the subsequent sections [145-146].

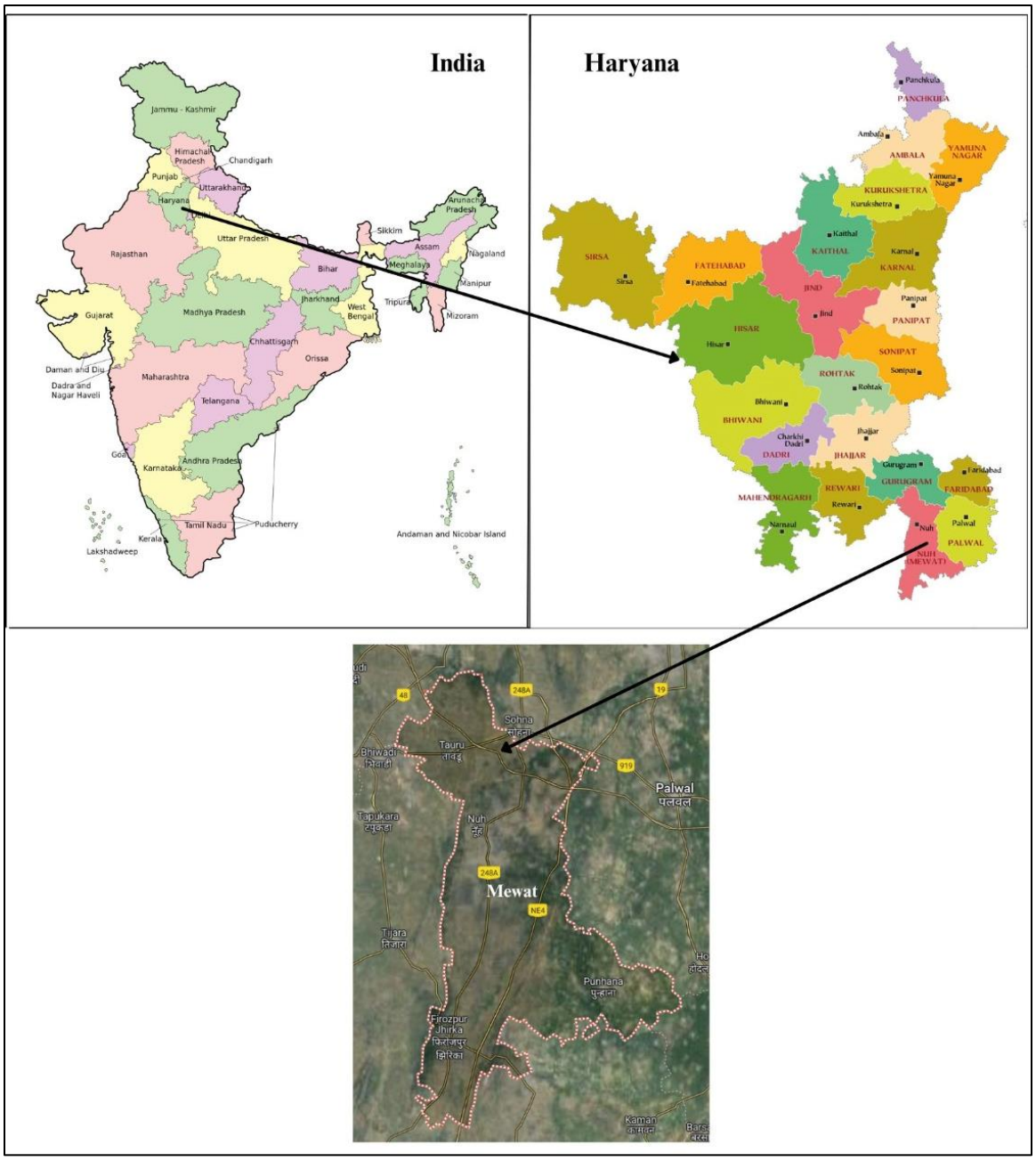

Fig. 4.2 Geographical Representation of the Study Area II [144]

4.3.1. RES Potential at Study area I

The potential of available RES i.e., solar, wind, biomass at study area I is given below:

Solar energy: Solar radiation is in abundant that can be harnessed for power generation. India receives a significant amount of solar radiation due to its geographical location. According to data obtained from the Indian Meteorological department, the country experiences approximately 250 to 300 sunny days in a year, indicating the immense potential for solar energy utilization.

To design and develop a SPV system, it is crucial to estimate the amount of solar radiation in a specific area. This information helps in determining the potential of solar energy generation and optimizing the size and configuration of the SPV system. The solar radiation data for different months for the proposed site is presented in Table 4.5. From the analysis of Table 4.5, it is evident that the village Sarai Jairam exhibits the highest annual average solar daily radiation of 5.25 kWh/m^2/day compared to the other villages considered in the study. This indicates that Sarai Jairam has the highest potential for solar energy generation among all the selected sites [147].

The annual average GHI at the selected site is 5.25 kWh/m^2/day, which is quite favorable for efficient power generation using solar energy. It signifies that the site receives an ample amount of solar radiation throughout the year, making it suitable for the installation of SPV system. Furthermore, the analysis of the monthly solar radiation data reveals that the month of May experiences the highest solar radiation with a value of 6.79 kWh/m^2/day, indicating the peak solar energy potential during that period. On the other hand, the month of December witnesses the lowest solar radiation with a value of 3.71 kWh/m^2/day, indicating the least amount of solar energy available during that time.

Table 4. 5 Monthly Solar Radiation Data at the Proposed Site I

Month	Daily solar radiation (kWh/m^2/day)			
	Sarai Jairam	**Nagla Beal**	**Nagla Pachauri**	**Barhan**
January	3.97	3.97	3.84	3.71
February	4.62	4.63	4.62	4.75
March	5.68	5.68	5.57	5.49
April	6.31	6.23	6.38	6.40
May	6.79	6.78	6.54	6.99
June	6.56	6.53	6.63	6.59
July	5.40	5.39	5.29	5.32
August	5.09	5.10	5.08	5.10
September	5.46	5.45	5.47	5.40
October	5.17	5.09	5.30	5.12
November	4.26	4.23	4.19	4.10
December	3.71	3.76	3.83	3.40
Average	5.25	5.24	5.23	5.20

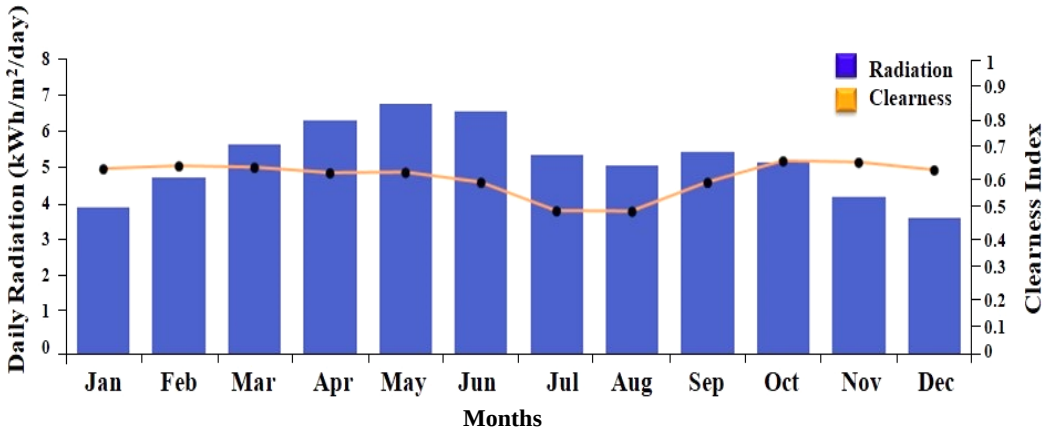

Fig. 4.3 Daily Average GHI for the Proposed Site [147]

To visualize the variation of GHI at the proposed site, Fig. 4.3 illustrates the graphical representation of the solar radiation data which provides a visual understanding of how the solar radiation levels fluctuate throughout the year at the selected site. Further, the annual solar energy potential (E_{PV}) of the selected site has been estimated as 1916 kWh/m^2/year using following equation.

$$E_{PV} = Q_{PV} \times 365 \quad (4.1)$$

Where, Q_{PV} is an annual average solar daily radiation (5.25 kWh/m^2/day)

Wind energy: Wind energy is a RES that can be harnessed to generate electricity using WT. In India, small WT, also known as aero generators, are typically designed to operate efficiently at wind speeds up to or around 10 m/s.

In the present study, the monthly wind speed data for the proposed site, as depicted in Fig. 4.4, indicates that the average annual wind speed at the selected area is 3.27 m/s. This wind speed is relatively low for efficient power generation using wind energy [148].

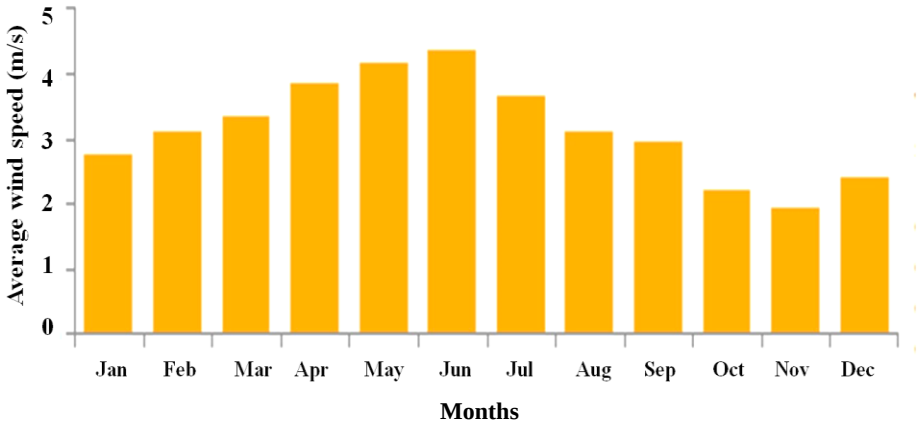

Fig. 4.4 Monthly Wind Speed at the Proposed Site I [148]

Considering the low wind speeds observed at the site, it has been determined that wind energy is not a viable source for power generation in the study area I. Therefore, in the context of this study, wind energy has not been considered as a significant source for electricity production at the selected site [148].

Biomass: Biomass is indeed a valuable and abundant source of energy, particularly in rural areas where crop residues and woody biomass are readily available. In the present

study, the focus is on the biomass potential of crop residues, specifically the residues from wheat and rice crops, in study area I [149].

Based on the grain productivity, crop residue ratio and collection efficiency of 50%, the annual availability of the biomass potential (Q_{BMG}) has been computed using equation 4.2, 4.3 and is presented in Table 4.6 [145].

$$Q_{BMG} = N_{CR} \times S_{CR} \times 0.001 \quad (4.2)$$

Where, N_{CR} is the gross crop residue available (kg/year) and S_{CR} is surplus crop residue fraction. The value 0.001 is used to adjust the unit of gross crop residue from kg to ton. Further, the gross crop residue of crop has been estimated as [146]:

$$N_{CR} = \mathrm{C}_{IA} \times \mathrm{C}_{Y} \times \mathrm{C}_{RR} \quad (4.3)$$

Where, C_{IA} represents crop irrigated area in hectare; C_{Y} is crop yield in kg/hectare; C_{RR} is crop residue ratio. The crop residue ratio is the ratio of residue yield (ton/hectare) to the crop yield (ton/hectare).

Table 4. 6 Biomass Potential from Crop Residue at Study Area I

Description	**Wheat**
Study area I	2248.64
Total irrigated area (hectare), C_{IA}	2248.64
Average production of crop (tons/hectare), C_{Y}	1.09
Grain productivity (ton), $\mathrm{C}_{IA} * \mathrm{C}_{Y}$	2451
Crop to residue ratio, C_{RR}	1.31
Availability of gross crop residue (tons/year), $N_{CR} = \mathrm{C}_{IA} \times \mathrm{C}_{Y} \times \mathrm{C}_{RR}$	3210.83
Surplus residue fraction, S_{CR}	0.5
Total surplus crop residue (tons/year), $N_{CR} * S_{CR}$	1605.42
Total biomass available (tons/year)	1605.42
Annual energy potential (kWh/year)	14,59,469

Based on the estimation of biomass potential from crop residues in study area I, the total biomass availability is calculated to be 1605.42 tons/year It is assumed that 0.0011 tons of biomass are required to generate 1 kWh of electricity [146]. Using this conversion factor, the total annual energy potential from biomass in study area I is determined to be 1,459,469.57 kWh/ year This indicates the significant energy potential that can be harnessed from the biomass resources available in the given area. By utilizing biomass for electricity generation, the study area can contribute to renewable energy production and reduce dependence on fossil fuels. Further, the Fig. 4.5 depicts the availability of biomass at selected site for study area I.

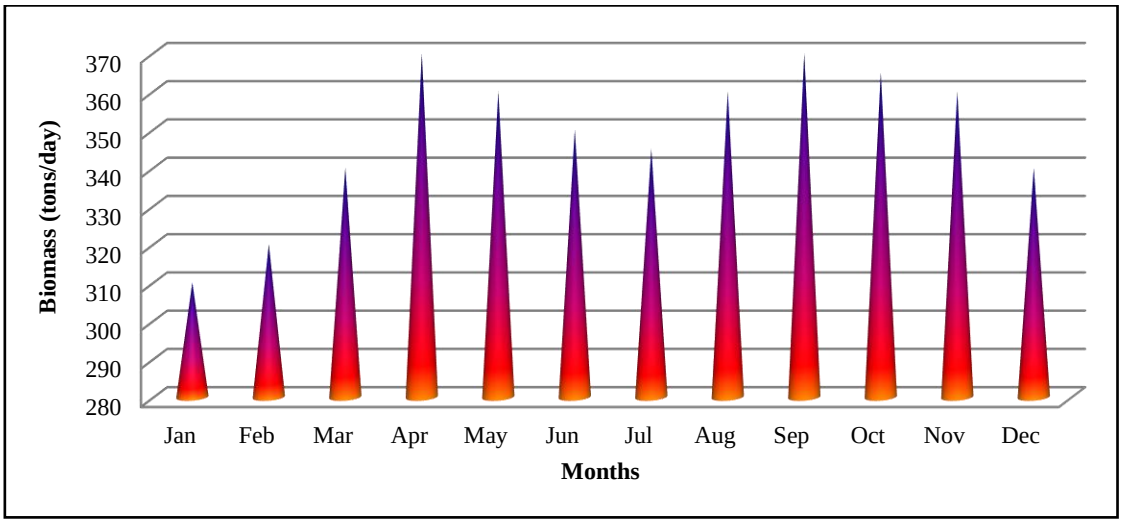

Fig. 4.5 Availability of Biomass at Selected Site [145]

Biogas: Biogas systems offer a renewable and sustainable energy solution by using organic waste materials and converting them into usable energy. They supply an environmentally friendly alternative to traditional fossil fuel-based power generation and helps in reducing GHG emissions.

The biogas system utilizes anaerobic digestion to convert organic materials such as animal dung, food waste, or human sewage into biogas. This process involves the use of bacteria to break down the organic matter in the absence of oxygen, resulting in the production of biogas.

The biogas produced typically consists of methane (CH_4) in the range of 50-60% and carbon dioxide (CO_2) in the range of 30-40%. It may also contain small amounts of other gases and impurities. The biogas can be used as a fuel for various purposes, including power generation. To evaluate the biogas potential in study area I, the animal dung obtained from different animals such as buffaloes, cows, sheep, and goats is considered. The biogas potential is calculated based on the number of animals and their corresponding dung production [150].

The calculation of biogas potential is typically done using the following formula [150]:

$$P_{BG} = C_D \times Y_{BG} \quad (4.4)$$

Where, P_{BG} is biogas potential; C_D is cattle dung availability (kg/day); Y_{BG} is biogas yield (m^3/kg).

The availability of cattle dung at the study area I is about 106959 kg/day. The biogas production evaluation is based on the cattle dung obtained from different animals and it is estimated that 1 kg of cow and buffalo dung can produce 0.036 $m^3$of biogas, whereas sheep and goat produce 0.070 m^3 and 0.078 m^3 respectively [145]. By assuming 50% collection efficiency, the availability of biogas in the study area I is computed as 1899.40 m^3/day. Further, it is estimated that 0.5 m^3 of biogas can produce one kWh of electricity. Thus, the annual energy potential of selected site is calculated as 3798.8 kWh/day and 13,86,562 kWh/year.

Further, the total annual energy potential of different RES at the study area I is estimated and given in Table 4.7

Table 4. 7 Estimated Potential of Different RES in Study Area I

Sr. No.	RES	Annual energy potential
1	Solar energy	1916 kWh/m^2/year
2	Biomass	14,59,469 kWh/year
3	Biogas	13,86,562 kWh/year

Based on Table 4.7, it is observed that study area I has significant potential of different RES, including biomass, biogas, and solar energy. Among these, biomass is identified as having the highest potential, followed by biogas and solar energy. The village of Sarai Jairam is found to have the maximum potential for RES among all the villages in study area I. Therefore, Sarai Jairam village has been selected as the ideal location for the installation of an HRES.

4.3.2. RES Potential at Study area II

In the study area II, a comprehensive investigation was conducted to gather data and estimate the potential of RES. The collected data aimed to provide a detailed understanding of the RES potential in the selected area, enabling the assessment of their feasibility and contribution to the energy requirements.

Solar energy: Monthly average solar radiation data from the National Aeronautics and Space Administration (NASA) has been collected for study area II. The data, presented in Fig. 4.6, provides valuable insights into the solar potential of the area. Based on the data obtained, it is observed that all villages in study area II receive the same amount of average daily solar irradiance, which is 5.26 kWh/m^2/day. This indicates that the solar radiation levels are consistent across the villages, and any one of the four villages can be selected for

solar power generation. Furthermore, the data shows that the highest solar radiation of 6.722 kWh/m^2/day occurs in June, while the lowest radiation of 3.534 kWh/m^2/day is recorded in December. These variations in solar radiation levels throughout the year are essential to consider when designing and optimizing SPV systems [147].

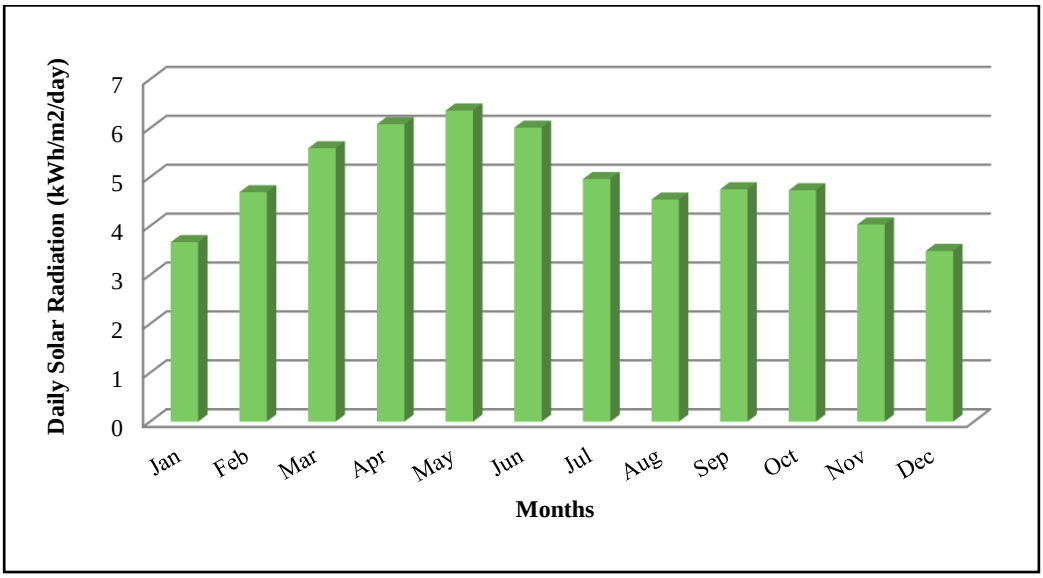

Fig. 4.6 Monthly Average Daily Solar Radiation of Study Area II [147]

Based on the annual average solar radiation, the annual energy potential from solar energy is calculated to be 1919 kWh/m^2/year. This estimation quantifies the amount of energy that can be potentially harvested from solar radiation in the study area II over the course of a year. The availability of consistent solar irradiance and the estimated annual energy potential demonstrate the viability and potential of solar energy as a renewable resource for power generation in study area II.

Wind energy: Based on the data collected, Silkhoh village is found to be suitable for wind power generation in study area II. The average annual wind speed at this site is recorded as 4.436 m/s, with a wind power density of 124 W/m^2. This indicates that Silkhoh village has favorable wind conditions for harnessing wind energy.

The availability of average wind speeds for each month at the selected site is illustrated in Fig. 4.7. It is observed that the highest average wind speed of 4.994 m/s occurs in the months of September and October, while the lowest wind speed of 3.275 m/s is recorded in November. These variations in wind speeds throughout the year are key factors to consider when designing wind power systems. The annual energy potential (E_W) from wind energy is evaluated as 1086 kWh/m^2/year by using equation (4.5).

$$E_W = P_D \times 365 \times 24 \qquad (4.5)$$

Where, P_D is wind power density of the given area (kW/m^2)

This estimation quantifies the amount of energy that can be potentially generated from wind resources in study area II over the course of a year. The suitability of Silkhoh village for wind power generation, along with the observed wind speeds and the calculated energy potential, highlights the potential of wind energy as a renewable resource for power generation in study area II [148].

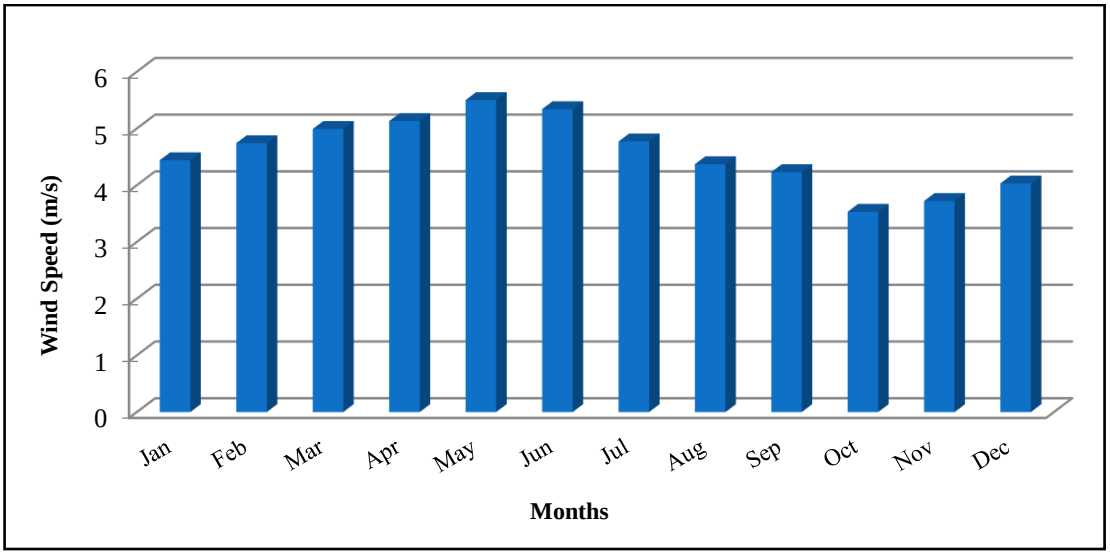

Fig. 4.7 Wind Speed Availability in the Study Area II [148]

Biomass: The total availability of crop residues at the selected sites is calculated to be 805 tons per year. This shows a significant quantity of biomass that can be utilized for energy

production through bio-generators. The annual energy potential from biomass is estimated as 731818 kWh/year. Further, the Fig. 4.8 depicts the availability of biomass at selected site for study area II [151].

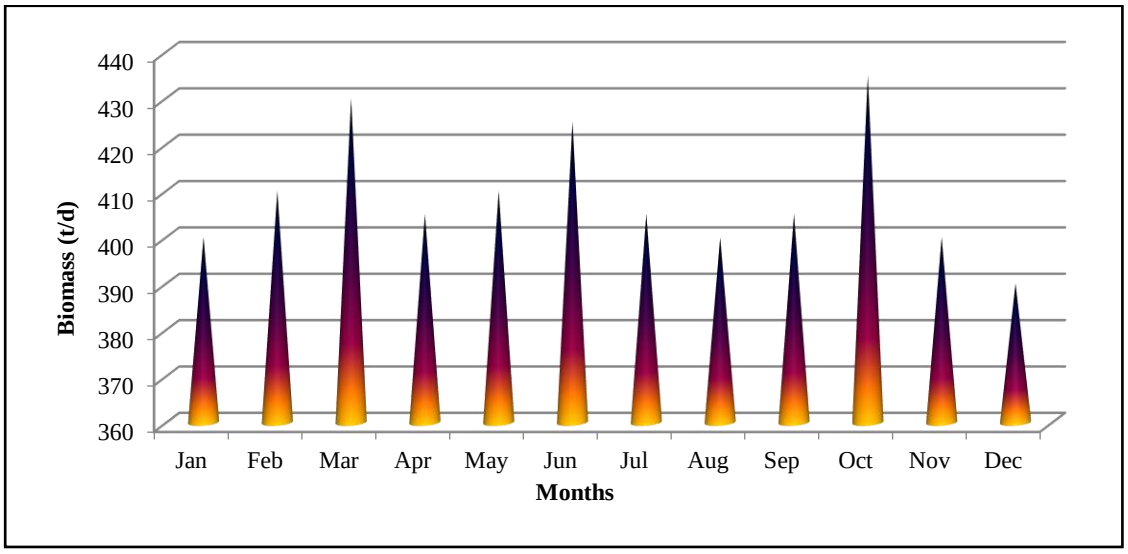

Fig. 4.8 Availability of Biomass at Selected Site for Study Area II [151]

Biogas: Based on the available data, it is figured out that the study area II has a substantial cattle population of 615, which has the potential to produce 236 m^3/day of biogas. This shows a significant amount of biogas production that can be harnessed from the cattle population in the area. Considering the biogas production potential from the cattle population, the annual energy potential from biogas is calculated to be 172280 kWh/year This estimation reflects the considerable energy generation potential that can be derived from biogas resources in study area II. Considering the various RES assessed in study area II, the potential of different RES is summarized in Table 4.8. Based on the analysis presented in Table 4.8, the selected site in study area II has significant potential for RES. This potential opens opportunities for the development of a renewable energy-based power

generation system in the region [151]. Considering the maximum availability of RES, Silkhoh village has been identified as the suitable location for the installation of the

Table 4. 8 Potential of RES at Study Area II

Sr. No.	RES	Annual energy potential
1	Solar energy	1919 kWh/m^2/year
2	Wind energy	1086 kWh/m^2/year
3	Biomass	731818 kWh/year
4	Biogas	172280 kWh/year

RES-based power production system. This selection is based on the understanding that Silkhoh village offers the highest potential for harnessing RES among the villages in the study area.

4.4 ASSESSMENT OF ELECTRICAL LOAD OF SELECTED SITES

In the present study, two specific study areas, as described in Section 4.2, have been selected for the development of HRES. To design the HRES for the electrification of these sites, the electrical load demand data has been collected by visiting the sites frequently and also taking into consideration the living standards of the local population, the type and number of electrical appliances used by them, and the daily operating hours of these appliances. The study areas experience a significant variation in average monthly temperatures, ranging from 4°C to 46°C throughout the year. These varying temperature and climatic conditions have an impact on the energy consumption patterns of various appliances. To account for these variations, the entire year has been subdivided into three seasons: summer season (April to July), moderate season (August to November), and winter season (December to March). This division allows for a more accurate representation of the load profiles and energy requirements for each season.

Additionally, the electrical load has been categorized into distinct types, including residential, commercial, municipal/governmental premises, and agricultural load. Each category represents a distinct set of ED associated with specific activities and infrastructure. By considering these load categories, the study accounts for the diversity of energy needs in the selected areas and ensures that the HRES design adequately address the requirements of each sector.

The detailed description of the load demand for each category, including the specific appliances, operating hours, and energy consumption patterns, is provided in the following sections of the study. This comprehensive understanding of the load demand allows for accurate sizing and optimization of the HRES components, ensuring that the system can reliably meet the energy requirements throughout the year while considering the specific climate and usage patterns of the study areas.

4.4.1. Residential Load

In the present study, the residential load for study area I and study area II has been estimated, including various electrical appliances commonly found in households. The load includes appliances such as LED lights, fans, refrigerators, televisions (TVs), coolers, mobile chargers, and water pumps. The residential load demand along with rating and operational hours of different appliances along with number of appliances has been presented in Table 4.9.

For study area I, the daily energy consumption during the summer, moderate, and winter seasons has been computed as 2101.62 kWh/day, 2085.66 kWh/day, and 1143.43 kWh/day respectively. The estimated annual residential load for study area I is 799,879.18 kWh/year. Among the villages in study area I, Barhan village has the highest residential

load, accounting for 67.86% of the total residential load. Sarai Jairam village follows with a contribution of 19%, Nagla Beal contributes 7.2%, and Nagla Pachauri village has the lowest contribution at 5.94%.

Table 4. 9 Residential Load Demand for Different Seasons

Appliances	**Rating (KW)**	**Quantity**	**Operating hours**			**Seasonal load (kWh/day)**		
			Summer season	Moderate season	Winter season	Summer season	Moderate season	Winter season
Water pump	0.5	1	1	1	1	0.5	0.5	0.5
Refrigerator	0.4	1	5	4	4	2	1.6	1.6
Cooler	0.3	1	5	5	0	1.5	1.5	0
Fan	0.075	2	18	14	0	2.7	2.1	0
LED TV	0.08	1	6	6	8	0.48	0.48	0.64
Mobile charger	0.018	1	5	4	4	0.09	0.072	0.072
LED light	0.02	2	18	18	18	0.072	0.72	0.72
Total energy requirement per day for (Study area I)						2101.62	2085.66	1143.43
Total energy requirement per day for (Study area II)						3140.51	2049.36	1162.14

Similarly, for study area II, the daily energy requirement during the summer, moderate, and winter seasons has been obtained as 3140.51 kWh/day, 2049.36 kWh/day, and 1162.14 kWh/day, respectively. The estimated annual residential load for study area II is 897,987.99 kWh/year. In study area II, Silkhoh village has the highest residential load, accounting for 61% of the total residential load and Nanuka village has the lowest contribution at 2 %.

The contribution of electrical appliances' load in the total residential load is illustrated in Fig. 4.9. Among the appliances, the refrigerator has the highest contribution, while the mobile charger has the lowest contribution. The fan load is the second-highest contributor to the residential load.

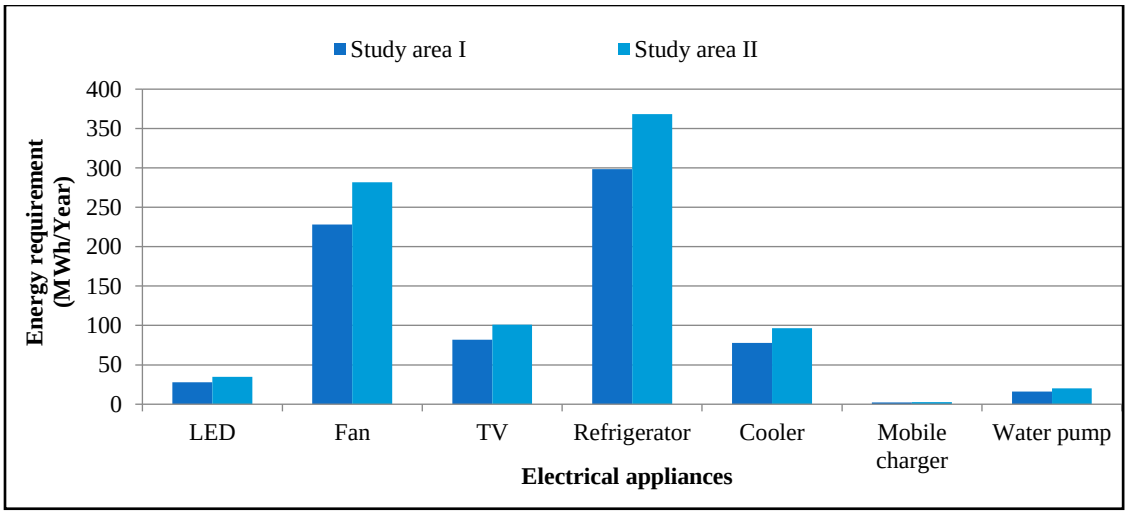

Fig. 4.9 Breakdown of Electrical Appliance Contributions in the Residential Load for Study Area I and II

4.4.2. Municipal/Governmental Buildings Load

In this work, the load demand for municipal/governmental buildings in study area I and II has been estimated. The load demand includes various facilities such as schools, Panchayat Ghar (village administrative center), Gramin health care center (rural health center), veterinary hospital, and streetlights. Table 4.10 presents the seasonal load demand for the municipal/government building along with the number and of appliances, their ratings and operational hours.

For study area I, the daily energy consumption during the summer, moderate, and winter seasons has been estimated as 107.09 kWh/day, 105.98 kWh/day, and 86.89 kWh/day, respectively. Fig. 4.10. shows the share of several types of loads in Municipal/Governmental buildings load for study area I.

Among the buildings, streetlights contribute the highest percentage of load demand, accounting for 27% in study area I. Veterinary hospital follows with a contribution of 23%,

Gramin health center with 21%, and school with 16%. The Panchayat Ghar has the lowest contribution of 13% in study area I. The estimated annual load for municipal/governmental buildings in study area I is 37,446.36 kWh/year.

Table 4. 10 Municipal/Governmental Buildings Load for Different Seasons

Load	Appliances	Rating (kW)	Quantity (no.)	Operating hours			Seasonal load (kWh/day)		
				Summer season	Moderate season	Winter season	Summer season	Moderate season	Winter season
Gramin Health Care Centre	LED light	0.012	6	10	10	12	0.72	0.72	0.864
	Fan	0.045	6	8	8	0	2.16	2.16	0
	Refrigerator	0.2	1	6	6	4	1.2	1.2	0.8
	Water heater	1	1	4	4	6	4	4	6
Panchayat Ghar	LED light	0.012	2	4	4	5	0.096	0.096	0.12
	Fan	0.045	2	8	6	0	0.72	0.54	0
Veterinary Hospital	LED light	0.012	2	10	10	12	0.24	0.24	0.288
	Fan	0.045	2	10	8	0	0.9	0.72	0
	Refrigerator	0.2	1	10	8	8	2	1.6	1.6
	Medical equipment	-	-	-	-	-	3.2	3.2	3.2
School	LED light	0.012	5	6	6	8	0.36	0.36	0.48
	Fan	0.045	5	8	6	0	1.8	1.35	0
	Submersible Pump	0.5	1	2	2	2	1	1	1
Street lights	LED light	0.03	36 for study area I	8	8	10	8.64	8.64	10.8
			30 for study area II	8	8	10	7.2	7.2	9
Daily energy consumption for 4 villages of study area I (kWh/day)							107.09	105.98	86.89
Daily energy consumption for 4 villages of study area II (kWh/day)							97.01	95.99	76.989

Similarly, for study area II, the daily energy requirement during the summer, moderate, and winter seasons has been calculated as 97.01 kWh/day, 95.99 kWh/day, and 76.989 kWh/day, respectively.

Fig. 4.11 illustrates the distribution of various types of loads in the Municipal/Governmental buildings for study area II. In study area II, the veterinary hospital has the highest contribution to the load demand at 24%, followed by the Gramin health center and streetlights, both contributing 22%. The school contributes 17%, while the Panchayat Ghar has the lowest contribution of 15%. The estimated annual load for municipal/governmental buildings in study area II is 35,555.37 kWh/year

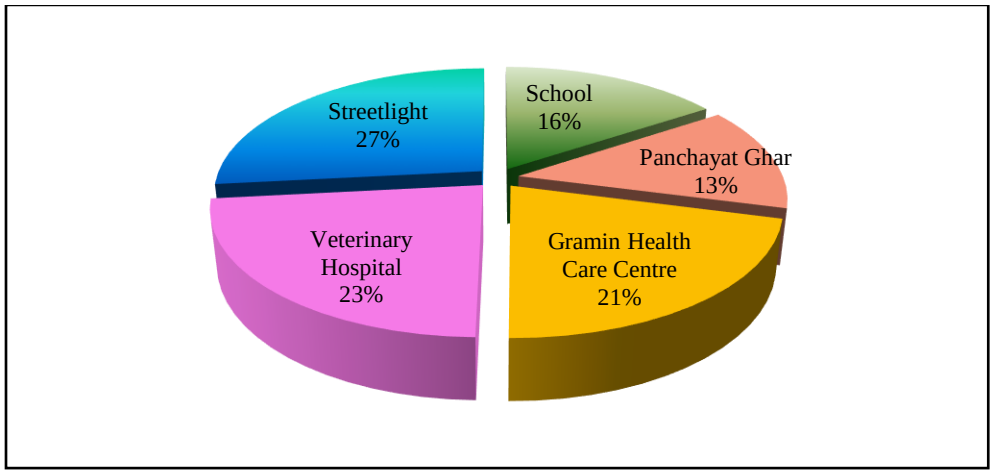

Fig. 4.10 Share of Distinct Types of Loads in Municipal/ Governmental Buildings Load for Study Area I

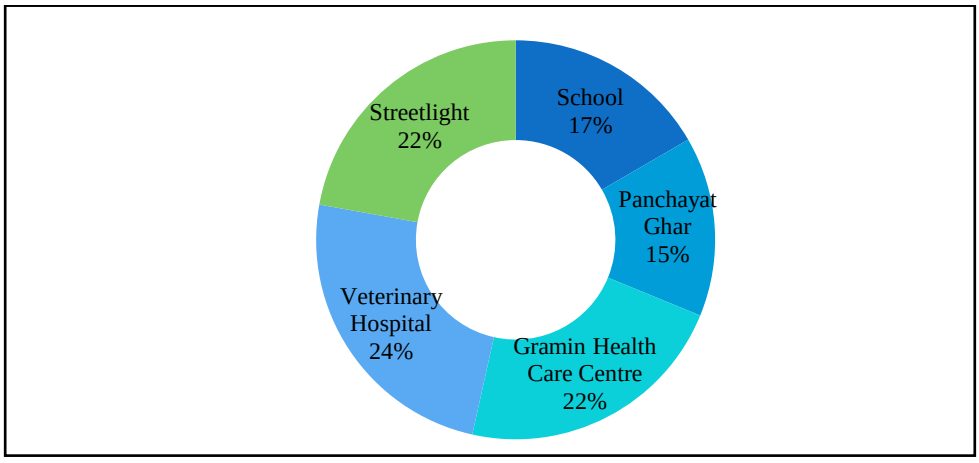

Fig. 4.11 Share of Distinct Types of Loads in Municipal/ Governmental Buildings Load for Study Area II.

4.4.3. Agricultural Load

The agricultural load has been considered in the present study as a significant component due to its importance in the rural Indian economy. Currently, several irrigation pumps used in agricultural activities are connected to DG, leading to environmental pollution. Therefore, the aim of the study is to address this issue by incorporating the agricultural load into the HRES. The agriculture load has been presented in Table 4.11 along with rating of irrigation pump, operational hours and quantities.

Table 4. 11 Agriculture Load for Different Seasons

Load	Appliances	Rating (KW)	Quantity (no.)	Operating hours			Seasonal load (kWh/day)		
				Summer season	Moderate season	Winter season	Summer season	Moderate season	Winter season
Agriculture	Irrigation pump	2.5	48	4	4	4	120	120	120
Total energy requirement per day for 4 villages							120	120	120

For both study area I and study area II, the agricultural load demand has been estimated as 43,800 kWh/year for each study area. This represents the energy needed to operate 12 irrigation pumps. Additionally, the daily energy consumption for each season has been computed as 120 kWh/day for each study area I and study area II. This value reflects the energy consumption of the irrigation pumps during the summer, moderate, and winter seasons.

4.4.4. Commercial Load

In the context of this current study, the expected increase in population and subsequent rise in load demand in the near future has been considered. To address this, the

commercial load from 8 shops in each village and total 32 shops in each study areas has been considered. Commercial load for different seasons has been presented in Table 4.12.

Table 4. 12 Commercial Load for Different Seasons

Load	Appliances	Rating (W)	Quantity (no.)	Operating hours			Seasonal load (kWh/day)		
				Summer season	Moderate season	Winter season	Summer season	Moderate season	Winter season
Shop	Tube light	12	1	4	4	5	0.048	0.048	0.072
	Ceiling Fan	45	1	9	9	0	0.405	0.405	0
Total energy requirement per day for 32 shops							14.496	14.496	1.92

The total commercial load demand for the proposed area is computed as 3,732 kWh/year for each of study area I and study area II. This load demand represents the electrical energy required to operate the shops in the respective study areas. Further, the total electrical load demand for both study areas has been summarized in Table 4.13.

Table 4. 13 Total Electrical Load for Both Study Areas

Load	Study Area I	Study area II
Residential (kWh/year)	799879.18	897987.99
Municipal/Governmental load(kWh/year)	37446.36	35555.37
Agricultural load (kWh/year)	43800	43800
Commercial load (kWh/year)	3732	3732
Total (kWh/year)	884857.5	981075.4

Further, Fig. 4.12 and Fig. 4.13 present the percentage-wise contribution of the electrical load in terms of residential, municipal/governmental, agricultural, and commercial loads for both study areas. It is evident from Fig. 4.12 and Fig. 4.13 that the residential load has the highest contribution to the total electrical load in both study area I and II.

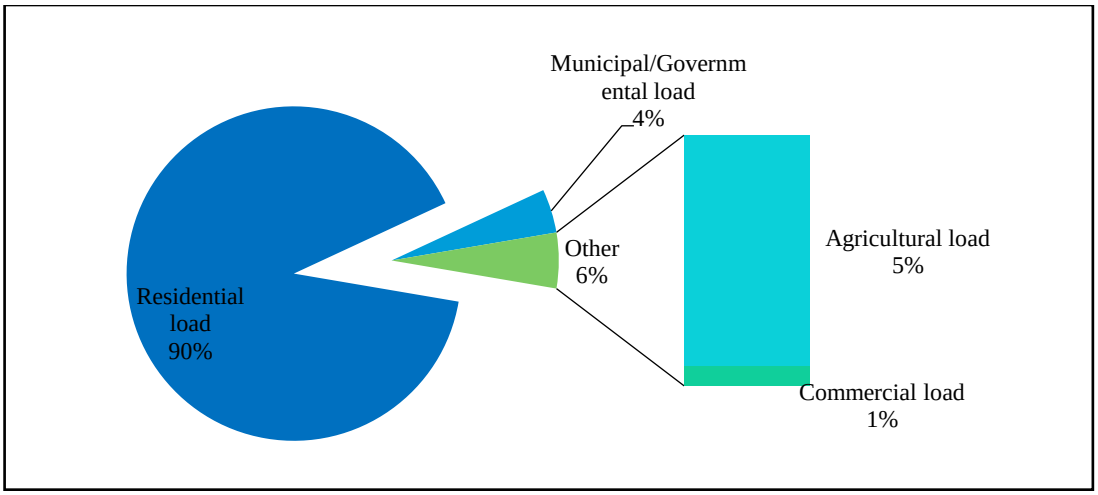

Fig. 4.12 Share of Diverse Types of Loads in Total Electrical Load for Study Area I

In study area I, the residential load accounts for 90% of the total electrical load, making it the dominant sector in terms of energy consumption. The municipal/governmental load is the second highest, contributing 4% of the total electrical load. The agricultural load follows with a contribution of 5%, and the commercial load has the lowest contribution of 1%.

Similarly, in study area II, the residential load holds the highest proportion, accounting for 92% of the total residential load. The agricultural load follows with a contribution of 4%, indicating its significance in this study area. The municipal/governmental load contributes 3% of the total electrical load, while the commercial load has the smallest contribution of 1%.

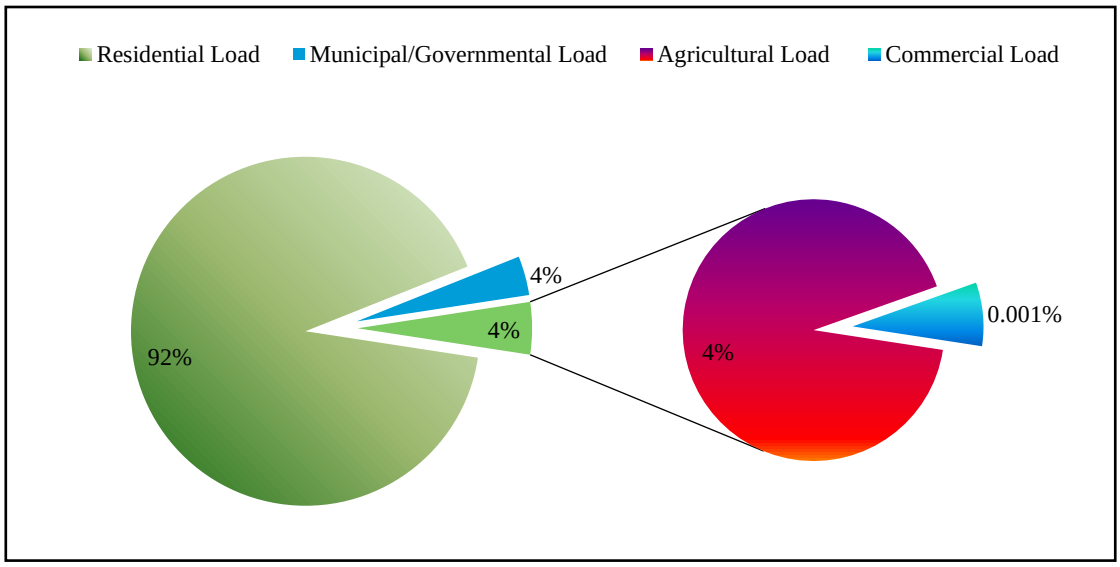

Fig. 4.13 Share of Distinct Types of Loads in Total Electrical Load for Study Area II

4.4.5. Season Wise Load Description

To meet the varying ED throughout the year, the impact of temperature variation on energy consumption of appliances has been taken into consideration. To account for this, the study has divided the year into three distinct seasons, each spanning four months. The three seasons considered in the current study is summer, moderate and winter seasons. Summer season includes April, May, June, and July. It represents the period of hot temperatures and increased energy consumption for cooling purposes. moderate season includes August, September, October, and November. It represents a transitional period with milder temperatures compared to summer but not yet reaching the winter conditions. Winter season consists of December, January, February, and March. It represents the colder period with lower temperatures and increased energy consumption for heating purposes. Based on the energy consumption patterns associated with these seasons, the daily energy consumption for study area I and study area II has been

calculated. In study area I, the daily energy consumption during summer, moderate, and winter seasons is estimated to be 3021.58 kWh/day, 2421.98 kWh/day, and 1387.58 kWh/day, respectively. Similarly, in study area II, the daily energy consumption during summer, moderate, and winter seasons is calculated as 3597.89 kWh/day, 2798.41 kWh/day and 1601.21 kWh/day, respectively.

Table 4. 14 Seasonal Load Demand for the Proposed Area

Season	**Month**	**Study area I (kWh/day)**	**Study area II (kWh/day)**
Summer season	April-July	3021.58	3597.89
Moderate season	August-November	2421.98	2798.41
Winter season	December-March	1387.58	1601.21

From Table 4.14, it is observed that the summer season has the highest load demand in both study area I and study area II, while the winter season has the lowest load demand. The summer season typically experiences elevated temperatures, leading to increased energy consumption for cooling purposes. On the other hand, the winter season has lower load demand as the temperatures are colder, requiring less energy for cooling and more for heating. This leads to a decrease in overall energy consumption during the winter season.

To further analyze the load demand patterns, Table 4.15 presents the peak load demand for each season in study area I and II.

Table 4. 15 Peak Load Demand of Each Season for Study Area I and II

Season	**Study area I (kW)**	**Study area II (kW)**
Summer season	177.01	218.02
Moderate season	176.92	209.20
Winter season	118.23	147.04

4.5 HOMER PRO SOFTWARE

HOMER Pro is a software specifically designed for the optimization and analysis of HRES. It is widely recognized and used by researchers, engineers, and decision-makers in the field of renewable energy. This software allows users to model and simulate various configurations of hybrid power systems by integrating multiple energy sources, energy storage systems, and conventional generators. The software aids in designing efficient and cost-effective systems that can meet specific EDs while maximizing the utilization of RES. HOMER Pro determines the most feasible solutions by conducting comprehensive simulations and optimizations of various HRES configurations. It analyzes multiple factors like energy production, cost, and system reliability to identify the optimal and economically viable energy solution. Further, the key features of HOMER PRO are described in the subsequent section [152].

4.5.1. Key Features of HOMER PRO

1) System Optimization

It employs sophisticated optimization algorithms to figure out the optimal configuration of a hybrid power system. It considers a range of factors such as energy resource availability, load demand, equipment costs, and system performance to find the most cost-effective solution.

2) Renewable Energy Integration

The software supports the integration of multiple RES, including SPV, WTs, hydro, biomass, and more. Users can input resource data and HOMER Pro calculates the optimal combination and sizing of these sources based on the energy requirements and availability.

3) Energy Storage Analysis

HOMER Pro enables the modelling and analysis of energy storage systems within the hybrid power system. It allows users to evaluate diverse types of energy storage technologies, such as batteries, flywheels, and pumped hydro storage, and determines their optimal sizing and operation for the given system.

4) Load Profiling

HOMER Pro allows users to input load profiles, representing the ED over time for different applications or sectors. This feature helps in accurately assessing the system's ability to meet the specific load requirements and optimize the system design accordingly.

5) Economic Analysis

HOMER Pro incorporates economic analysis tools to assess the financial feasibility of the designed hybrid power system. It calculates metrics such as the COE, NPC, and payback period to evaluate the economic viability of the system.

HOMER Pro software provides a comprehensive framework for designing and optimizing HRES by considering the available energy resources, load demand, economic factors, and system constraints. Its optimization capabilities, combined with economic analysis, assist in making informed decisions about the system configuration, sizing, and operation, ultimately leading to more efficient and cost-effective renewable energy solutions.

4.6 PROBLEM FORMULATION

The main objective of this study is to develop a reliable HRES that minimizes the cost. To achieve this objective, the NPC and COE are considered as the objective function.

The optimization of the NPC and COE is performed using HOMER Pro software, considering various constraints such as upper and lower bounds, storage limit of the battery, power reliability in terms of unmet load, and others. The details of objective function and constraints are discussed in chapter 3 and HOMER Pro software description is provided in sections 4.5.

The mathematical modelling of different system components is provided in chapter 3, which includes the modelling of RES, BESS, and other relevant components.

Furthermore, the current study also considers the land requirement for the installation of the hybrid system. The computation of land requirement is performed based on specific criteria and factors, which are discussed in detail within the study. This information helps in determining the spatial requirements and feasibility of implementing the hybrid system in the selected study areas.

By integrating mathematical modelling, OT, and consideration of land requirement, the study aims to develop a comprehensive and HRES that minimizes costs while meeting the desired performance and power reliability criteria.

4.6.1. Land Used for Installation of Hybrid System

In the present study, the consideration of social and environmental impacts includes the assessment of land usage for the installation of the hybrid system. The land used for the installation of the hybrid system (H_L) is considered during the optimization process.

$$H_L = \sum_{j=1}^{N_{res}} L_j \times S_j$$

The land requirement for each RES is represented by L_j, which denotes the land needed for the installation of 1 kW of jth RES in terms of m^2/kW. The optimal size of each RES is

represented by S_j, and N_{res} represents the total number of RES considered in the proposed HRES.

The land requirement for the installation of 1 kW of SPV, WT, BMG and BGG are 30 m^2, 110 m^2, 90.2 m^2, 144 m^2 respectively [153-154].

4.6.2. Economical and Technical Dataset

Economic data includes CC, OMC, RC etc. of components of hybrid system. In the present study, the lifespan of the proposed system has been considered as 25 years. Annual real interest rate of 8% is taken to convert one-time costs to annualized costs.

The economic data used for the development of hybrid model has been provided in Table 4.16 [155]. It has been observed that the CC and RC of WT is highest among all the components. The lifespan of SPV system and WT has been taken as 25 years which is equal to the project lifetime. The life of one battery is to be 5 years The cost of biomass fuel has been taken as $0.015/kg [155].

Table 4. 16 Economic Data of Renewable Energy Systems

Components	**Capacity considered**	**CC**	**RC**	**OMC**	**Lifespan**
SPV	1kW	$1333/kW	$1333 /kW	$ 26/year	25 years
WT	3.3 kW	$3500 /WT	$ 3500 /WT	$ 60/WT/year	25 years
BMG	1kW	$1033 /kW	$ 750 /kW	$ 0.01//kW/ hour	15000 hours
BGG	1kW	$660 /kW	$ 450 /kW	$ 0.01/kW /hour	20000 hours
Battery	12V, 200 Ah	$284 /kW	$ 220/kW	$6/battery/year	5 years/battery
Converter	1kW	$117 /kW	$ 117 /kW	$3/kW /year	10 years

4.6.3. Input Data for Feasibility Analysis and Sizing of HRES

Input data comprising of hourly load demand (kW), monthly average daily solar radiation (kWh/m^2/day), monthly average wind speed (m/s) and monthly average biomass

and biogas availability (tons/year), required for the feasibility analysis and sizing of HRES has been already presented in sections 4.3 and 4.4.

4.7 FEASIBILITY ANALYSIS AND SIZING OF HRES FOR STUDY AREA I

Depending upon the availability of RES different HRES models for OFG and grid connected scenario have been formulated for study area I and Study area II and presented in Table 4.17. Hourly simulations were conducted over the course of one year using the HOMER Pro software to assess selected models. Subsequently, a techno-economic analysis was conducted to evaluate the performance of these developed models. After careful consideration, the model that demonstrated the highest feasibility, as determined based on NPC and COE, was chosen among all the alternatives.

Table 4. 17 Proposed Hybrid Models for the Study Area I

MODEL	HRES	DESCRIPTION
H-11	OFG	BMG/SPV/ BESS
H-12		BGG/ SPV/BESS
H-13		BMG/SPV/ BGG/BESS
H-14	Grid connected	BMG/SPV/ BGG/BESS

Furthermore, techno-economic analysis was conducted using the HOMER Pro software for all the aforementioned HRES. The models were evaluated based on their NPC and COE and the model with the lowest values for these metrics was selected as the best option. The results of the various OFG and grid connected HRES are presented in Fig. 4.14 and Fig. 4.15 alongwith Table 4.18. The detailed discussion of these results is provided in the subsequent sections.

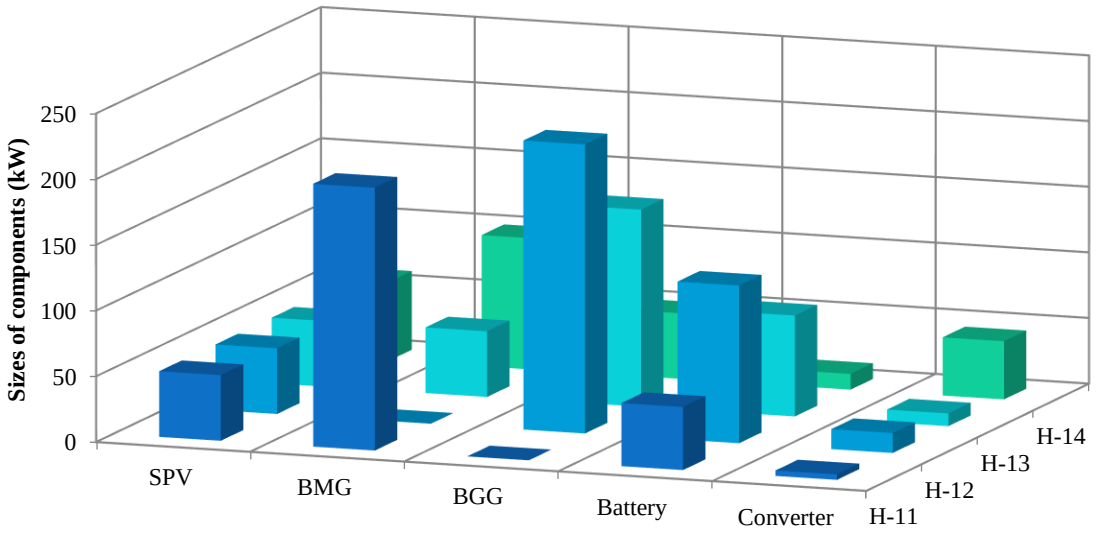

Fig. 4.14 Sizes of Various Components for Different Models

4.7.1. Model H-11: BMG/SPV/ BESS

After conducting research, it has been determined that the optimal size for the H-11 hybrid model comprises a 50 kW SPV system, a 200 kW BMG, a 48 kWh BESS, and 4.16 kW converters. The estimated values for the total NPC, operating cost, and COE for this model are $1,208,108, $73,679 per year, and $0.116 per kWh, respectively.

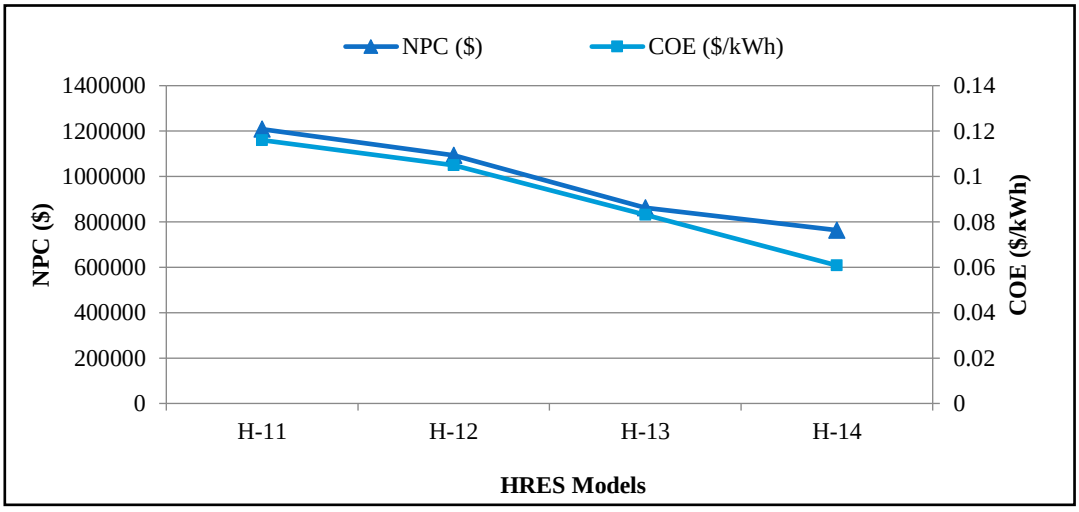

Fig. 4.15 NPC and COE for Different Models

Table 4. 18 Results of OFG and Grid Connected HRES Models for Study Area I

RES	HRES (OFG)			HRES (Grid-connected)
	H-11	H-12	H-13	H-14
SPV system (kWh/year)	78680 (7.6%)	78680 (7.6%)	78680 (7.6%)	94416 (6.62%)
BMG (kWh/year)	952794 (92%)	-	104844	876000 (61.4%)
BGG (kWh/year)	-	963196 (92.4%)	681761	438000 (30.7%)
Total electrical power production (kWh/year)	1031474	1041876	865285	1426615
Excess electricity (kWh/year)	227222 (22%)	236940 (22.7%)	59918 (7%)	0
GS (kWh/year)	-	-	-	617632
GP (kWh/year)	-	-	-	18199

4.7.2. Model H-12: BGG/ SPV/BESS

Based on the results, the optimal size for model H-12 is determined to be a 50 kW SPV system, a 220 kW BGG, a 120 kWh BESS, and 15.2 kW converters. The estimated values for the NPC and operating cost of this model are $1,092,454 and $68,723 per year, respectively. The computed COE for this model is $0.105 per kWh.

4.7.3. Model H-13: BMG/SPV/ BGG/BESS

It has been revealed that the optimum size of the hybrid model H-13composed of 50 kW SPV system, 150 kW BGG, 50 kW BMG, BESS of 76.8kWh with 9.7 kW converter. The NPC, TAC and COE are calculated as $862284, 48057$/year and $0.0831/kWh respectively.

4.7.4. Grid Connected System

High COE and excess electricity are the major disadvantages of OFG systems. Therefore, a comparative study has been conducted between OFG and grid connected scenario of HRES.

4.7.5. Comparison between OFG and Grid Connected Models

The best OFG hybrid model has been compared with grid connected model H-14 and it is found that, grid connected scenario offers least NPC, TAC and COE of $763228, 38536 $/year and $0.0608/kWh, respectively. The optimum size of the considered model in grid connected scenario consists of 60 kW SPV, 50 kW of BGG, 100 kW of BMG, 12kWh of battery, 44.3kW of converter. The excess energy of this model is found to be 0 as surplus electricity has been sold to grid.

It has been concluded that, the grid connected model H-14 is best among all OFG and grid connected models in terms of NPC, TAC, COE, unmet load, excess energy etc.

4.8 ANALYSIS OF VARIOUS PARAMETERS OF PROPOSED MODEL FOR STUDY AREA I

The optimized results pertaining to best model have been analyzed based on NPC, amount of energy generated, excess electricity generated, energy sold and purchased, and land requirement etc. as discussed in the following sections.

4.8.1. Share of Different Costs in NPC

The cash flow summary in terms of NPC of proposed HRES of study are I is presented in Fig. 4.16.

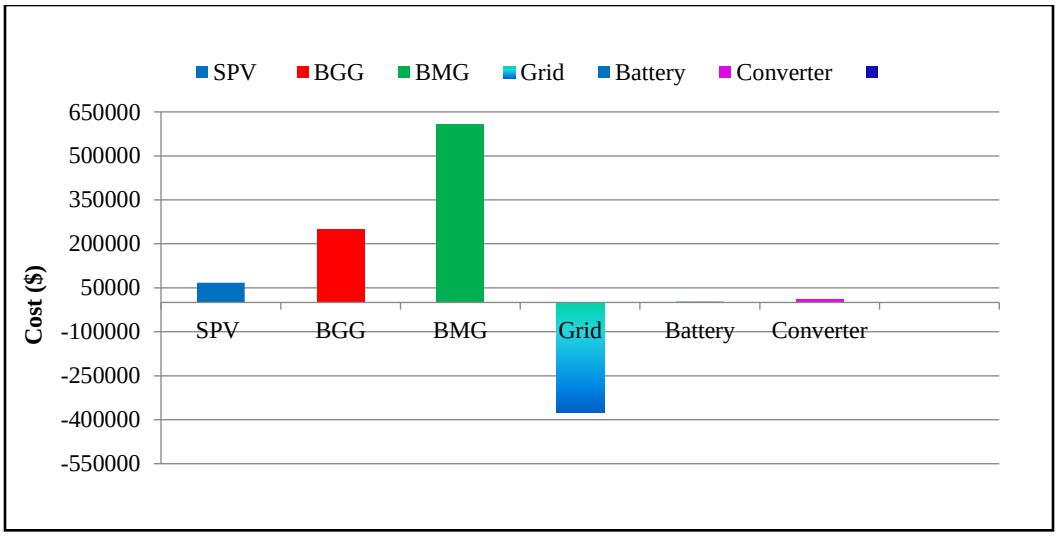

Fig. 4.16 Cash Flow Summery in Terms of NPC of Proposed HRES for Study Area I

It is evident from Fig. 4.16 that major portion of NPC is due to the cost of BMG followed by BGG and SPV respectively. All costs are expenditures incurred upon SPV, BGG, BMG, battery and converter, so they appear as positive values, whereas the net worth of energy sold to, and purchased from the grid is negative, indicating that the revenue from selling power to the grid exceeds the expenditure on purchasing power from the grid. Further, the share of different cost like CC, OMC, RC, FC and SV in the NPC is shown in Fig. 4.17, As it is evident from the Fig. 4.17 that the highest share in the NPC is of RC which accounts for 59%. This high RC is due to BMG, BGG, batteries, and converters as they must be replaced throughout the project's lifetime. The majority of operating cost is because of biogas system due to its FC and remaining is due to SPV, biomass, converter, and battery. The FC in the NPC is due to the cost of biomass.

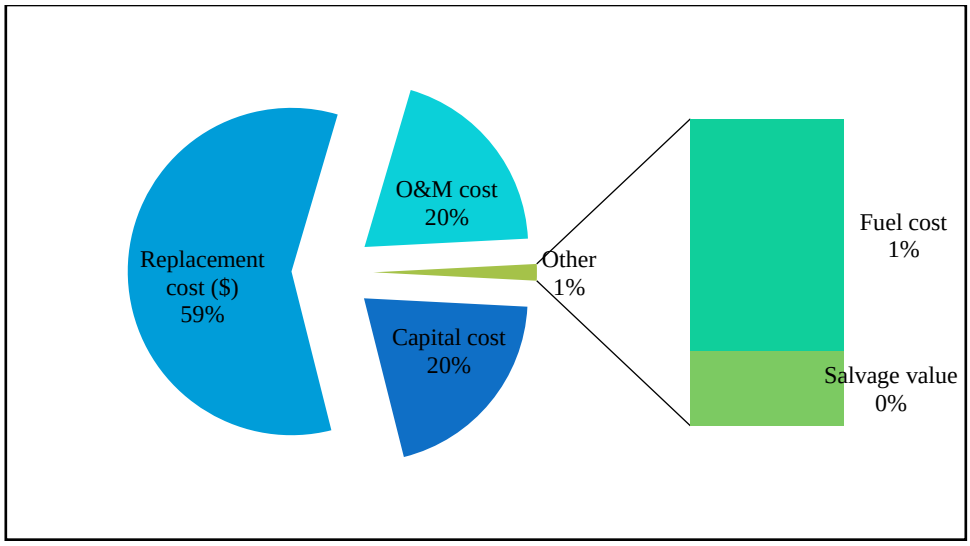

Fig. 4.17 Breakdown of NPC of Grid Connected HRES

4.8.2. Energy Generation by Best Hybrid Model

The monthly average electricity production by different RES of proposed system is depicted in Fig. 4.18. It has been seen that the contribution of BMG is highest which is 62.1%, followed by BGG, 31%, SPV, 5.57% and grid contribute for1.34%

4.8.3. Excess Electricity

Based on the simulation output, it is revealed that excess electricity is generated more in OFG mode compared to grid connected mode.

4.8.4. Monthly Average Energy Sold and Purchased

The energy sold to the grid is 603337 kWh/year which is higher than energy purchased 18962 kWh/year Further, the proposed hybrid model purchased less energy in winter season and sold more energy in summer season.

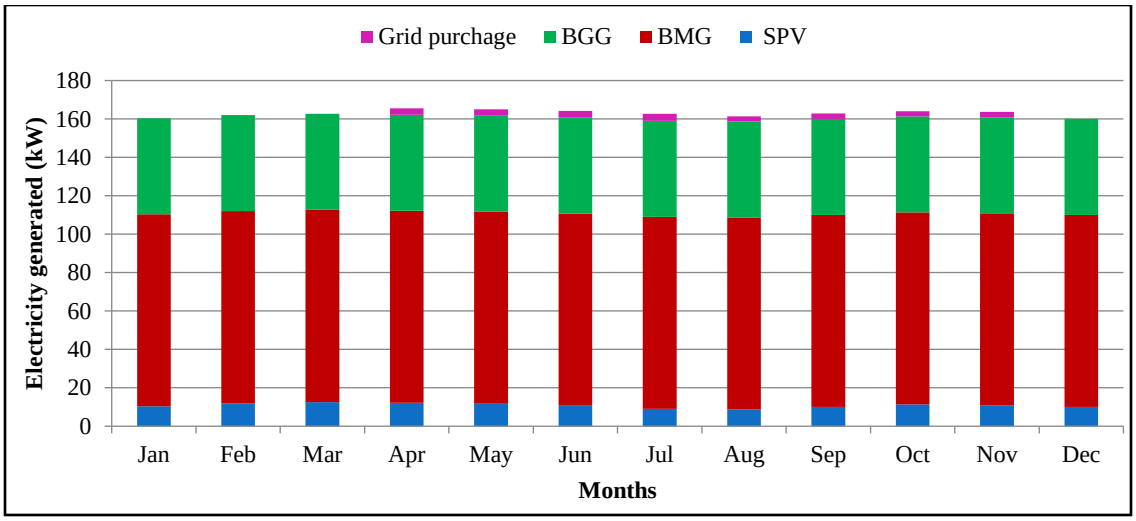

Fig. 4.18 Monthly Average Electricity Generation of Proposed Model for Study Area I

4.8.5. Land Needed for Proposed Hybrid Model

The proposed hybrid model needs 28208 m^2 of land for installation of proposed hybrid system.

$$\text{Land needed } (m^2) = ((60 \times 30) + (100 \times 90.2) + (50 \times 144) = 18020\ m^2$$

4.9 RESULTS OF HYBRID MODELS FOR STUDY AREA II

Based on the availability of RES, the main aim of this study is to design an optimal hybrid model to meet the present and future ED of cluster of villages of study area II. The proposed HRES has been simulated by using HOMER Pro tool for a year using technical and economic data as inputs. At each hour, load is fulfilled with the generator outputs and/or battery supply/grid. At first, five different viable options of hybrid models based on RES for OFG systems have been considered as given in Table 4.19. Further, these models are compared in terms of least NPC, TAC and COE to select the best choice. Finally, the best OFG model is compared with grid connected hybrid system.

Table 4. 19 OFG and Grid Connected Models for the Study Area II

Model	Description
H-21	BMG/WT/BGG/BESS
H-22	BMG/ SPV/WT/BESS
H-23	BGG/ SPV/WT/BESS
H-24	BGG/ SPV/BMG/BESS
H-25	WT/BGG/ SPV /BMG /BESS
H-26	Grid connected WT/BGG/ SPV /BMG /BESS

4.9.1. Results of OFG and Grid Connected Hybrid Models

The possible OFG and grid connected models are simulated in HOMER Pro to meet the full hourly demand of the area for 0% unmet load. After hourly simulation, the obtained results are presented in Fig. 4.19, Fig. 4.20 and are summarized in Table 4.20. Further, the results of each model have been discussed in the following sections.

1) Model H-21: BMG/WT/BGG/BESS

The Model H-21 consists of 36 kW of WT, 150 kW BMG, 50kW of BGG and BESS of 835 kWh (348 nos.) along with 54.5kW converter. The NPC and operating cost of this option are estimated as $1052540 and 57511$/year respectively at the computed COE of $0.0799/kWh.

1) Model H-22: BMG/ SPV/WT/BESS

Based on hourly calculation for Model H-22, the optimum size of SPV system, WT, BMG, BESS, and converter are estimated as 80 kW, 45 kW, 150 kW, 1538.4kWh (641 nos.) and 92 kW respectively. The NPC, TAC and COE are estimated as $1052540, 70715$/year and $0.103/kWh respectively.

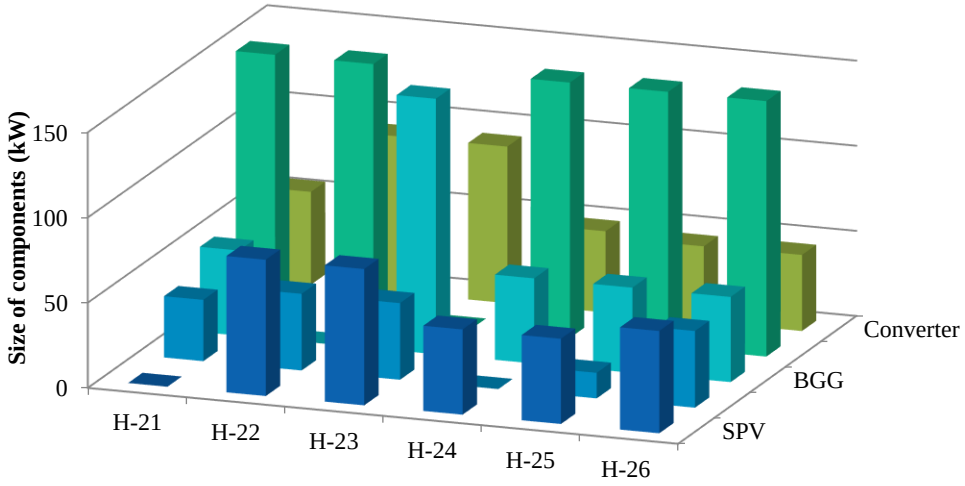

Fig. 4.19 Sizes of Various Components for Different Models

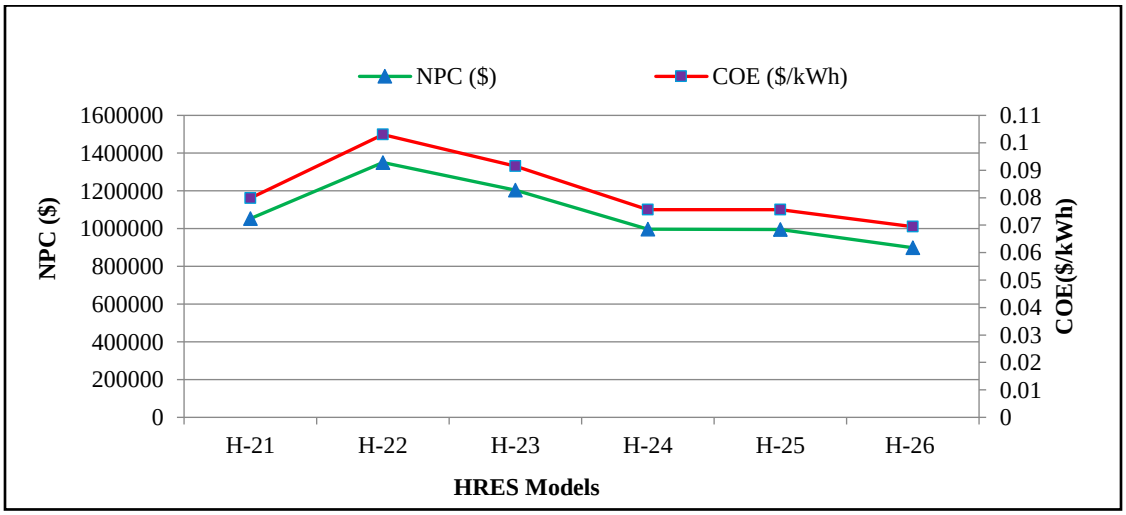

Fig. 4.20 NPC and COE for Different Model

2) Model H-23: BGG/ SPV/WT/BESS

After hourly simulation, the optimum size of SPV system, wind energy system, BGG and battery of model H-23 are obtained as 80kW, 45 kW, 150kW and 1540.8 kWh (642 nos.) respectively. The NPC, TAC and COE of ModelH-23 are calculated as $1203656, $63694, and $0.0915 /kWh, respectively.

Table 4. 20 Electrical Energy Output of OFG Hybrid Models

RES	HRES (OFG)					HRES (Grid-connected)
	H-21	H-22	H-23	H-24	H-25	H-26
SPV system (kWh/year)	-	128960 (11.9%)	128960 (11.9%)	80600 (7.82%)	80600 (7.8%)	96720 (5.09%)
Wind energy system (kWh/year)	38,863 (3.78%)	48578 (4.49%)	48578 (4.48%)	-	16139 (1.57%)	48578 (2.6%)
BMG (kWh/year)	828256 (80.6%)	904315(83.6%)	-	814183 (79%)	800,550 (77.6%)	1314000 (69.2%)
BGG (kWh/year)	160,498 (15.6%)	-	906167 (83.6%)	136405 (13.2%)	134,444 (13%)	438000 (23.1%)
Total electrical power production (kWh/year)	1,027,617	1081853	1083705	1031187	1,031,787	1899925
Excess electricity (kWh/year)	3,435 (0.33%)	39118 (3.62%)	41225 (3.8%)	3632 (0.35%)	4,829 (0.47%)	1118 (0.059%)
GS (kWh/year)	-	-	-	-	-	876152
GP (kWh/year)	-	-	-	-	-	2627

3) Model H-24: BGG/ SPV /BMG /BESS

The optimum size of the model H-24 consists of 50 kW SPV system, 50kW BMG, 150 kW BGG, BESS384 kWh (160 nos.) with 47.7 kW converter. The NPC, TAC and COE are estimated as $996071, 55250$/year and $0.0757/kWh, respectively.

4) Model H-25: WT/BGG/ SPV/BMG/BESS

It is evident that the optimum size of model H-25 composed of 50 kW of SPV system, 15 kW of WT, 150 kW BMG, 50 kW of BGG and BESS of 384 kWh (160 nos.) along with 44.3 kW converter. The total NPC, TAC and COE of this model have been computed as $995331, 54711.61/year and $0.0.0756 /kWh, respectively.

4.9.2. Comparison between OFG and Grid Connected RES Models

From Fig. 4.19 and Fig. 4.20, it has been found that the Model H-25 offer least NPC, TAC, COE of $1549976, $121250, and $0.124/kWh, respectively. The optimum size of model H-25 composed of 50 kW of SPV system, 15 kW of WT, 150 kW BMG, 50 kW of BGG and BESS of 384 kWh (160 nos.) along with 44.3 kW converter.

Further, the comparison of the best OFG and grid connected model has been carried out and shows that grid connected scenario offers least NPC, TAC and COE of $1046260, $88457 and $0.091/kWh respectively. The optimum size of the considered model in grid connected scenario consists of 60 kWof SPV, 45 kW of WT, 150 kW of BMG, 50 kW of BGG, 14.4 kWh (6 nos.) of battery, 44.7 kW of converter. There is no excess energy as surplus electricity has been sold to grid.

It has been concluded that, the grid connected scenario is best model among all OFG and grid connected models in terms of NPC, TAC, COE, and excess energy etc.

4.10 ANALYSIS OF VARIOUS PARAMETERS OF PROPOSED OPTIMAL MODEL FOR STUDY AREA II

The following sections describes the various parameters of proposed optimal systems like land needed for HRES, energy generation by different components, different costs contributing to NPC.

4.10.1. Breakdown of NPC of Grid Connected RES Model

The cash flow summery in terms of NPC is shown in Fig. 4.21. It has been observed that BMG have the highest cost which contribute to total NPC which is due to the high RC because their less operational life. All expenses encompass expenditures related to SPV,

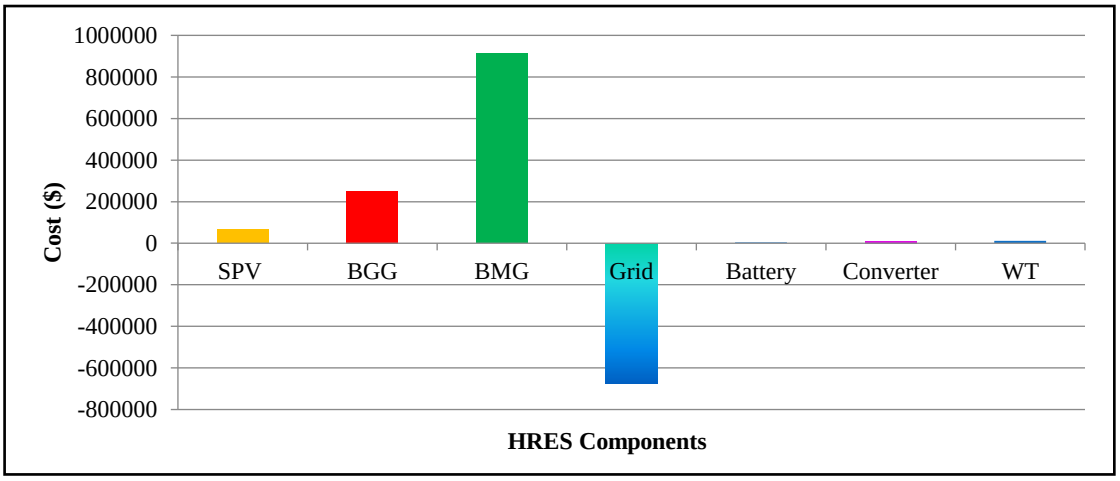

Fig. 4.21 Cash Flow Summery in Terms of NPC of Optimal HRES for Study Area II

BGG, BMG, battery, WT, and converter, resulting in their representation as positive values. In contrast, the net balance of energy transactions with the grid is negative, signifying that the income derived from selling power to the grid surpasses the costs of purchasing power from it. The share of different costs in NPC for grid connected HRES model has been presented in Fig. 4.22. The highest share in NPC is due to RC which accounts for 49% followed by OMC 27%.

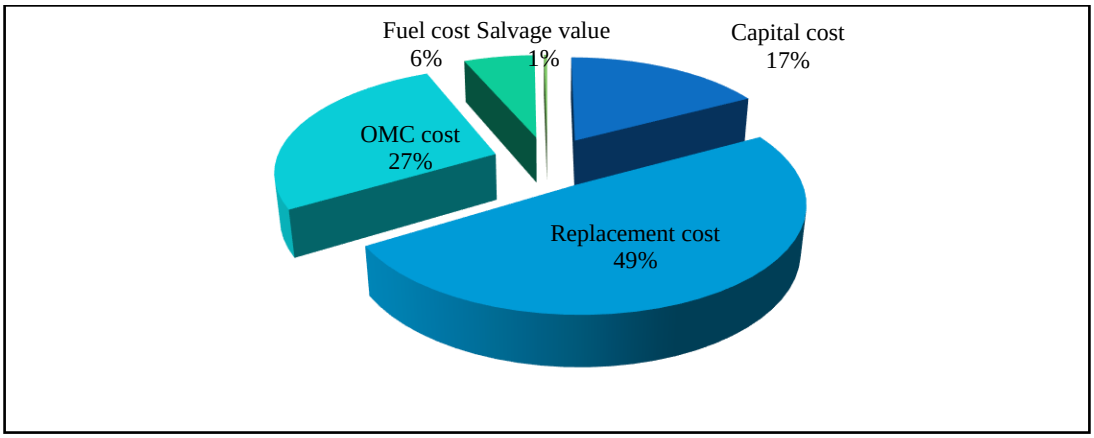

Fig. 4.22 Breakdown of NPC of Proposed (H-26) Grid Connected Model

4.10.2. Energy Generation by Optimal Hybrid Model

The monthly average electricity generation of best model has been demonstrated in Fig. 4.23. It has been found that BMG contributes highest followed by BGG, SPV, WT and grid, respectively. Out of total annual electricity production of 1899925 kWh/year (100%), BMG contributes 69.2% followed by BGG of 23.1%, SPV of 5.1%, and WT of 2.6% and grid of 0.12% respectively. The proposed hybrid model fulfils the electricity needs through SPV, wind, biomass, biogas, battery, and grid. It has been observed that due to availability of plenty of biomass in the study area the electricity production due to BMG is highest.

4.10.3. Excess Electricity

Based on the simulation output, it has been found that excess electricity is generated more in OFG mode as compared to grid connected mode which is almost 0%.

4.10.4. Land Needed for Proposed Hybrid Model

The proposed hybrid model requires 27480 m^2 of land for installation of proposed HRES.

$$\text{Land needed } (m^2) = ((60 \times 30) + (45 \times 110) + (150 \times 90.2) = 27480\ m^2$$

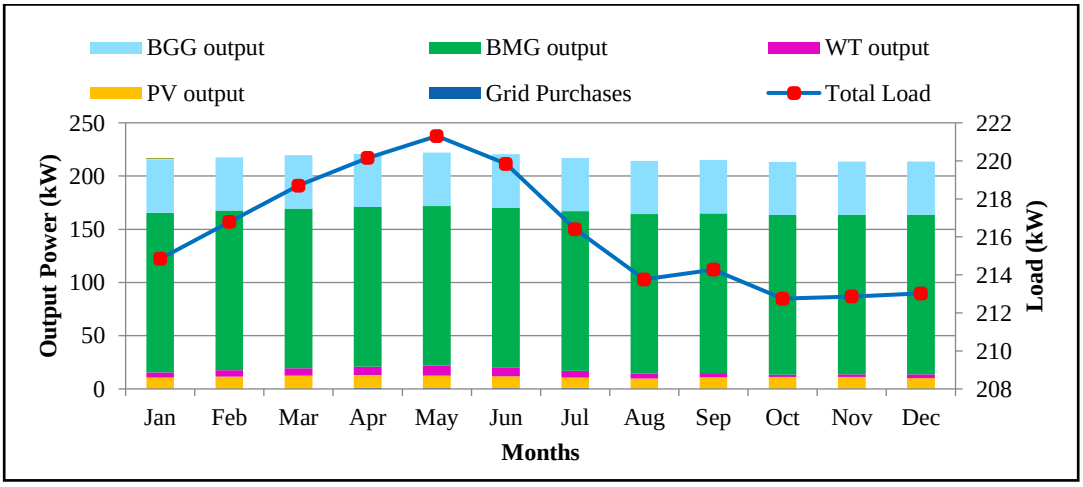

Fig. 4.23 Monthly Average Electricity Generation of Proposed Model

4.11 CONCLUSION

In this chapter, the feasibility and techno-economic analysis of hybrid models based on RES for a cluster of villages located in the Mewat and Agra districts of Haryana and Uttar Pradesh state respectively, India, has been presented. This study aims to facilitate the development of hybrid models for both OFG and grid-connected scenarios in similar remote and rural areas. Further, a comparative analysis of the results obtained from various hybrid system models in both OFG, and grid-connected scenarios has been presented. Based on the findings, it can be concluded that the grid-connected hybrid system offers the lowest NPC and COE compared to the OFG models.

The optimum size of grid connected HRES for study area I consists of 50 kW SPV, 100 kW of BMG, 50 kW of BGG, 12 kWh of battery, 44.3 kW of converter. The proposed model will be able to provide a reliable power supply at least NPC, TAC and COE of $763228, 38536 $/year and $0.0608/kWh, respectively. Further, the optimum size of grid connected HRES for study area II comprised of 50 kW of SPV system, 15 kW of WT, 150 kW BMG, 50 kW of BGG and BESS of 384 kWh (160 nos.) along with 44.3kW converter. This system offers least NPC, TAC and COE of $1046260, $88457, and $0.091/kWh, respectively.

CHAPTER 5

INVESTIGATION OF ISSUES IN GRID INTEGRATION OF VARIOUS RES

5.1 INTRODUCTION

The depletion of fossil fuel reserves and the associated environmental challenges have spurred a significant uptick in the utilization of RES. However, due to the inherent unpredictability in the generation of most RES, their seamless integration into the electricity grid has become a complex and time-intensive endeavor. This approach gives rise to a diverse array of challenges, spanning both technical and non-technical domains. Within this chapter, we delve into an extensive exploration of the benefits, difficulties, and challenges that may emerge during the intricate process of integrating various RES into the grid. Additionally, we present several viable alternatives that can be considered [156]. Fig. 5.1 visually illustrates the integration of diverse RES within the grid, providing a comprehensive representation of the energy landscape.

5.2 BENEFITS OF INTEGRATION OF RES

RES can be employed as a stand-alone or grid connected for power generation. But, when they are incorporated into larger electric power networks, their advantages are considerably increased. The enormous generation capacity in comparison to other forms of power generation is one of RES's key attributes that influences their inclusion into power networks. In terms of network topology, RES is also influenced by their geographic and topological positions. Another aspect that needs to be addressed when integrating RES into

electricity grids is their fluctuation. By allowing for the successful implementation of cleaner, more environmentally friendly energy technologies into the electricity network, renewable integration lessens the country's reliance on imported coal. Larger resources like wind farms, solar farms, etc. are often connected at the transmission level while smaller RES are typically connected at the distribution level.

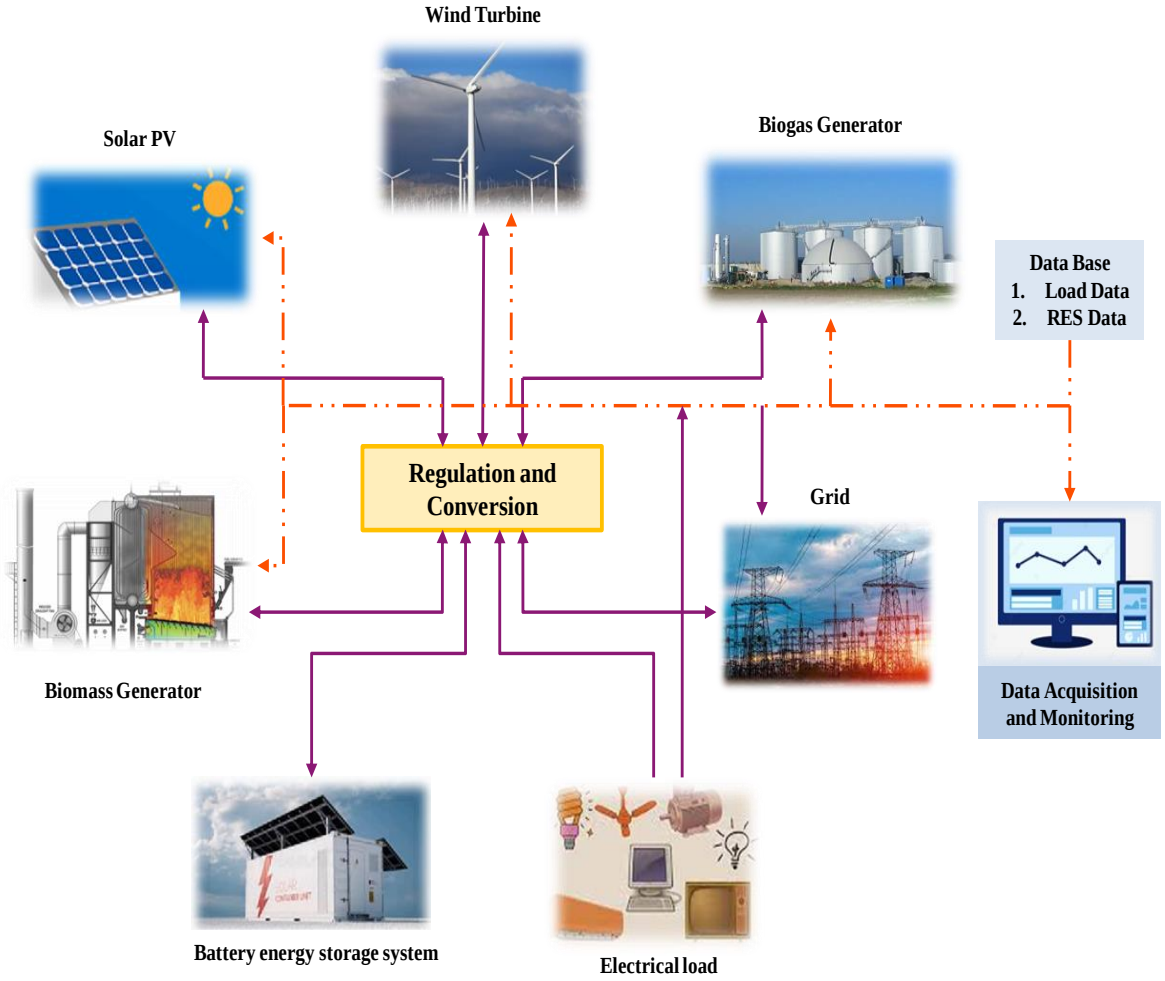

Fig. 5. 1 Grid Components Integrated with Various RES

Fig. 5.2 illustrates the various benefits of integration of various RES into the grid and the following sections briefly examine the benefits of RES integration [157].

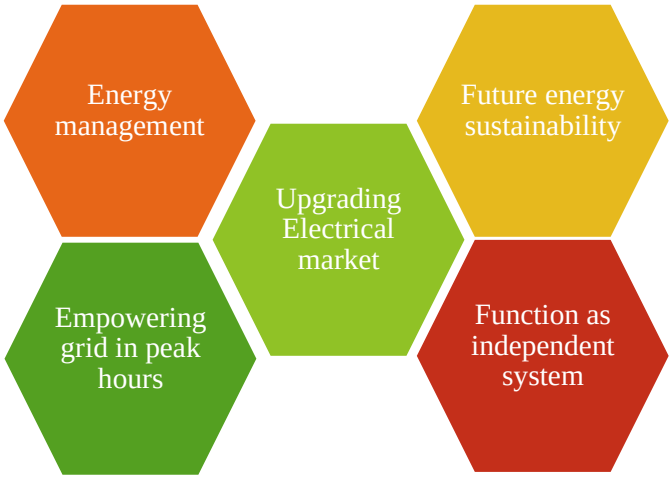

Fig. 5. 2 Benefits of Integration of RES

5.2.1. Future Energy Sustainability

The integration of RES into the grid presents an opportunity to reduce dependence on fossil fuel-generated power. One of the most sought-after outcomes of this integration is the environmental benefit derived from the increased presence of RES. This advantage is closely linked to a reduction in the emission of GHG. RES technologies, such as solar and wind power, are environmentally friendly and have a positive impact on the ecosystem [157]. Beyond diversifying the energy resource portfolio, renewable energy also boasts a unique characteristic: it produces no pollution. This quality is instrumental in combating climate change and its adverse effects. Moreover, RES plays a pivotal role in generating local economic value and promoting employment opportunities, thereby fostering regional growth. In this manner, the utilization of RES aligns with sustainability objectives [158].

.

5.2.2. Empowering Grid in Peak Hours

The incorporation of more RES along with the implementation of storage facilities will enhance the capabilities of the smart grid by furnishing it with up-to-the-minute data. This, in turn, will encourage the utilization of RES whenever suitable. As the proportion of RES within the energy generation mix grows, it leads to a decrease in both operational inefficiencies and peak energy demand. This trend aligns with efforts to optimize the grid's performance and efficiency [158].

5.2.3. Energy Management

The implementation of smart metering facilitates the uptake of energy management approaches like demand side management (DSM) on a customer level. This, in turn, enables the effective utilization of DR practices, ultimately resulting in optimized energy usage and substantial energy savings [158].

5.2.4. Function as Independent System

During a power outage, a RES system can function as an independent system, minimizing the disruption to customers. A grid connected HRES is used by industrial and commercial users, which helps to minimize the demand for electrical power. There are instances where a standalone system helps to preserve energy in residential settings [158].

5.2.5. Upgrading Electrical Market

At the national level, trading of power is made easier by the provision of a digital platform by power exchange. Since 2011, India has been actively trading in renewable energy, and the country currently ranks fourth in terms of the potential size of its market [158].

5.3 ISSUES AND CHALLENGES IN INTEGRATION OF RES WITH GRID

In today's world, one of the most critical issues is to figure out how to incorporate a larger proportion of renewable energy into the overall energy production. The increasing proportion of RES in the grid poses a number of problems and difficulties, many of which are caused by the intermittent nature of these RES. In most cases, these concerns are crucial for the wind and solar generation. The integration of RES like biomass, hydro, and geothermal energy into the grid poses no substantial challenges and can be predicted more accurately [159]. The several difficulties and problems associated with integration are shown in Fig. 5.3 and discussed in the subsequent sections.

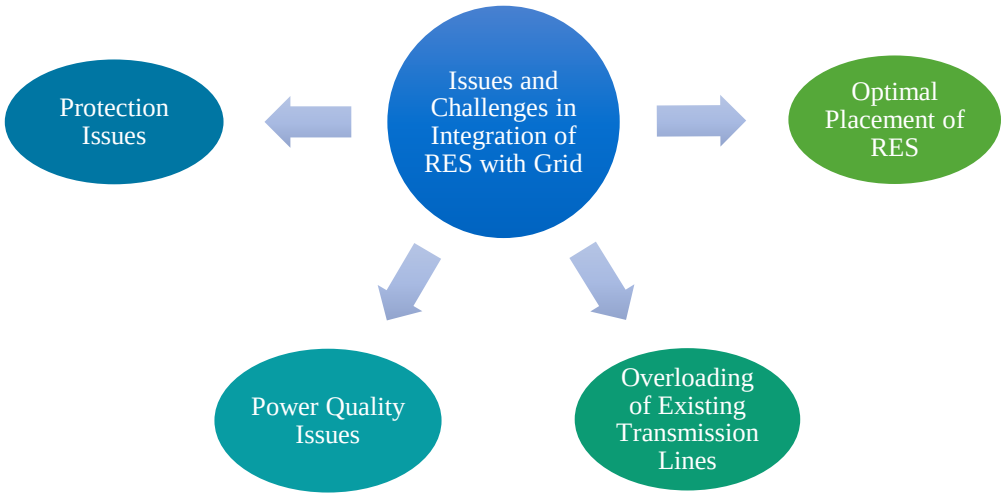

Fig. 5. 3 Issues and Challenges in Integration of RES with Grid

5.3.1. Power Quality

It is essential to maintain overall power quality of the system for the proper functioning of a power generation system and the utilities. Power quality must be upheld

while achieving total balance between electricity produced and electricity used by the customer. Among the many factors for power quality, voltage fluctuations and maintaining a uniform sinusoidal wave are key challenges that must be addressed across the electricity generating process [158].

Due to the increasing use of renewable energy and the loading effect of transmission lines in response to slight disruptions, the power quality and subsequently the stability of the power system is impacted. As a result, maintaining a healthy, stable, and smart power transmission and distribution system is a difficult task. This section discusses the power quality challenges that arise because of the integration of RES into the grid. Voltage, frequency variations, and harmonics are major power quality concerns. As RES are integrated into the grid, the frequency and voltage become unstable. Weather changes and hour of day have a continual impact on grid output and functioning. Voltage and frequency swings are produced by the unpredictability of RES, resulting in grid disruptions. The system also incorporates harmonics. A pure sinusoidal wave has no harmonics. The presence of harmonics in a system causes sinusoidal wave distortion. Harmonics are caused by the imperfect operation of electrical and mechanical devices. Harmonics can be generated into wind farms because of electronic devices used in WT for regulating purposes, such as inverters, and due to large power transformers used to step-up voltage for transmission purposes. These harmonics can be of various orders, with the third and fifth order harmonics being the most significant and having the highest impact on power quality when compared with the other higher order harmonics [158].

The introduction of harmonics causes a decrease in capacitive impedance in the system that causes considerable heating in electronic devices. In power generation, these

harmonics generate circulating currents, which increase system losses. Voltage instability also arises in wind farms owing to power variance when wind speed varies over time. Voltage swell is the inverse of voltage dip. It is a sudden rise in voltage at the frequency that is beyond of normal limits, lasting more than one cycle which is 20 milliseconds and usually less than a few seconds. The effects of voltage swells include loss of data, flickering lights and displays, and the failure or destruction of sophisticated equipment. DSG, such as solar and wind power, will result in an overall rise in voltage with an increased risk of voltage swells. Voltage swells can also occur because of connecting massive single-phase equipment. A connection of this type causes a voltage drop in the phase where the device is attached. But, due of the voltage drop across the neutral wire, the voltage in the other two phases rises. Severe voltage surges may develop because of excessive output from SPV systems. The combination of SPV and electric vehicle charging, when one or both are coupled to single phase, increases the danger of voltage swells [158].

Single phase faults cause the most significant voltage swells because the voltage in the phases that are not affected by the fault also increases while the fault is occurring. This is the scenario that occurs when there is a fault in a single phase of a long overhead wire that also has a high ground resistivity. The over voltages will be lower for cables, and they will also be reduced for low ground resistivity. Customers with low voltage who live in distant areas are the ones who are most likely to experience voltage surges particularly when they arise on a continual basis, they might cause harm to the equipment. In most cases, SPV systems will have anti-islanding protection installed, as voltage surges will cause the protection to trip. Because low-voltage networks do not often include measuring points, the customer frequently is not aware of the existence of swells or the effect that they

have on his or her own equipment. When it comes to SPV systems, flicker is the result of power changes brought on by passing clouds. In the case of WT, flicker is brought about by fluctuations in the output power because of changes in wind speed, wind shear, and the effects of the tower's shadow. When compared to their fixed-speed counterparts, variable-speed WT has demonstrated much superior performance in terms of flicker emission [158].

5.3.2. Overloading of Existing Transmission Lines

The unpredictable nature of solar and wind power adds another layer of complexity to the process of achieving an equilibrium between demand and supply. In the middle of the day, when demand is at its highest, the present transmission system struggles to keep up a balance between demand and supply. The distributed nature of these energy supplies adds another layer of complication to the existing grid. If the producers suddenly create an excessive amount of power, there is the potential for a surge, which would result in the shutdown of the entire system. A transmission line has a certain capacity, and if this limit is exceeded, the line will be damaged because of the thermal loads [160].

5.3.3. Protection Issues

The unpredictable nature of solar and wind power creates additional challenges when attempting to achieve balance. Changing short circuit levels, reverse power flow, a lack of continuous fault current, blinding protection, and islanding are the primary protection concerns associated with the connecting of RES to the grid and presented below [160].

1) Change in Short Circuit Levels

Direct grid tied synchronous machine-based RES increases the number of network faults. Only small and unreliable fault currents may be produced using induction generators. As was previously observed, a high fault level signifies a robust grid, in which the impacts of adding a new DSG on the point of common coupling (PCC) voltage is probably not going to be too severe. But another challenge regarding system protection is the rise in network fault brought on by the installation of DSG.

When it comes to determine the rating of current transformer (CT) , circuit breakers (CB), and the coordination between over current relays, the primary criterion that is employed is the short circuit current level in the network. The equivalent impedance of the system at the failure location is what is used to quantify the short circuit level. The addition of generators to a system has the potential to lower the corresponding system impedance, which would result in a rise in the fault level. In this scenario, the fault current may be greater than the capability of the CB that is already installed. In addition, CT saturation can be caused by high fault currents. In addition, altered fault levels might make it difficult for over-current relays to work in cooperation with one another, which can result in an inefficient functioning of protective systems [5].

2) Lack of Sustained Fault Current

For protection relays to accurately identify fault currents and differentiate them from regular load currents, faults must generate a substantial and extended increase in current levels, which can then be detected by the relays. When fault currents stem from RES and are limited in their magnitude, it presents a challenge for overcurrent-based protection relays to effectively discern faults. This complexity arises due to the

characteristic lower fault currents often associated with RES compared to traditional power sources. Within the realm of renewable energy generation, the prevalent types of generators encompass induction generators, small synchronous generators, and power semiconductor converters. Induction generators possess restricted capacity to contribute significant fault currents to asymmetrical faults, while their ability to maintain sustained fault currents in three-phase faults is limited. Similarly, small synchronous generators tend to struggle with providing fault currents that significantly exceed their rated current. The constraints of power semiconductor devices, found in power electronics converters, lie in their inability to withstand prolonged high overcurrent levels. As a result, power electronics converters incorporate internal limitations to control the current flow. In cases where fault currents are inadequate to sustain a fault condition, the capacity of relays to detect faults is compromised [160].

3) Blinding of Protection

It is anticipated that the proportion of the grid to the overall fault current would decrease when DSGs are present. This reduction introduces the possibility that certain short-circuits might go unnoticed, primarily due to the diminished grid contribution to the short-circuit current, which may not surpass the pickup current of the feeder relay. This situation arises because the grid's contribution is comparatively smaller. Ensuring the proper functioning of over-current relays, directional relays, and reclosers relies on the accurate detection of unusual current patterns. Consequently, protections dependent on these devices face an elevated risk of malfunctioning as a consequence of the decreased grid contribution [160].

4) Islanding

Islanding is the state that occurs when a portion of the network is separated from the main grid and continues to function as its own independent system. This system may be provided with electricity by one or even more generators. The isolated network will exhibit unusual changes in frequency and voltage as a direct consequence of islanding. The opening of an auto protective relay during a failure has the potential to result in the establishment of two separate systems that function at frequencies that are distinct from one another. If the auto recloser is allowed to shut while the two systems are operating out of phase, the outcome might be catastrophic. Furthermore, the configuration of the transformer connection can play a significant role in the occurrence of islanding operations, potentially leading to the formation of an ungrounded system. The presence of such an islanded system can pose risks to maintenance workers who might unknowingly interact with an isolated portion of the network. Given that islanding is recognized as a potentially hazardous situation, it is recommended that Distributed Synchronous Generators (DSGs) be promptly disconnected from the primary grid once an islanding condition is detected [160].

5.3.4. Optimal Placement of RES

The selection of a suitable connection point for the RES to the grid is one of the most important tasks involved in the process of integrating them. It is possible that the performance of the network will suffer if crucial factors, such as the connecting point and the capacity of the RES, are not accurately specified. This circumstance has the potential to result in an increase in the amount of energy loss and voltage variations,

Injecting RES close to load centers or distribution transformers would result in variations in the flow of power, which will influence the overall voltage of the system. Abnormal voltage variation causes power fluctuations in a low-voltage (LV) system, and the problem significantly gets the worst at high renewable penetration levels, when there will be a sudden surge in the operating voltage, primarily under situations of reduced ED [161].

5.4 SOLUTIONS TO ADDRESS RES INTEGRATION CHALLENGES

This section provides a variety of possible solutions to the issues that are caused by the unpredictability and uncertainty of HRES power generation, and these answers are being considered as potential remedies. While deciding on a certain approach, the features of the network and how cost-effective the technology is to implement are the most important factors to consider. Grid infrastructure, operational procedures, the type of production, and regulatory considerations are all factors that influence the various solutions that are the most economically feasible and practical. In general, systems require more flexibility to be able to absorb the added unpredictability that is brought about by renewable. Better forecasting, operational procedures, energy storage, demand side flexibility, flexible generators, and other techniques can all contribute to the attainment of flexibility [160].

5.4.1. Forecasting of Wind and Solar Resources

The forecasting of wind and solar energy production holds the potential to substantially mitigate the uncertainty associated with these RES. This predictive capability

not only aids in minimizing the requirement for operational reserves but also empowers grid operators to more effectively allocate resources, adjusting their commitments to align with the variations in wind and solar power generation proportions. Forecasting methodologies encompass two distinct approaches: short-term and long-term forecasting. Short-term forecasts, often presented in hourly intervals, tend to be less intricate compared to their long-term counterparts. The accuracy of short-term forecasts typically falls within the range of 3 to 6% of rated capacity when predicting one hour in advance, while extending to approximately 6 to 8% of rated capacity for predictions made a day in advance. These forecasting techniques provide a valuable tool for enhancing grid stability and optimizing energy resource allocation. The utilization of these forecasts not only aids in managing variability but also contributes to the efficient integration of RES into the power grid [160].

5.4.2. Operational Practices

Quick dispatch helps to control the uncertainty of renewable energy power by reducing the demand for regulatory resources, improving efficiency, and providing access to a larger collection of resources that may be used to balance the system. In addition, fast dispatch minimizes the amount of time it takes to balance the system. Because of rapid dispatch, the levels of load and generation may be more closely matched, which reduces the need for costlier regulating reserves [160]

5.4.3. Reserves Management

It is possible to apply modified reserve management strategies to assist in mitigating the effects of the variable output of wind and solar electricity. This includes putting restrictions on wind and SPV power ramps to decrease the need for backups and allowing

intermittent resources to supply backups or other support facilities like as control, inertia, and so on [160].

5.4.4. Interconnecting more Distributed Resources

The effects of intermittent renewable energy can be mitigated by linking a considerable number of small, distributed energy resources that are dispersed throughout a broader geographical region instead of big units concentrated in one area. Because local fluctuations only affect a limited number of units and not the overall output power, there will not be much variation in the total power that is produced [160].

5.4.5. Energy Storage

Energy storage has become a typical choice to limit the amount of power that must be curtailed as the percentage of RES has risen. The various energy storage options are superconducting magnetic energy storage, flywheel, electrochemical capacitors, pumped storage power plant, compressed air energy storage, hydrogen storage [160].

5.4.6. Use of HRES

Employing a hybrid configuration that combines both wind and SPV, along with other RES, holds the potential to mitigate power fluctuations to a certain extent. This advantageous outcome is attributed to the synergistic nature of the outputs from these HRES, which complement each other in terms of generation patterns. By harnessing the strengths of various RES within a hybrid framework, the resultant combined output tends to exhibit a more stable and consistent profile, thereby contributing to a reduction in power variations.

5.4.7. Demand Response

An effective approach to counteract the adverse impacts of abrupt ramps is to enhance demand-side flexibility. Beyond its role in peak demand reduction, DR can be harnessed for backup support and auxiliary services as well. When compared to the expenses associated with maintaining additional reserves, leveraging DR to restore system equilibrium during infrequent instances of substantial shortages or excesses of renewable power can yield substantial cost savings [160].

5.5 CONCLUSION

The recent public awareness of environmental problems, which are caused by the coal-fired power station, has stimulated interest in the development of current smart grid technology and its integration with climate-friendly green renewable energy. Due to the intermittent nature of RES, integrating it with the power grid presents huge technological challenges. These challenges need to be addressed to build a power system that is sustainable and environmentally friendly. In this chapter, we have covered the advantages of integrating RES into the grid, various possible issues and challenges that might arise, as well as suggested few solutions.

CHAPTER 6

INTELLIGENT MODELLING FOR THE SIZING OF HRES

6.1 INTRODUCTION

In chapter 4, the feasibility and techno-economic analysis along with design and development of HRES models for rural electrification has been discussed. These models have been developed using the HOMER Pro platform. However, the HOMER Pro has certain limitations, such as black box coding, which makes it challenging to comprehend the algorithms and calculations employed. Additionally, HOMER Pro lacks intra-hour variability and does not allow for flexible simulation models of system components [162].

To address these limitations, there is a need for intelligent approaches that can overcome these challenges. In this connection, extensive literature review suggests that intelligent approaches show more promising results compared to simulation tools like HOMER Pro [162]. Further, the size optimization of BMG and BGG in HRES has been rarely explored, as most studies have employed fixed generator sizes. Additionally, most of the research has focused on optimizing OFG HRES, while limited analysis has been conducted on grid-connected scenarios. Moreover, the application of intelligent optimization approaches for grid-connected systems remains largely unexplored.

To address the above stated issues, the present chapter aims to perform the size optimization of various OFG, and grid connected HRES for selected sites. Based on the availability of RES, different models have been selected to meet the load demand of

specific rural areas. The sizes and cost of different generators are then calculated using the recently developed AO algorithm and compared with the results of HS and PSO algorithms implemented on the MATLAB platform.

In the subsequent sections, the underlying basics, and theories of AO, HS, and PSO algorithms are explained. Furthermore, the chapter presents a systematic procedure for effectively implementing these algorithms through flowcharts, ensuring a comprehensive understanding of the optimization process.

6.2 THE AQUILA OPTIMIZATION (AO) APPROACH

The AO algorithm was created by Abualigah et al. in 2021 [163]. This algorithm is based on swarms and was inspired by the innate hunting behavior of aquila's. Aquila guards over a domain that has been estimated to cover up to 200 km^2 of land. They frequently construct large nests in lofty locations, as is their wont. Because of its boldness during the hunt, aquila is one that has been studied the most out of all the species of birds worldwide. While a male aquila began hunting by himself, he was able to bring down a significantly larger number of preys. Aquila use their swiftness and their sharp talons to pursue a wide variety of prey, including squirrels, rabbits, and a range of many other smaller critters. It has also been documented that they engage in predation on fully grown deer. After that, the ground squirrels constitute the second most significant portion of aquila's diet [163]. The majority of aquila can deftly and fast transition among hunting ways as conditions dictate. It is widely accepted that aquila makes use of four distinct hunting strategies, each of which possesses various distinguishing traits. Aquila can swiftly and successfully adapt its hunting strategies to suit the needs of a wide variety of prey, and

it then pursues its prey using a combination of its lightning-fast speed and its formidable feet and claws.

6.2.1. Mathematical Modelling of AO Technique

The AO algorithm simulates aquila's hunting behavior by mimicking the actions of each step of the hunt. The optimization procedure of the AO algorithm is represented through four methods, which describe the key steps involved in the algorithm. The following is an overview of the mathematical model of these steps in detail [164].

1) Expanded exploration

Aquilas utilize an expanded exploration strategy, wherein they ascend to considerable heights to scout for prey over a wide expanse in a single sweep. Once the prey's location is ascertained, the Aquila swiftly plunges down vertically to seize it. Consequently, the mathematical representation of this behavior can be expressed as follows:

$$Y_1(\varphi + 1) = Y_b(\varphi) \times \left(1 - \frac{\varphi}{T}\right) + (Y_m(\varphi) - Y_b(\varphi) \times r_1) \quad (6.1)$$

$$Y_m(\varphi) = \frac{1}{n}\sum_{j=1}^{n} Y_j(\varphi) \quad (6.2)$$

Where; $Y_1(\varphi + 1)$ is the solution of the next iteration of φ which is generated by first search method Y_1; $Y_b(\varphi)$ denotes the best position, $Y_m(\varphi)$ is the average location of all aquilas in the current iteration. φ and *T* are the current and maximum iteration, respectively. n is the population size, and r_1 denotes an arbitrary numeral between 0 and 1.

2) Narrowed exploration

Narrowed exploration is the most frequently employed hunting method. After landing within the designated area and flying around the target, it attacks the victim with brief

gliding moves using short glides. The position update formula is expressed by the following notation:

$$Y_2(\varphi + 1) = Y_b(\varphi) \times lf(d) + Y_r(\varphi) + (x - y) \times r_2 \quad (6.3)$$

Where; $Y_2(\varphi + 1)$ is the solution of the next iteration of φ which is generated by second search method Y_2 ; $Y_r(\varphi)$ an arbitrary location of aquila, d is size of dimension, r_2 is random value within the range (0, 1). $lf(d)$ is Levy Flight Function.

$$lf(d) = S \times \frac{U \times \sigma}{|V|^{\frac{1}{\beta}}} \quad (6.4)$$

Where; S and β are constants, U and V are random numbers

3) Expanded exploitation

In expanded exploitation, aquila descends vertically to conduct an initial attack after a rough estimation of the location of prey. Aquila takes advantage of the specified region to approach near and to attack the prey. Mathematically, this behavior can be formulated as follows:

$$Y_3(\varphi + 1) = \big(Y_b(\varphi) - Y_m(\varphi)\big) \times \alpha - r_4 + \big((ub - lb) \times r_5 + lb\ \big) \times \delta \quad (6.5)$$

Where; α, δ are exploitation adjustment parameters in the range of 0-1. *lb* and *ub* are lower and upper bound. r_4, r_5 are random numbers between 0 and 1.

4) Narrowed exploitation

Aquilas use this approach to pursue their prey in the direction of their escape trajectory and then attack the prey while it is still flying around in mid-air. In terms of mathematics, the following is the formulation of this conduct:

$$Y_4(\varphi+1) = qf \times Y_b(\varphi) - (g_1 \times Y(\varphi) \times r_6) - g_2 \times lf(d) + r_7 \times g_1 \quad (6.6)$$

Where; $Y(\varphi)$ is the current position, qf is the value of quality function. g_1 is movement parameter during tracking prey value of this varies from 2 to 0. r_6 , r_7 are random numbers between 0 and 1. The AO initiates the improvement process by generating a predetermined set of solutions known as the population. Over successive iterations, the AO employs search strategies to explore positions near the optimal solution or the best solution found so far. Each solution adjusts its position based on the best solution obtained through the AO's optimization processes. To emphasize a balance between exploration and exploitation in the AO's search strategies, the above four steps: expanded exploration, narrowed exploration, expanded exploitation, and narrowed exploitation have been utilized. The search process of the AO concludes once the termination criterion is satisfied. Further, the flow chart for the AO algorithm is presented in Fig. 6.1 [163].

6.3 HARMONY SEARCH (HS)

HS was motivated by the process of music improvisation, which involves a group of performers adjusting the pitch of their instruments to generate beautiful harmony. When the pitches of all musical instruments are synchronized or offer a pleasing harmony, each musician remembers the experience, maximizing their chances of providing a pleasing harmony the next time. Further, the following section summarizes the implementation steps for the HS [140]:

6.3.1. Steps for HS Algorithm

The process begins with the formulation of the problem. The following is a description of the optimization problem using the objective function f(z):

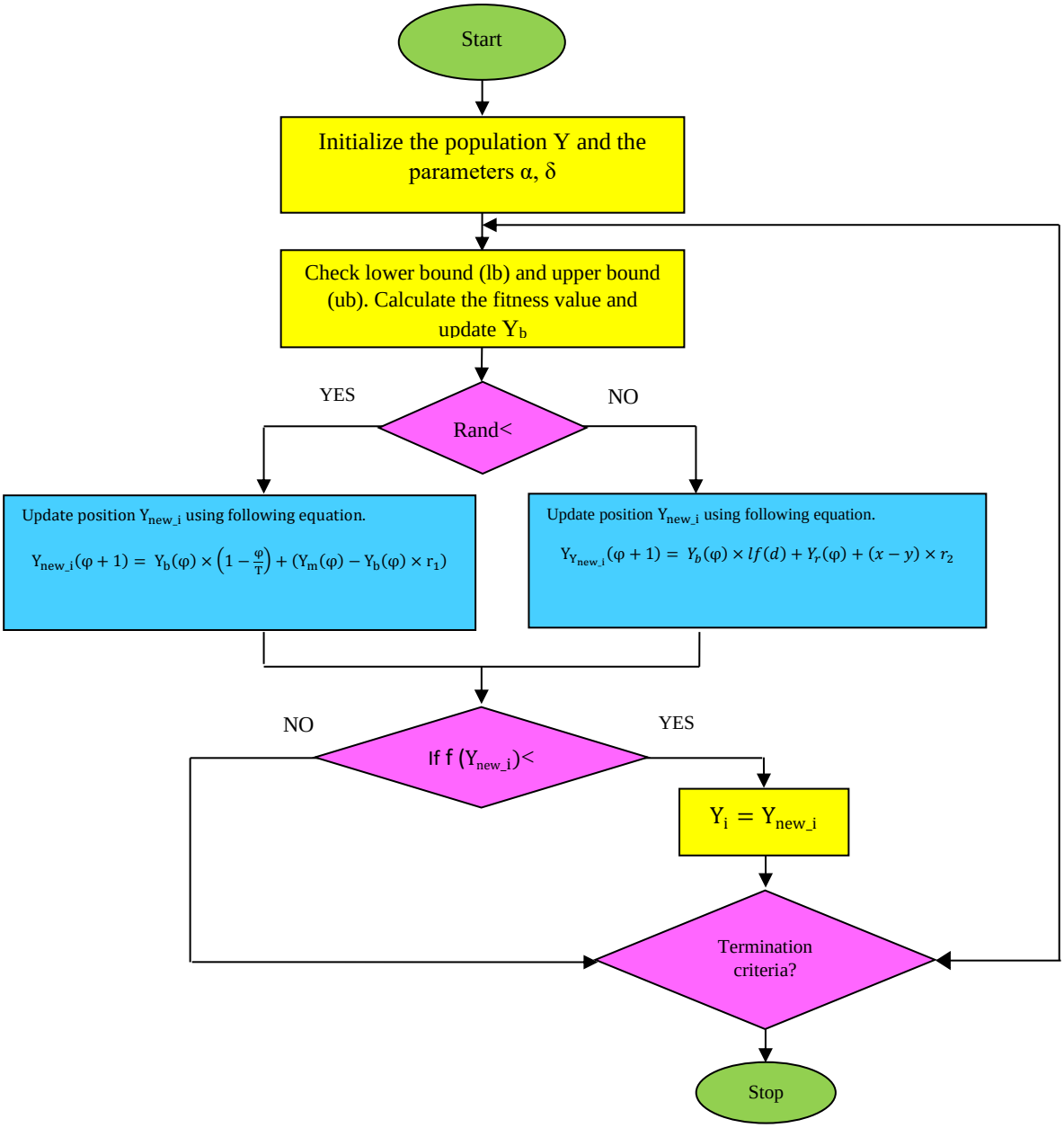

Fig. 6.1 Flow Chart of AO Algorithm

Min. f(z) Subjected to

$$z_k^{min} \leq z_k \leq z_k^{max} \qquad (6.7)$$

(k = 1, 2, 3, 4, n)

Here, $z = [z1, z2, z3, \ldots\ldots\ldots zn]^T$, are decision variables; *n* represents number of decision variables.

Further, the various steps for executing the HS code are summarized as follows:

- **HS Parameter Initialization**

Initialization of harmony memory matrix (HMM) elements is accomplished by using the following equation:

$$z_{kl} = z + rand(z_k^{max} - z_k^{min}) \quad (6.8)$$

Where, *l = 1,2,3, 4.....n; k = 1,2,3,4..... HMS*

Where, z_k^{max}, z_k^{min} are lower & upper limits of decision variable; HMS is harmony memory size.

Modifications to the new vector of harmony based on earlier perspectives are considered improvisation or harmony adjustment. To generate new harmony, the following operations are conducted with each decision variable [140].

A random number (RN) between 0 and 1 is created and compared with harmony memory consideration rate (HMR).

If RN > HMR, then z_{kl}^{new} can be updated as:

$$z_{kl}^{new} = z_l^{min} + rand(z_l^{max} - z_l^{min}) \quad (6.9)$$

Where, *l = 1,2,3, 4.....n; k = 1,2,3,4.....HMS*

If RN ≤ HMR, then the following equation is used to randomly select one of the decision variables stored in the current harmony memory [140]:

$$z_{kl}^{new} = z_{kl} \quad (6.10)$$

- HS addresses the pitch adjustment technique by which the new harmony will move to an adjacent value within the bounds of possibility. After HS parameter initialization, a random variable between 0 and 1 is created to execute the pitch adjustment process.
- **Updation**

  If the newly created harmony vector produces improved outcome, then the new harmony vector is considered in harmony memory.
- **Stopping Criterion**

The algorithms will be used again and again until the best outcomes are achieved. When the optimal outcomes are obtained, the algorithm will come to a halt, and the best results will be saved.

6.4 PARTICLE SWARM OPTIMIZATION (PSO)

PSO is a metaheuristic method for solving complex optimization problems that employs a population (swarm) of so-called particles. Every particle, which is made up of m decision variables, is represented by a vector, which describes its location in the search space. Particles focus on two knowledge sources which are acquired by means of the personal best and possible best experiences of the swarm and move by a specific speed through the search space. The procedure is carried out until the stopping requirement is reached [165].

To begin, in PSO, a population of particles is randomly generated in the search space using a uniform distribution. Every particle uses its memory to navigate through the search space to reach a better location than its current one. In its memory, a particle

memorizes the best experience it had its own (P_b) as well as the best experience of the group (G_b). The particle update sequence is as follows at each cycle [165].

$$\vartheta_j\,(i+1) = w_f \times \vartheta_j(i) + L_{c1} \times r_{a2}(g_{btj}(i) - y_j(i)) \tag{6.11}$$

$$y_j(i+1) = \vartheta_j(i+1) + y_j(i) \tag{6.12}$$

Where, ϑ_j is j^{th} particle velocity; y_j is j^{th} particle position; L_{c1}, L_{c2} symbolizes learning coefficients; r_{a2} denotes random number lies in between 0 to 1, w_f is weight factor of inertia, A higher weight factor leads to a global search, whereas a smaller number leads to a local search.

6.4.1. Steps for PSO Algorithm

The various steps involved in PSO algorithm are presented as follows [166]:

- **Initialization of the Problem**

The first step is formulation of objective function along with constraints. PSO parameters that may be adjusted are also specified.

- **Initialization of Particles**

The search space has been initialized with m particles, each with a different set of decision vectors generated at random. Initiation of each particle is done using this equation.

$$y(0) = y_{mn,j} + rand(y_{mx,j} - y_{mn,j}) \tag{6.13}$$

Initial and final values of y for each particle are denoted by y_{mx} and y_{mn}, respectively

- **Fitness Function Evaluation**

Based on the values of the decision variables affiliated with each particle, an objective function is calculated.

- **Updation**

P_b is calculated for each particle, and G_b is chosen based on the population's best. Additionally, each particle is free to move to the new location. More precisely, each particle's velocity and position are updated.

- **Stopping Criteria**

The algorithm is terminated when the maximum number of iterations is reached, and G_b is regardedt as he best solution.

6.5 Fitness Function

The NPC is the fitness function considered for this research and can be formulated as [3]:

$$NPC = npc_{pv} + npc_{wt} + npc_{bmg} + npc_{bgg} + npc_B + npc_{inverter} + \in_G^P - \in_G^S \qquad (6.14)$$

This NPC has to be minimized with certain boundary constraints and HRES components limit which are discussed in the subsequent sections.

6.6 DESIGN CONSTRAINTS

To solve the size optimization problem, the following constraints must be met by the possible solution during the system's operation [3]:

6.6.1. Upper and Lower Bounds of Components

To fulfill the load requirement, the size of system components such as n_{pv}, N_W, BGG_p^o, and BMG_p^o may differ in the developed framework. As a result, these components' upper and lower bounds are specified as [3]:

N_{pv} is an integer, $N_{pv}^{min} \leq N_{pv} \leq N_{pv}^{max}$ (6.15)

N_B is an integer, $N_B^{min} \leq N_B \leq N_B^{max}$ (6.16)

N_W is an integer, $(N_W)^{min} \leq N_W \leq (N_W)^{max}$ (6.17)

BMG_p^o is an integer, $(BMG_p^o)^{min} \leq BMG_p^o \leq (BMG_p^o)^{max}$ (6.18)

BGG_p^o is an integer, $(BGG_p^o)^{min} \leq BGG_p^o \leq (BGG_p^o)^{max}$ (6.19)

6.6.2. Storage Limits on BESS

The upper and lower limits (E_{bmn}, E_{bmx}) of the battery backup system have also been regarded as one of the criteria to run the battery safely and are represented as [3]:

$E_{bmn} \leq E_b(t) \leq E_{bmx}$ (6.20)

6.6.3. Power Reliability

A user experiences non-availability of energy when the ED exceeds the amount of available generation. Thus, the power reliability in terms of LPSP may be calculated using the formula discussed in section 3.4 of chapter 3.

6.7 TECHNICAL AND ECONOMICAL INPUT DATABASE

To identify the most appropriate size of the proposed HRES, it is necessary to know the techno-economic input parameters, which are presented as:

6.7.1. Electrical Load Demand (kW)

The ED for the designated regions has been meticulously calculated in section 4.4 of chapter 4. This calculation serves as a foundational step in the formulation of a HRES

aimed at electrifying the chosen location. Further, Fig. 6.2 displays the hourly ED that was measured for the site I throughout three distinct seasons.

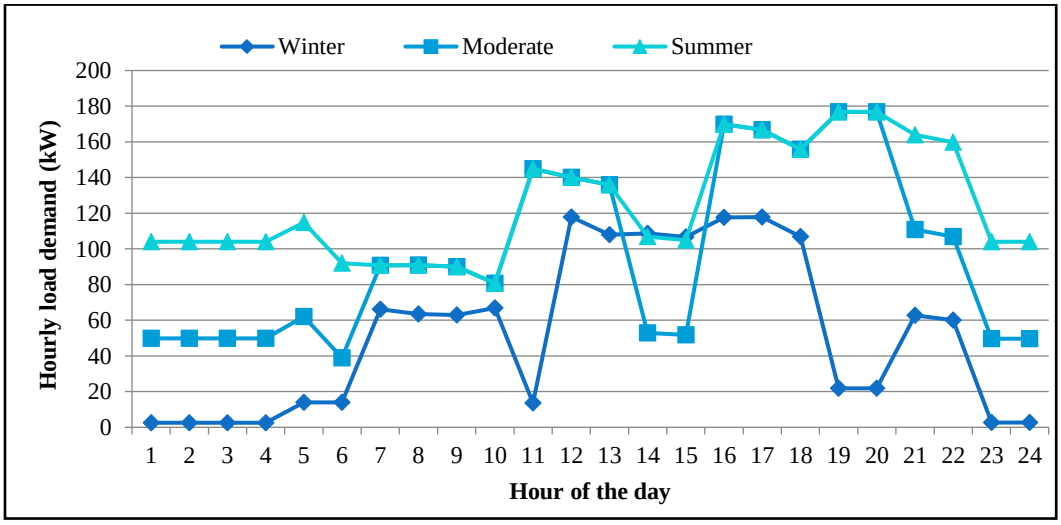

Fig. 6.2 Hourly Load Demand of Site I

The load deman for three seasons for study area I has been computed 3021.58 kW/day, 2421 kW/day, and 1387.58 kW/day, respectively. For site II, the load demand of these seasons is computed as 3597.89 kWh/day, 2798.4 kWh/day, and 1601.21 kWh/day, respectively. Further, Fig. 6.3 depicts the daily ED for the research area during the three seasons.

6.7.2. Solar Irradiance

The monthly average solar radiation data has been collected from NASA. Fig. 6.4 depicts the solar irradiation for the specified region I. The study area gets 5.267 kWh/m^2/day of solar radiation on average. Further, Fig. 6.5 illustrates the monthly daily average solar irradiation for the selected site II. It has been found that the solar irradiance varies throughout the year, with May having the most significant value of 6.74 kWh/m^2/day and December having the lowest value of 3.53 kWh/m^2/day.

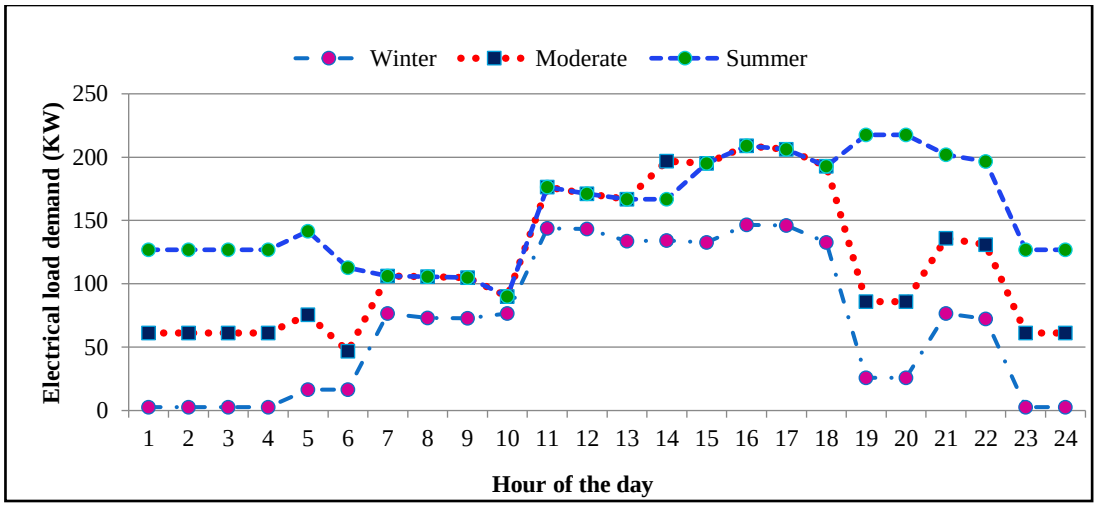

Fig. 6.3 Hourly Load Demand of Site II

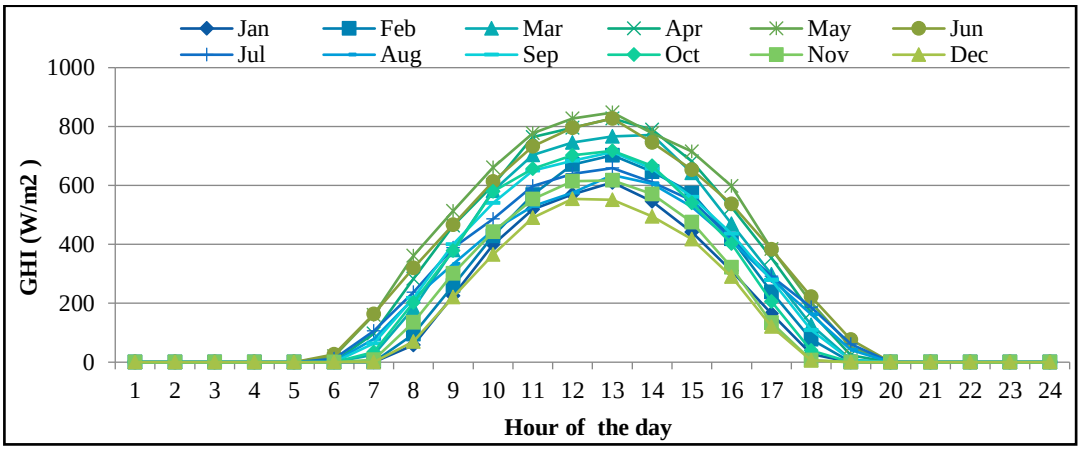

Fig. 6.4 Month-Wise Daily Solar Irradiations for Site I

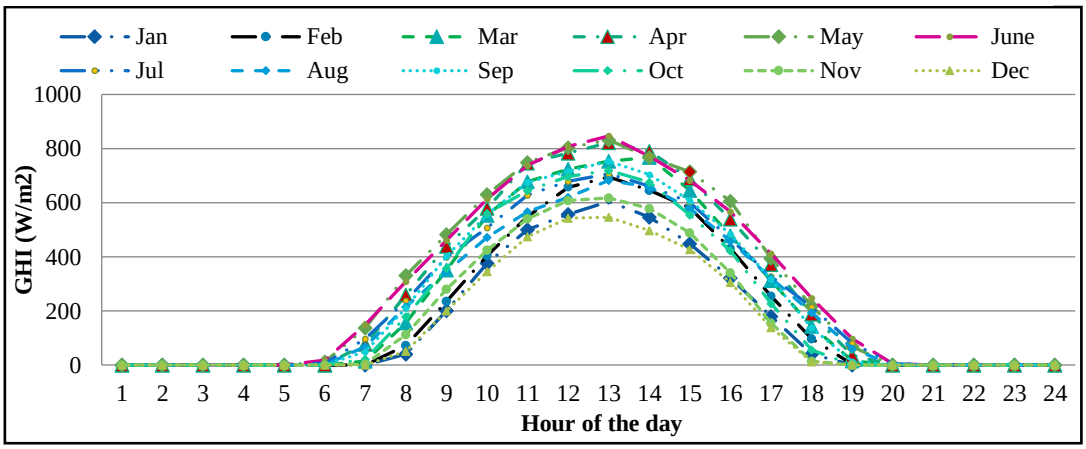

Fig. 6.5 Month-Wise Daily Solar Irradiation for Site II

6.7.3. Average Ambient Temperature

The ambient temperature that was measured throughout the investigation region I is depicted in Fig. 6.6. NASA was the source for the data collection used to determine the monthly average atmospheric temperature. The average temperature of the surrounding air fluctuates between 4°C and 43°C across the course of the year. Further, Fig. 6.7 illustrates the monthly hourly average ambient temperature of the selected site II.

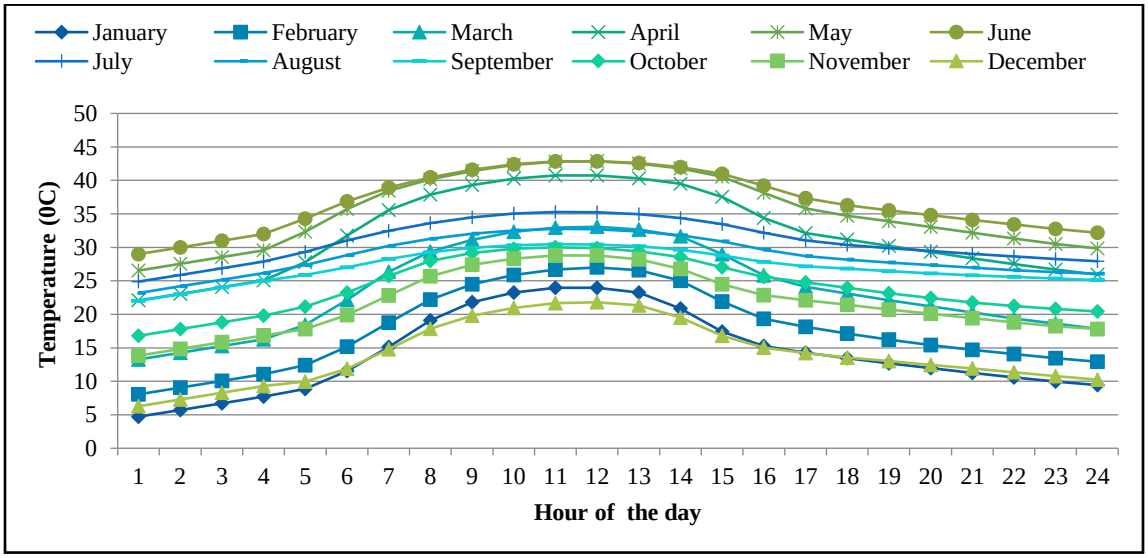

Fig. 6.6 Monthly Average Ambient Temperature for Site I

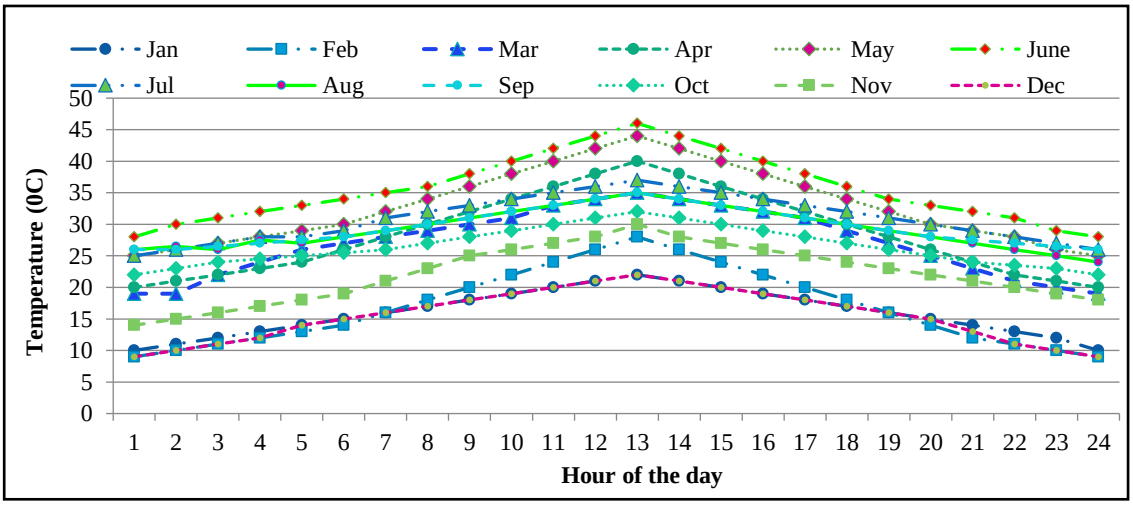

Fig. 6.7 Monthly Average Ambient Temperature for Site II

The annual range of the ambient temperature has been recorded as 9°C to 46°C

6.7.4. Wind Speed

Fig. 6.8 shows the monthly variations in the hourly wind speed at the site II. With a calculated wind power density of 124 W/m^2, the anticipated yearly average wind speed is 5.18 m/s.

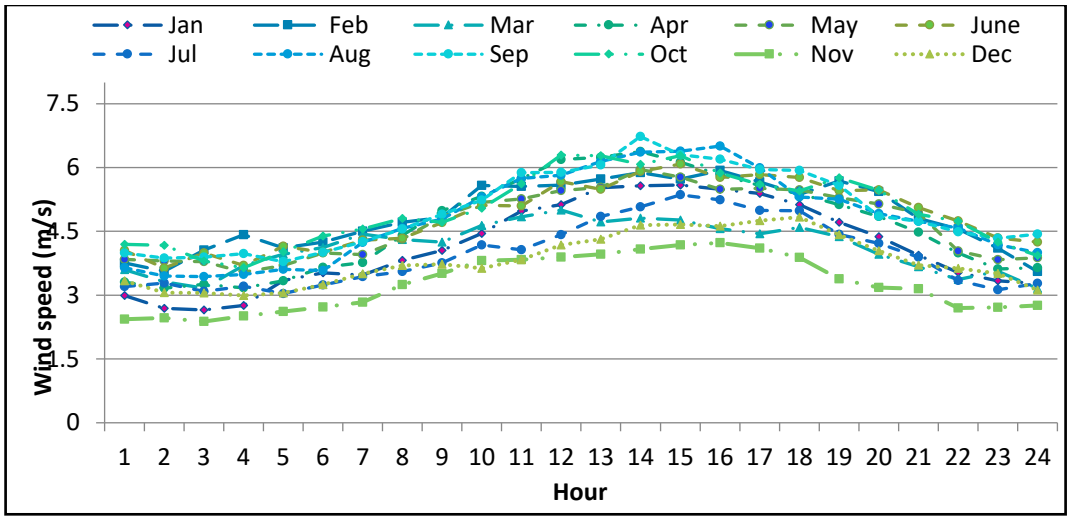

Fig. 6.8 Monthly Average Wind Speed for Site II

6.7.5. Scheduling of BGG and BMG

In the current research, BGG and BMG are scheduled for site I and site II to operate

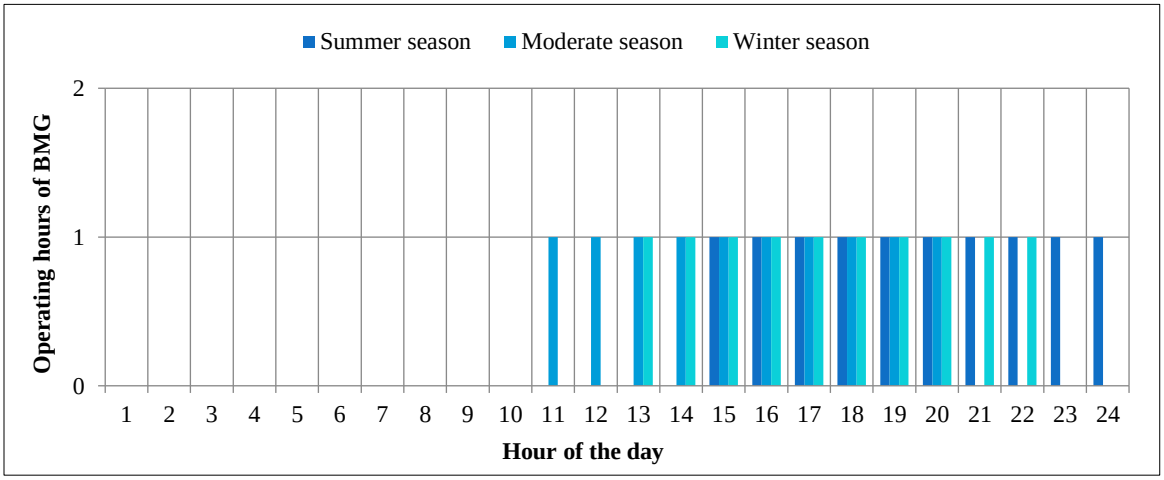

Fig. 6.9 Scheduling of BMG for Study Area I

As shown in Fig. 6.9 and Fig. 6.10, the BGG runs for 10 hours daily, while the BMG

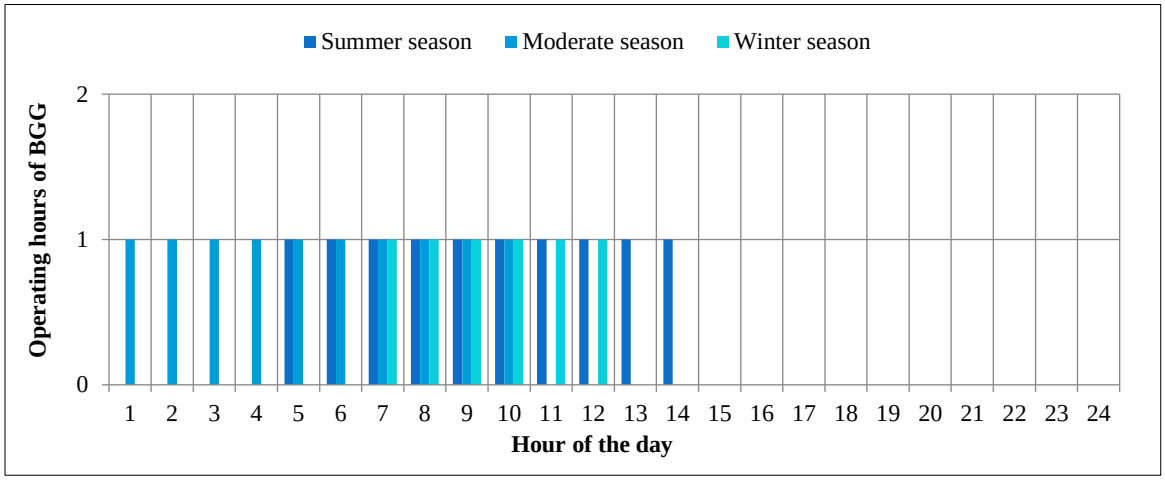

Fig. 6. 10 Scheduling of BGG for Study Area I

operates for 6 to 10 hours per day.

6.7.6. Parameters of AO, HS and PSO Algorithms

In order to achieve the best possible results with the fitness function, the algorithm specifications have been set to maximum iterations = 150 and run = 30. For AO; exploitation adjustment coefficients for AO; $\alpha = 0.1$; $\delta = 0.1$; Population size = 30, For

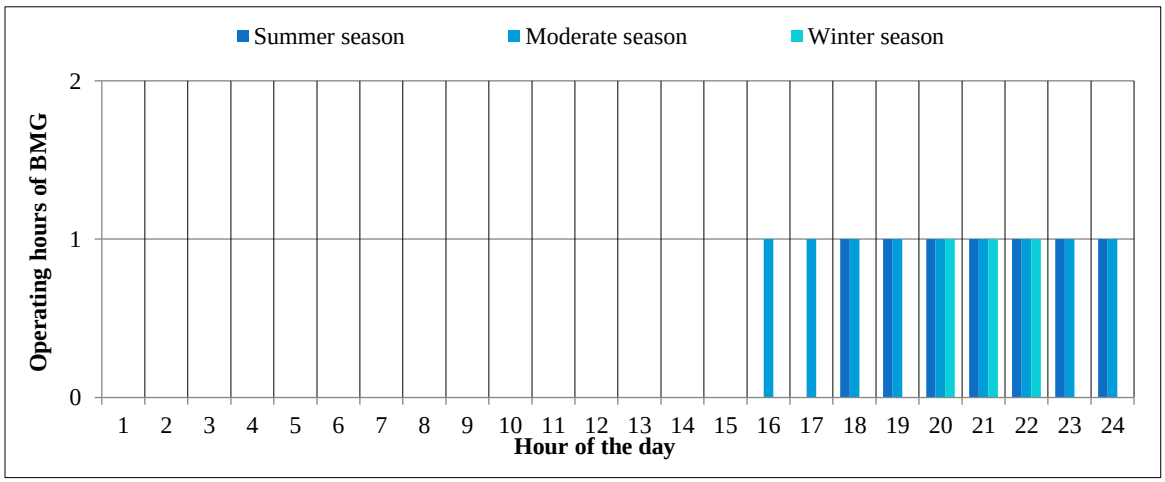

Fig. 6.11 Scheduling of BMG for Study Area II

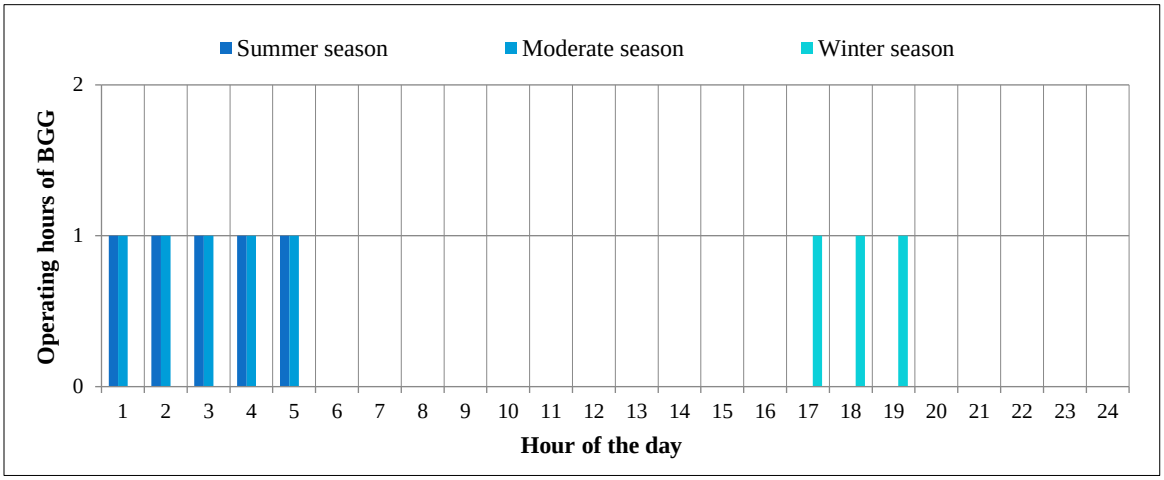

Fig. 6. 12 Scheduling of BMG for Study Area II

HS; HMR= 0.95; HMS=5; Pitch adjusting rate (PR) = 0.1; Maximum value of pitch adjustment rate (PRmx) =1; Minimum value of pitch adjustment rate (PRmn) =0.1. The setting of various parameters of the PSO algorithm is as follows: inertia (w) =5, cognition coefficient (C1) =2, and social coefficients (C2) =2.

6.7.7. Cost parameters of HRES Components

The economic implications of a variety of HRES components including CC, OMC, SV, and fuel price (FP) are outlined in Table 6.1. The OMC of SPV, BMG, and BGG are respectively 2%, 5%, and 5% of CC, whereas the SV of SPV, BMG, and BGG are respectively 10%, 30%, and 30% of CC.

Table 6.1 Various Costs of Different Components of HRES

RES	Capacity considered (W)	CC ($)	OMC	SV	FP ($/ton)
SPV	235	192	2%	10%	-
BMG	1000	1033	5%	30%	15
BGG	1000	660	5%	30%	8
WT	3300	3500	2%	30%	-

6.7.8. Project Parameters

This research has considered the system's life expectancy of 25 years; this is the period for which it functions properly. An annual rate of interest is considered to be 11%.

6.8 RESULTS AND DISCUSSION FOR SITE-I

As part of this investigation, an attempt has been made to determine the most optimal model for the HRES, considering the numerous distinctive types of RES. At the beginning, three different arrangements of HRES operating in OFG mode were taken into consideration:

i. Model H-11: BMG/SPV/ BESS
ii. Model H-12: BGG/ SPV/BESS
iii. Model H-13: BMG/SPV/ BGG/BESS

All the OFG models are optimized using the AO approach and analyzed in terms of the technical and financial concerns that need to be addressed to determine the optimal OFG model. Further, the optimal OFG model is then contrasted with the grid tied SPV/BMG/BGG/BESS HRES system, and the most optimal choice is identified because of this analysis. In the end, the outcomes have been evaluated and contrasted with those acquired through the HS and PSO.

6.8.1. Optimization Results of OFG HRES

The AO technique in MATLAB effectively replicates the stated OFG system, satisfying the total demand for the region. Table 6.2 shows the optimum outcome of the OFG system after hourly simulation. As it is apparent from Table 6.2, model H-13 has the minimum NPC and COE out of all the available options. The most efficient configuration

for an OFG consists of an SPV system with a capacity of 234.06 kW, a BMG with a capacity of 200 kW, a BGG with 188 kW, and a BESS capacity of 607.20 kWh. It costs $1089200 for the NPC and $0.159 for the COE/ kWh, respectively.

Table 6.2 Result of OFG HRES for Different Algorithms

Model	OT	PV_p^o (kW)	E_B (kWh)	BGG_p^o (kW)	BMG_p^o (kW)	NPC ($)	COE ($/kWh)
H-11	AO	282	1291	284	-	1183280	0.173
	HS	237.35	696	180	-	1225371	0.201
	PSO	246.75	720	120	-	128345	0.209
H-12	AO	279.89	1989	-	522	1190900	0.175
	HS	235	739.2	-	190	1299878	0.215
	PSO	240.87	7228.8	-	187	1290123	0.211
H-13	AO	234.06	607.2	200	188	1089200	0.159
	HS	232.65	684	165	209	1170769	0.197
	PSO	234.53	679.2	200	168	1185385	0.198

6.8.2. Optimization Outcome of Grid Connected HRES

MATLAB was used to minimize the objective function by employing the AO approach. The optimum values for each variable, as calculated by the hourly simulation is presented in Table 6.3. The optimal HRES consisted of 235 kW of SPV, 10 kW of BGG, 64 kW of BMG, and 50.40 kWh of battery storage. It is estimated that the total costs associated with NPC and COE will be $547,670 and $0.0768/kWh, respectively.

6.8.3. Assessment of OFG and Grid Connected HRES

A comparison has been carried out between the grid-tied approach and the optimal architecture for the OFG, with a specific focus on NPC and COE. The results, presented in

Table 6.2 and Table 6.3, indicates that both NPC and COE for the grid tied HRES are lower than those for the OFG configuration. Thus, the grid tied HRES is proven to be a more cost-effective option. Based on these findings, it has been concluded that the recommended sites would benefit significantly from adopting a grid interlinked HRES that incorporates SPV, BMG, BGG, and batteries. The schematic representation of this proposed system layout is depicted in Fig. 6.11.

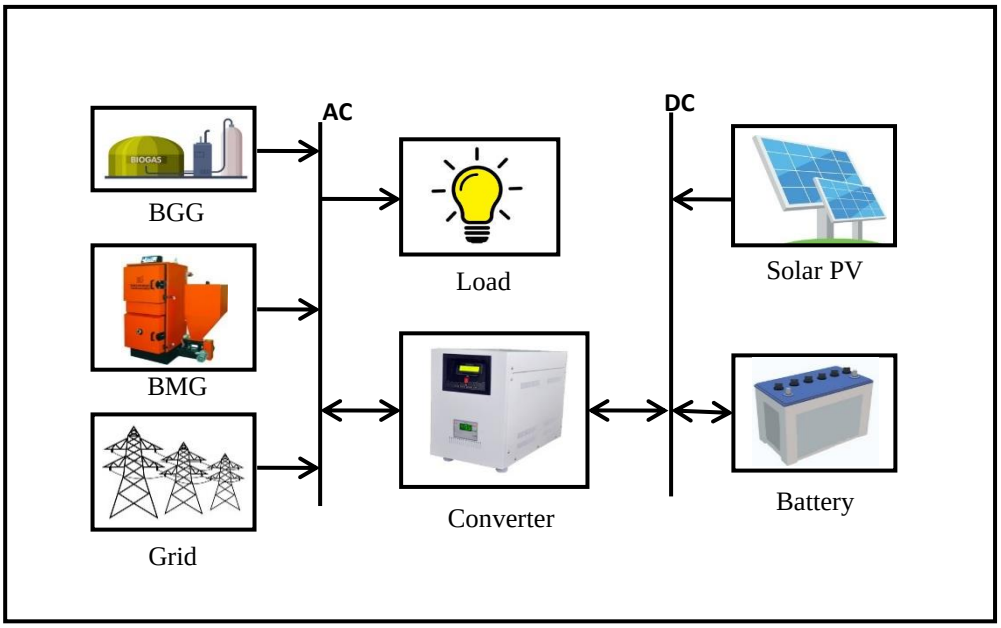

Fig. 6.13 Setup for Proposed HRES

6.8.4. Assessment of Various Optimization Techniques

Finally, different optimization strategies were contrasted to determine the most optimal results for the optimized configuration. The results of the AO method are contrasted against the outcomes of the HS and PSO techniques as shown in Table 6.4. AO produces more optimal results when compared to HS and PSO. Furthermore, several other parameters are investigated and displayed in Table 6.5, and the results make it extremely obvious that AO outperforms. In addition, the convergence curves for PSO, HS, and AO

for NPC are depicted in Fig. 6.12. It can be clearly seen from Fig. 6.12 that the AO converges very quickly and provides a satisfactory solution prior to twenty iterations. On the other hand, both HS and PSO converge after 135 iterations, which shows that AO converges faster than other OT.

Table 6.3 Various Algorithms' Findings for the Optimal Setup for 0% LPSP

Algorithms	**N_{pv}**	**N_B**	**PV_p^o kW**	**E_b kWh**	**BMG_p^o kW**	**BGG_p^o l**	**NPC, $**	**COE, $/kWh**
AO	1000	21	235	50.40	64	10	547670	0.076
HS	992	48	233.12	115.2	91	27	572490	0.082
PSO	638	117	149.93	280.8	118	58	759350	0.112

Table 6.4 Algorithm Comparison for Optimum Configuration

Algorithms	**NPC, $**	**COE, $/kWh**	**Best**	**Average**	**Worst**	**Standard deviation (SD)**
AO	547670	0.076	5.45×10^5	5.48×10^5	5.83×10^5	3.17×10^2
HS	572490	0.082	5.69×10^5	5.73×10^5	6.01×10^5	8.15×10^3
PSO	838060	0.121	8.40×10^5	8.41×10^5	8.78×10^5	8.79×10^3

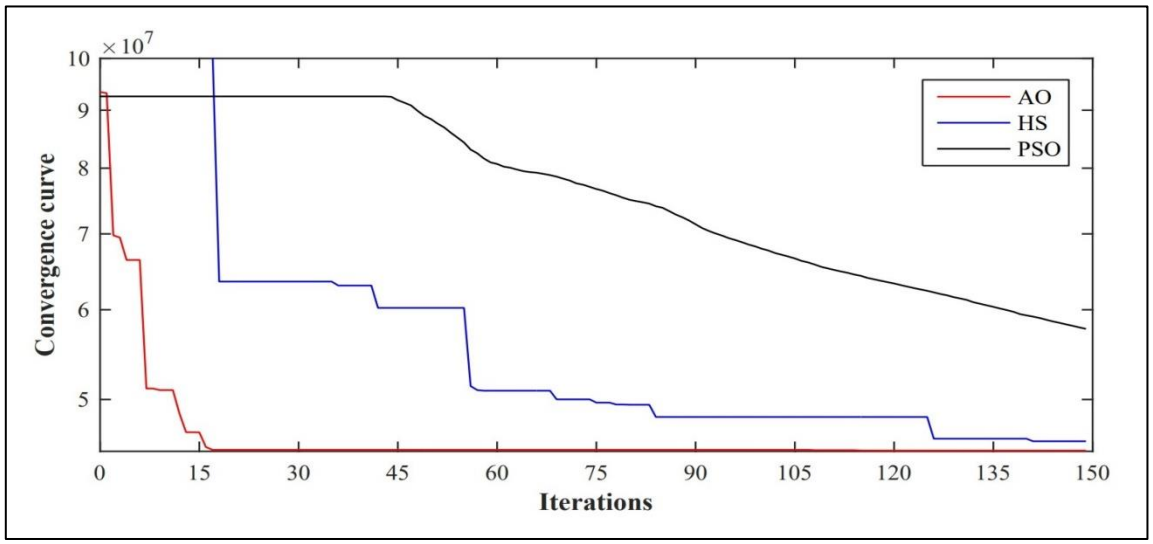

Fig. 6. 14 Convergence Curve for AO, HS and PSO

6.8.5. Annual Energy Generation from Various RES

Fig. 6.13 depicts the different RES' contributions to the annual electrical power generation. It is found that highest amount of electricity was produced by SPV which accounts for 73%, followed by biomass 24% and biogas 3% respectively.

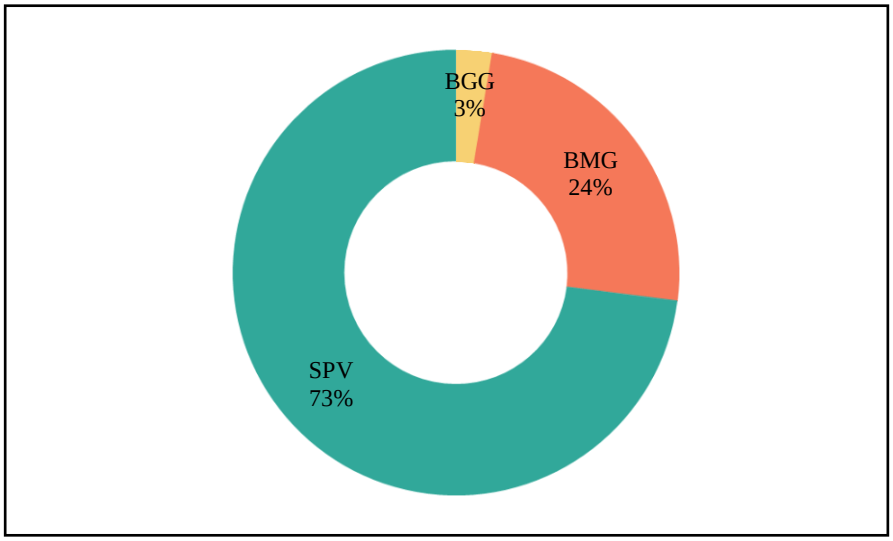

Fig. 6.15 Annual Energy Generation from Various RES

6.8.6. Contribution of Various Costs in NPC

Table 6.5 presents the contributions of CC, OMG, fuel expenses, SV, GP, and GS towards the overall NPC of the HRES. It is observed that the cost of electricity purchased from the utility has significantly increased and represents the most substantial share among all the components in the HRES, amounting to a total of $342,880.

Table 6.5 Proportion of Various Costs in NPC

Various Cost	Cost in $
CC	115950
O&M	102110
Fuel	41012
Salvage value	9004.4
GP	342880
Revenue from GS	45279

6.8.7. Contribution of Different RES in NPC

The percentages of each individual component that make up the overall NPC are displayed in Fig. 6.14. The percentage of the NPC that is contributed by BMG is 56%. This is followed by SPV panels, which contribute 21%, converters, which contribute 9%, BGG, which contributes 7%, and batteries, which contribute 7%.

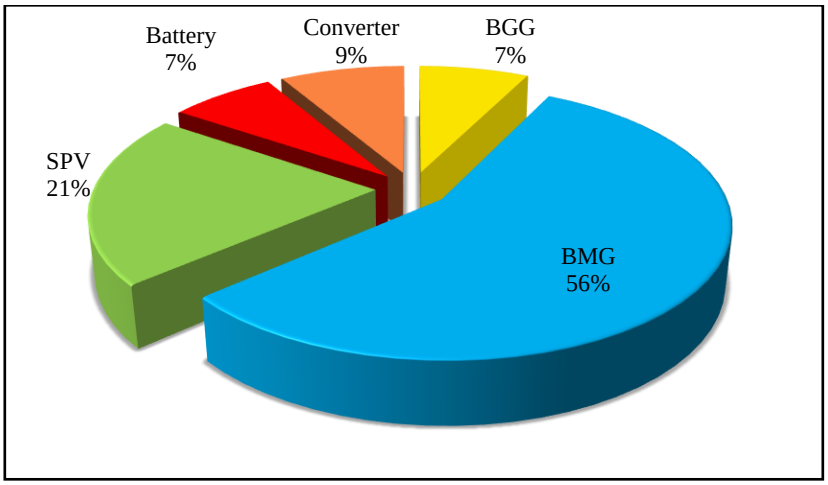

Fig. 6.16 Proportion of Different Renewable Technologies in NPC

6.8.8. Grid Purchase and Grid Sale

In the scenario under consideration, the overall cost of GP is $342,880, and the earnings from GS come to $45,279. In addition, the annual turnover of energy through the utility grid amount 43,656 kWh, while the annual buyouts of energy are 305,085 kWh. Further, a schematic illustration of GP and GS energy levels throughout the three different seasons is presented in Fig. 6.15.

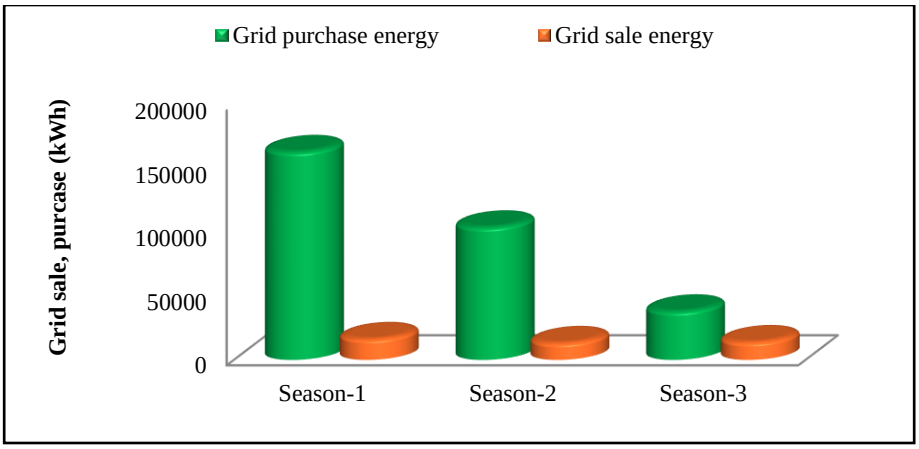

Fig. 6.17 Grid Purchase and Sold Energy for Different Seasons

6.9 RESULT AND DISCUSSION FOR SITE II

In research area II, an attempt has been made to determine the optimal design and size taking into accounts the various forms of RES. First, the following four OFG HRES models have been taken into consideration:

(i) Model H-21: OFG SPV/BMG/Battery

(ii) Model H-22: OFG SPV/Wind/BMG/Battery

(iii) Model H-23: OFG SPV/Wind/BGG/Battery

(iv) Model H-24: OFG SPV/Wind/BMG/BGG/Battery

(v) Model H-25: Grid tied SPV/Wind/BMG/BGG/Battery

Utilizing the AO, HS, and PSO algorithms, all OFG models are optimized. Additionally, all algorithms are also used to simulate and optimize the grid connected HRES model. Finally, the most acceptable model has been identified after comparing grid connected and OFG models in terms of technical and financial considerations.

6.9.1. Optimization Results of OFG HRES

Using AO, HS and PSO algorithm in MATLAB, the hourly simulation of specified OFG models has been carried out for one year. Table 6.6 shows the outcome of the evaluated models with the optimal sizes of component and costs. The optimal model H-24 has the least NPC and COE, as shown in Table 6.6 The optimal hybrid OFG model has a 398 kW SPV array, a 2860 kWh BESS, a 210 kW WT, a 230 kW BMG, a 42 kW BGG.

Table 6.6 Result of OFG HRES using AO Algorithm

Model	Algorithm	PV_p^o (kW)	E_B (kWh)	W_p^o (kW)	BMG_p^o (kW)	BGG_p^o (kW)	NPC (10^6\$)	COE (\$/kWh)
H-21	AO	450	1928.8	-	270	20	1.701	0.205
	HS	412	2503	-	181	38	1.851	0.225
	PSO	420	2544	-	174	36	1.864	0.227
H-22	AO	364	2168	270	20	-	1.723	0.209
	HS	410	1987	318	70	-	1.810	0.218
	PSO	450	2019	210	110	-	1.835	0.221
H-23	AO	470	2987	640	-	34	1.750	0.210
	HS	430	3765	601	-	32	2.1098	0.284
	PSO	378	3998	610	-	28	2.210	0.297
H-24	AO	398	2860	210	230		1.639	0.198
	HS	320	2927.2	200	242		1.651	0.201
	PSO	289	2986	240	276		1.798	0.207

The total NPC and COE are calculated as $\$1.639\times10^6$ and \$0.198/kWh, respectively. In addition, the AO method with H-24 in OFG mode, yields more promising results than those of the HS and PSO algorithm.

6.9.2. Optimization Outcome of Grid Connected HRES Model

The size optimization of grid tied SPV/WT/BMG/BGG/Battery HRES has been conducted using AO, HS and PSO algorithms in MATLAB. The optimal sizes of the components for the grid connected HRES were determined through hourly simulations and are presented in Table 6.7. The most optimal system was obtained using the AO algorithm. The optimal model H-25 consists of a 237.4 kW SPV array, an 82.5 kW WT, a 30 kW BGG system, a 15 kW BMG, and a 43.2 kWh BESS.

The total NPC for the optimal HRES configuration is estimated to be $\$6.61 \times 10^5$, with a corresponding COE of \$0.0737/kWh. These results signify the cost-effectiveness of the optimized HRES model in meeting the energy demands of the grid-tied system

Table 6.7 Algorithm Comparison for Grid Connected Optimum Configuration (H-25)

OT	PV_p^o (kW)	W_p^o (kW)	BMG_p^o (kW)	BGG_p^o (kW)	E_B (kWh)	NPC (10^5\$)	COE (\$/kWh)
AO	237.4	82.5	30	15	43.2	6.61	0.0737
PSO	217.14	102.3	19	29	110	8.32	0.0950
HS	232.65	95.7	20	31	89	8.01	0.0902

6.9.3. Assessment of OFG and Grid Connected HRES

A comparison is conducted between the grid-tied approach and the optimal architecture for an OFG. The comparison focused on two important metrics: NPC and COE. The results, as presented in Table 6.6 and Table 6.7, show that both NPC and COE are lower for the grid tied HRES compared to the OFG configuration. Due to the lower NPC and COE values, it can be concluded that the grid-tied system is more cost-effective than the OFG configuration. This implies that the grid-tied approach would be more economically viable for the suggested sites.

The recommended grid interlinked HRES consists of various components, namely SPV, BMG, BGG, WT, and batteries. This system configuration is considered beneficial for the suggested sites, due to factors such as improved reliability, cost savings, and efficient utilization of RES. To provide a visual representation of the proposed system, a schematic layout is provided in Fig. 6.16. This diagram illustrates the arrangement and interconnection of the SPV panels, BMG system, BGG system, batteries, and any other relevant components in the grid interlinked HRES.

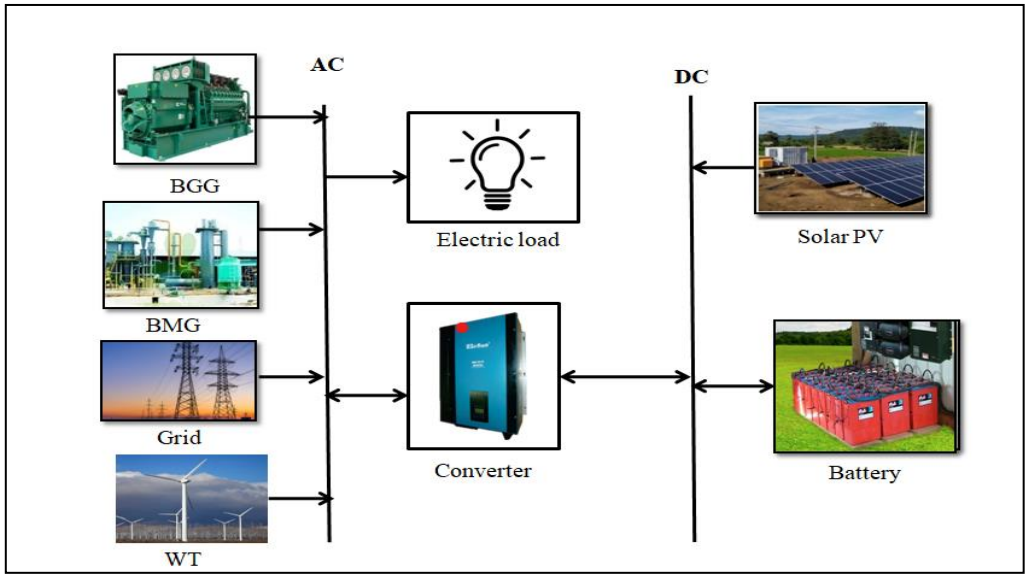

Fig. 6.18 Setup for Proposed HRES for Site II

6.9.4. Assessment of Various Optimization Techniques

Based on the comparison and analysis presented, the AO method outperforms the HS and PSO techniques in terms of optimizing the given configuration. This conclusion is supported by both Table 6.7, which shows that the AO method produces more optimal results, and Table 6.8, which demonstrates the superiority of AO across multiple parameters related to the performance or characteristics of the optimized configuration.

Moreover, the convergence behavior of the optimization methods was assessed using convergence curves for NPC in Fig. 6.17. The curves depict the progression of NPC values over iterations for each technique. The findings indicate that the AO method achieves optimal solution within the first thirty-two iterations, suggesting a relatively fast convergence. In contrast, both HS and PSO techniques converge after 120 iterations, indicating that AO converges faster than the other OT. Overall, based on the results presented, the AO method is the most effective and efficient optimization strategy for the given configuration.

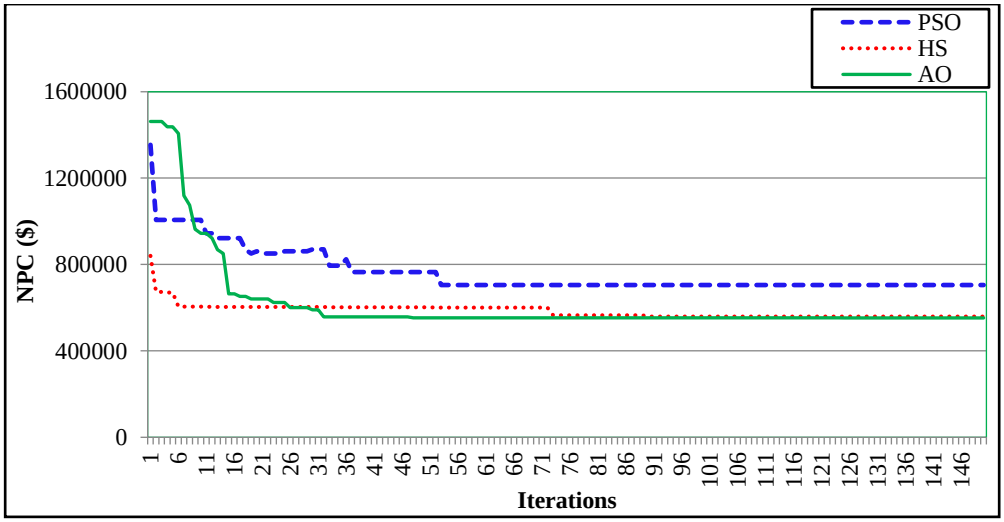

Fig. 6.19 Convergence Curve for AO, HS and PSO

Table 6.8 Algorithm Comparison for Optimum Configuration

Algorithms	NPC, ($)	COE, ($/kWh)	Best	Average	Worst	SD
AO	661020	0.0737	667850	673650	694237.5	98
HS	679871	0.0902	679881	679976	698456	110
PSO	701362	0.0950	707431	708458	713987	116

6.9.5. Annual Energy Generation from Various RES

In Fig. 6.18, the illustration highlights the diverse contributions of various RES to the overall annual electrical power generation. Among these sources, the most considerable proportion of electricity generation is attributed to SPV, accounting for approximately 63% of the total. Following SPV, wind energy holds the second-largest share, contributing around 17% to the overall electricity production. BGG ranks third, constituting approximately 15% of the generated power. Lastly, BMG contributes around 5% to the total electrical output.

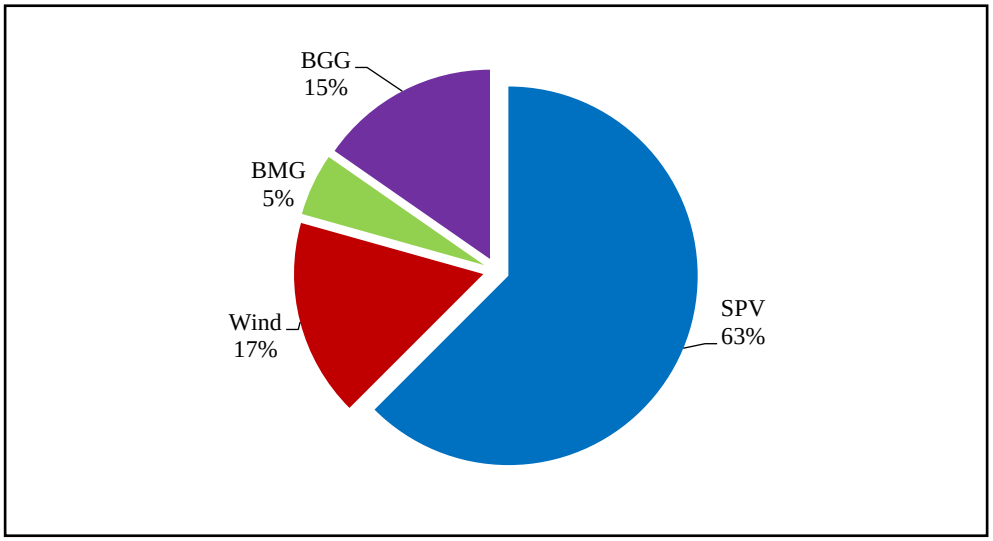

Fig. 6.20 Annual Energy Generation from Various RES

6.9.6. Contribution of Different RES in NPC

Fig. 6.19 presents the breakdown of individual components contributing to the overall NPC. Among these components, BGG account for the largest proportion, contributing approximately 36% to the total NPC. Following closely, WT contributes approximately 33% to the NPC. SPV systems make up around 18% of the NPC, while BMG constitute approximately 12%. Lastly, batteries contribute a modest 1% to the overall NPC.

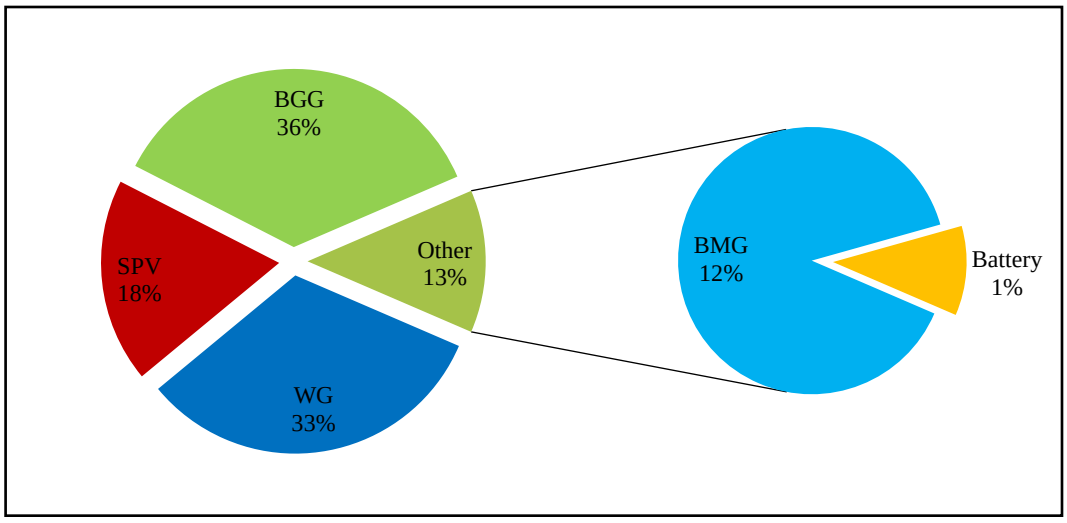

Fig. 6.21 Proportion of Different Renewable Technologies in NPC

6.10 CONCLUSION

In the current chapter, the focus has been on determining the optimal sizing of HRES for specific sites. The primary objective was to minimize the NPC of the selected HRES while adhering to constraints related to component boundaries, battery storage limits, and system reliability. To achieve this, various models were analyzed in both OFG and grid-connected scenarios using novel AO algorithm. The results of AO algorithms were then compared with HS and PSO algorithms. After a thorough comparison, it was found that a grid connected HRES consisting of SPV, BMG, BGG, and battery storage offered the most optimal solution for study area I. Through hourly simulations, the optimum sizing for the grid scenario in study area I was determined as follows: a 235 kW SPV, a 10 kW BGG, a 64 kW BMG, and 50.40 kWh of battery storage. The total NPC for this HRES has been estimated $\$6.41 \times 10^5$, while the COE calculated as \$0.0887/kWh.

In study area II, after considering both technical and economic aspects, the optimal solution for a HRES was found to be a combination of SPV, WT, BMG, BGG, and battery

storage. This configuration addresses the unique requirements and constraints of study area II while maximizing efficiency. The recommended sizing for the components of the grid tied HRES in study area II is as follows: a 237.4 kW SPV array, an 82.5 kW WT, a 30 kW BGG system, a 15 kW BMG, a 43.2 BESS. These component sizes are carefully determined to achieve the best technical performance and economic feasibility for study area II. The total NPC for this HRES is estimated to be $\$6.61 \times 10^5$, with a corresponding COE of \$0.0737/kWh.

These results provide valuable insights into the economic viability of the proposed HRES in both study areas. Moreover, it is important to note that the installation of the proposed hybrid system in study area I would require approximately 14262.8 m^2 of land, while study area II would necessitate approximately 21870m^2 of land. These land use estimates provide a practical understanding of the spatial requirements associated with implementing the recommended HRES in their respective study areas.

The findings and results of this study hold potential for the development of HRES in similar areas. The insights gained from this research can serve as valuable guidance for future endeavors aimed at establishing sustainable and efficient energy solutions in similar regions.

CHAPTER 7

DEVELOPMENT OF RENEWABLE ENERGY BASED INTELLIGENT MODELS FOR ENHANCING RELIABILITY OF POWER IN RURAL INDIA

7.1 INTRODUCTION

The world is currently exploring the use of alternative sources of energy to generate electricity. Due to the lower installation costs and growing environmental concerns, RES sources are being used in the generation of electrical energy. RES are becoming more appealing as ED and fossil FC increase. The hybridization of these resources has the potential to reduce unpredictability and intermittency while increasing efficiency. The forecasted data of solar and wind helps to optimize the scheduling and maintenance of power generation facilities and thus can helps in optimal sizing of HRES. This leads to better operational efficiency and reduced downtime. The present chapter deals with the size optimization of HRES using forecasted data using recently developed algorithms: CPA, TSA, AO [139].

The accuracy of size optimization of HRES can be improved by using accurate weather data that can be obtained through forecasting [167]. Thus, to increase the precision of the size optimization, hourly forecasting of GHI, temperature, and wind speed for one year has been performed using GPR, SVR, XGBT, and DT techniques for study area I and study area II. The results of all four FM are then compared and revealed that the results obtained from GPR are better than those of other FM for both the sites. Further, the forecasted data for solar, wind, and temperature obtained from GPR are used for sizing the

HRES. The NPC is utilized to analyze the viability of the HRES while considering system reliability. Furthermore, recently developed optimization algorithms, namely the CPA, TSA, and AO algorithms have been applied for the sizing of a grid connected HRES to meet the energy needs of a remote site in the Indian province of Haryana and Uttar Pradesh. Moreover, a comparison of CPA, AO, and TSA has been conducted and revealed that TSA offers more promising outcomes.

7.2 COLONY PREDATION ALGORITHM (CPA)

The CPA is a novel stochastic optimization approach developed by Chen et al., the behavior of social animals serves as the basis for this algorithm. The main focus herein is on colony predation, a strategy used by animals to evade predators and boost hunting success rates. Wolf packs, hyena packs, lion packs, piranha packs, and other animals that hunt in packs frequently use this tactic. Predators frequently obtain additional prey through colony predation, improving individual survival rates. This is a strategy used by animals that live in colonies to ensure their survival and maximize the effectiveness of their hunt for food. Hyenas and wolves, for instance, communicate and work together through colony predation to capture more prey than they could individually. The two most popular strategies for increasing the likelihood of successful hunting are dividing and encircling animals. Another tactic animals use in circumstances when consumption surpasses their produce. In this behavior, they will switch to another prey, increasing their predation's effectiveness. CPA draws inspiration from collective hunting; a strategy herd animals use to increase individual survival rates. CPA also considers the natural phenomena of survival of the fittest [168].

7.2.1. Mathematical Modelling of CPA Technique

The CPA employs primarily five key steps to enhance hunting success rates. The mathematical modelling of these hunting steps used in CPA is explained below [168].

Step 1: Communication and Collaboration

Predation success rates are higher for animals that hunt in groups, because they communicate and work together more efficiently.

The following formulae, describes how individuals communicate and hunt for food in groups.

$$Y_n^m(\tau+1) = Y_n^{m_1}(\tau) + (1-p).\left(\frac{Y_1(\tau)+Y_2(\tau)}{2}\right) \quad (7.1)$$

Where; p is the random number lies between 0 to 1; the individual looking for food is marked by $Y_n^{m_1}(\tau)$; the two closest positions to prey in the n^{th} dimension are indicated by $Y_1(\tau)$ and $Y_2(\tau)$; $n\epsilon$ *1,2,…., dim*; *dim* is the dimension of population; the individual's latest updated position is represented by $Y_n^m(\tau+1)$.

Step 2: Disperse Food

The initial approach in colony prediction separates the prey from its group by driving it in various directions. The predation strategies of the individuals in the search were mathematically modeled and as follows:

$$Y(\tau+1) = Y_b - P_s\,.(k_1.(u_b - l_b) + l_b) \quad (7.2)$$

Where; the position of a population is denoted by $Y(\tau+1)$, the position of food is marked by Y_b; P_s denotes the strength of prey, $k_1$represents [K_1; K_2;K_3; …K_n], which is a random number between 0-1; u_b, l_b are the upper and lower bounds respectively.

Step 3: Encircle Food

The hunting party uses the second tactic to encircle and approach animals. This step can be mathematically mimic using the following equation:

$$Y(\tau + 1) = Y_b - 2 \cdot P_s \cdot d \cdot e^l \cdot tan\left(\frac{\pi}{4} \cdot l\right) \quad (7.3)$$

Where the distance that separates the current member from the prey is represented by d; the random number is defined by l which lies between 0 and 1. The value of *d* is calculated as follows:

$$d = |Y_b - Y(\tau)| \quad (7.4)$$

The current hunter population is marked by $Y(\tau)$.

Step4: Supporting Closest Individual

Recognizing the group's potential challenges in pursuing prey, the closest individual requests peer assistance, which can be described as follows.

$$Y(\tau + 1) = P_{nearest} \quad (7.5)$$

Where, location of the nearest predator is marked by $P_{nearest}$.

Step 5: Searching for the Food

If no prey is located nearby or if the food supply is too far away from the prey, the surviving individuals will seek another food source. In the following way this behavior may be expressed as follows:

$$d_1 = |2 \cdot k_4 \cdot Y_{rand} - Y(\tau)| \quad (7.6)$$

$$Y(\tau + 1) = Y_{rand} - P_s \cdot d_1 \quad (7.7)$$

Where, random number is defined as k_4 and its value lies between [0 and 1]. An individual's random position is indicated by Y_{rand} ; d_1 represent the distance of random group movement.

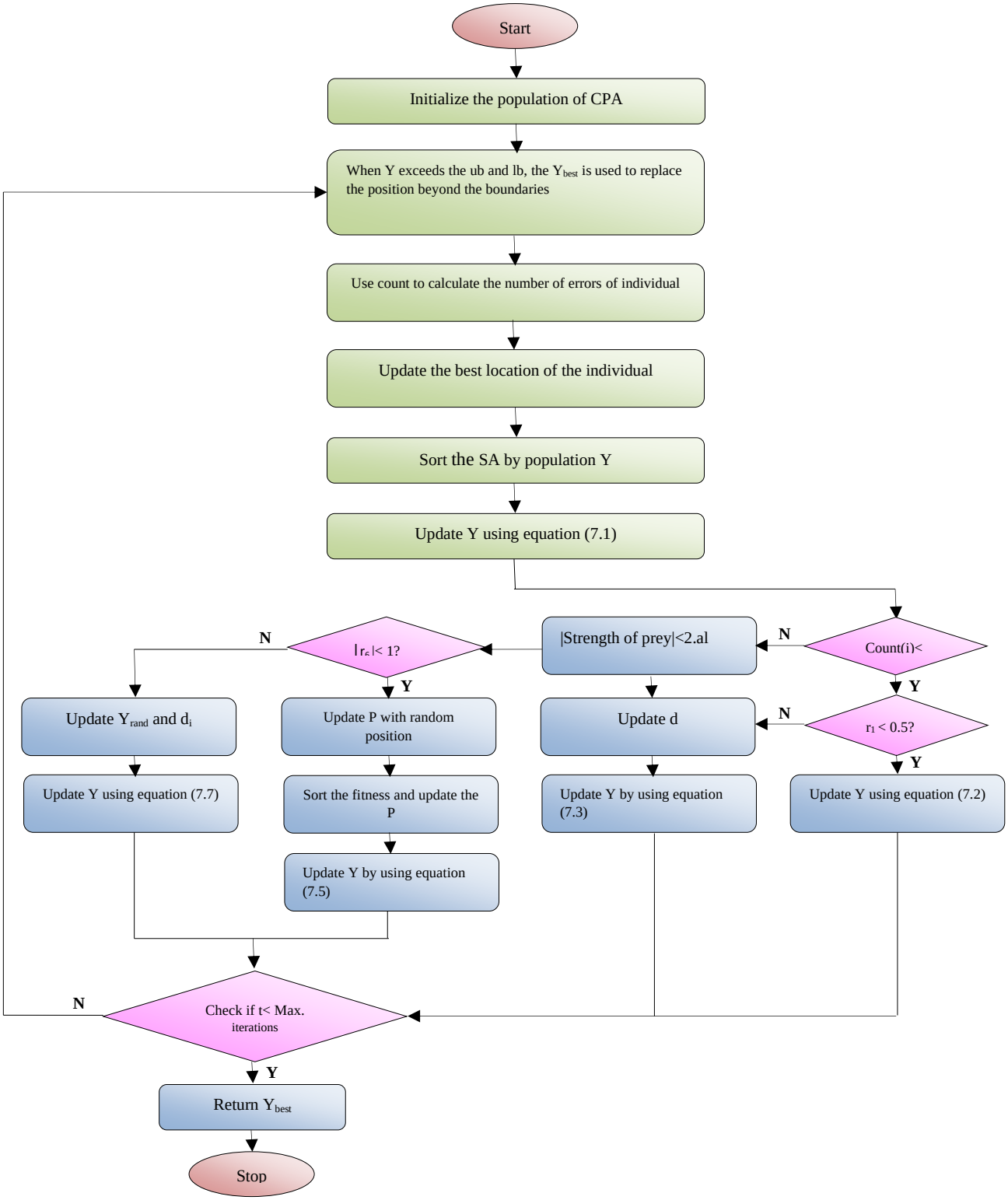

Fig. 7.1 Flowchart of CPA Algorithm

Further, CPA stands out as a distinctive optimizer with consistent performance, has demonstrated significant potential in addressing various optimization problems. One of its notable strengths lies in its ability to swiftly shift from exploration to exploitation in the initial stages, granting more time for the exploitation phase. Moreover, CPA ensures the inclusion of perturbations within the algorithm, safeguarding against premature convergence to local optima. This combination of features makes CPA a promising and efficient algorithm for optimization tasks. Additionally, the flowchart for proposed CPA is presented in Fig. 7.1 [168].

7.3 TUNICATE SWARM ALGORITHM (TSA)

TSA is an algorithm that takes inspiration from tunicate colonies. Tunicate is a group of marine animals. They make dwellings on piers, rocks, or the undersides of boats and ships. Most often, they resemble small blobs of color. The tunicate can emit intense blue-green light, or bioluminescence, which makes it visible from a distance. They have two ends: an open end and a closed end. The open end is utilized for propulsion, such as jet propulsion employing atrial siphons. Tunicates move by using bursts of fluid. The force of this explosion is so intense that it can cause tunicates to travel vertically in the water. The shape of this animal is measured in millimeters. Tunicates have the expertise and ability to locate food sources in the water even when there is no information available on food sources. The most crucial tunicate activities are their jet propulsion and swarm intelligence, which they use to identify the optimal food supply [169].

7.3.1. Mathematical Modelling of TSA Technique

The mathematical modelling of the initial behavior of the tunicates, which is the jet's propulsion, needs to satisfy three requirements. These requirements aim to avoid conflicts amongst tunicates, modify the potential tunicate's position, and get closer to the potential tunicate. Conversely, the swarm behavior keeps track of fellow seekers' presence to arrive at the most appropriate and optimal solution. The mathematical modelling of these behaviors is described in the following subsections [169].

Step 1: Preventing Search Agent Disputes

To prevent the disputes among search agents (SA), vector $\vec{B}$ is used to calculate the new search agent location

$$\vec{B} = \frac{\vec{H}}{\vec{N}} \tag{7.8}$$

$$\vec{H} = r_2 + r_3 - \vec{E} \tag{7.9}$$

$$\vec{E} = 2 \cdot r_1 \tag{7.10}$$

Where, the gravity force is indicated by $\vec{H}$; $\vec{E}$ represents deep ocean advection; r_1, r_2, r_3 denote random values between 0 and 1; $\vec{N}$ represents the social forces among SA.

The following formula is used to compute the vector *N*:

$$\vec{N} = [Q_{min} + r_1 (Q_{max} - Q_{min})] \tag{7.11}$$

Where; Q_{min} , Q_{max} represent initial and subordinate speeds to make social interaction.

Step 2: Movement towards the Direction of Best Neighbor

After avoiding the disputes between neighbors, the SA moves towards the direction of best neighbor

$$\overrightarrow{P_D} = | \overrightarrow{F_S} - R_{rand} \cdot \overrightarrow{Q_p}(y) | \quad (7.12)$$

Where, the distance between the food source and SA is denoted by $\overrightarrow{P_D}$; the current iteration is represented by y, $\overrightarrow{F_S}$ indicates the position of optimum food source; $\overrightarrow{Q_p}(y)$ is the position of tunicate; and R_{rand} represents random value between 0 and 1.

Step 3: Converge towards the Best Search Agent

The SA can keep its position towards the optimal location of SA which is near to food source.

$$\overrightarrow{Q_p}(y) = \overrightarrow{F_S} + \overrightarrow{B} \cdot \overrightarrow{P_D} \text{ , } if\ R_{rand} \geq 0.5 \quad (7.13)$$

$$\overrightarrow{Q_p}(y) = \overrightarrow{F_S} - \overrightarrow{B} \cdot \overrightarrow{P_D} \text{ , } if\ R_{rand} < 0.5 \quad (7.14)$$

Where; $\overrightarrow{Q_p}(y)$ stands for the updated position of tunicate with respect to the position of food sources, $\overrightarrow{F_S}$

Step 4: Swarm Behavior

To mathematically imitate the swarm behavior of tunicates, the first two optimal solutions remain intact, and the locations of the remaining SA are updated based on the optimal location of the SA. To describe the tunicate swarm behavior, the following formula can be used:

$$Q_P(\vec{y} + 1) = \frac{\overrightarrow{Q_P}(y) + \overrightarrow{Q_P}(y+1)}{(2 + r_1)} \quad (7.15)$$

As the swarm behavior updates the positions of other search agents towards the best optimal solution and the stopping criteria are met, the TSA algorithm efficiently converges towards the optimal design of the problem. TSA exhibits remarkable robustness in handling dynamic and uncertain environments, due to its collective behavior, which enables adaptive and effective adjustments to changes. Further, the flowchart for TSA is presented in Fig. 7.2 [169].

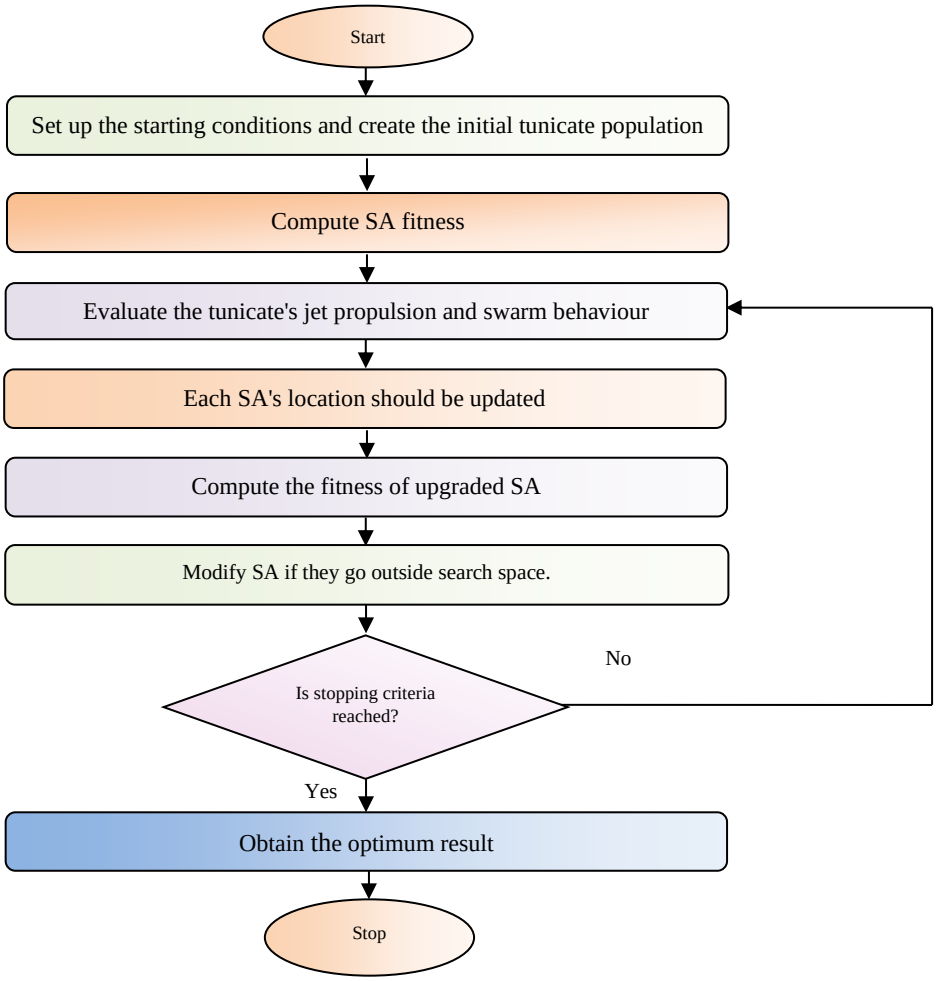

Fig. 7.2 Flowchart of TSA Algorithm

7.4. RESULTS AND DISCUSSION FOR STUDY AREA I

The current study integrates ML-based forecasting techniques with optimization algorithms to size HRES. By utilizing forecasted data, more accurate and reliable sizing results can be achieved, leading to improved cost-effectiveness and performance of the RES. Therefore, the current work focuses on the hourly forecasting of GHI, temperature, and using ML techniques such as SVR, GPR, XGBT, and Decision Trees (DT). The forecasting results are compared using statistical indicators, and GPR is identified as the best solution.

The forecasted data obtained through GPR is then utilized for sizing HRES. Three optimization algorithms, namely: CPA, TSA, and AO, are employed in MATLAB to perform hourly simulations over one year for a selected grid linked HRES. The objective of this research is to minimize the NPC while ensuring the reliability of the power supply. A comparative analysis is conducted between the sizing results obtained using forecasted data and those obtained without forecasted data. The results of the TSA algorithm using forecasted data are found to be more optimal, leading to a reduction of 0.22% in the COE.

7.4.1. Performance Indicators for Forecasting

It is not easy to assess the accuracy of an FM without doing the performance assessment; therefore, statistical indicators have been used for the performance evaluation. The indicators that are employed for comparative research are termed as Root Mean Square Error (RMSE), Mean Absolute Error (MAE), and Correlation Coefficient (R^2). The MAE measure is useful for determining FM prediction errors. The correlation coefficient reveals

how closely two models are related to each other, whereas the RMSE indicator analyzes the model's overall accuracy.

In the study, different FM are trained using four years of data, specifically from 2016 to 2019, for wind speed, GHI, and temperature. The training phase is crucial as it allows for a better understanding of the model's accuracy and helps in selecting the best-performing FM.

7.4.2. Training and Testing Phase

Once the FM are trained, they are evaluated in the real prediction stage, also known as the testing phase. In this phase, the trained models are utilized to forecast GHI and temperature. The effectiveness of each FM is evaluated by comparing the predictions with the actual values using the data from 2020. The performance indicators for GHI and temperature for both the training and testing phases are calculated and presented in Table 7.1 and Table7.2 respectively. These indicators provide insights into the accuracy and reliability of the FM, allowing for the selection of the most effective FM for the specific variables being forecasted.

Table 7.1 Training and Testing Performance Comparison for GHI

ML Model	**Training Phase**			**Testing Phase**		
	RMSE	MAE	R^2	RMSE	MAE	R^2
DT	0.089109341	0.051650366	0.908232	0.240235	0.1759061	0.896154
SVR	0.094136684	0.051410203	0.897586	0.16992	0.1282659	0.944546
GPR	**0.098263664**	**0.05953362**	**0.888409**	**0.187653**	**0.1360788**	**0.945525**
XGBT	0.090643674	0.051363595	0.905045	0.174715	0.1299993	0.918481

Table 7.2 Training and Testing Performance Comparison for Temperature

ML Method	Training Phase			Testing Phase		
	RMSE	MAE	R^2	RMSE	MAE	R^2
DT	0.0840803	0.009655748	0.9178016	0.261181	0.0352136	0.905154
SVR	0.0899271	0.008861715	0.908895	0.566462	0.0288729	0.891659
GPR	**0.0895453**	0.008216276	**0.933532**	**0.801434**	0.0305253	**0.921403**
XGBT	0.09705954	0.007940475	0.92675	0.694554	0.0577127	0.910532

7.4.3. Optimization Results of Proposed HRES

This study aimed to optimize the size of HRES for the outlying region of Agra, India. The optimization focused on a grid connected SPV/BMG/BGG/Battery configuration using forecasted data. Four distinct ML techniques, namely SVR, DT, GPR, and XGBT, were utilized for forecasting. Among these methods, GPR exhibited exceptional forecasting accuracy, making it the most effective approach for the study.

After obtaining the forecasted data for GHI, and temperature for study area I, the optimal grid linked HRES, involving various RES, was developed to fulfil the energy needs of the given site based on minimal NPC and COE. Three recently developed optimization approaches viz. TSA, CPA, and AO were applied to optimize the size of the selected HRES. Further, the hourly simulation for selected HRES has been conducted in MATLAB for one year to facilitate this analysis, 150 iterations were performed. An Intel® Core TM i7-8250 was used to create and evaluate the recommended optimizers. Further, the yearly real interest, inflation and escalation rates are fixed at 0.11, 0.075, and 0.05, respectively. The parameters of the TSA, CPA and AO algorithms are set as follows: TSA: maximum

iteration = 150, SA =30, CPA: maximum iteration = 150; dimensions = 5; SA = 30; AO: exploitation adjustment coefficients; $\alpha = 0.1$; $\delta = 0.1$; Population size = 30,

maximum iteration= 150. Further, various optimization results obtained from applying these algorithms with and without forecasted data, were compared, and presented in Table 7.3. The optimization results for the selected grid linked HRES, along with their respective sizes obtained using the forecasted data, and are illustrated in Table 7.4.

Table 7.3 Algorithms Results With and Without Forecasting

Parameters	**TSA**		**CPA**		**AO**	
	With Forecasted data	**Without Forecasted data**	**With Forecasted data**	**Without Forecasted data**	**With Forecasted data**	**Without Forecasted data**
Energy generated by SPV (W)	442958	453271	441185	458765	442515	461256
NPC ($)	493100	499987	533291	594858	497713	533291
COE ($/kWh)	0.0627	0.0639	0.0763	0.0794	0.0674	0.0763
GP energy	203178	210231	256181	258693	273570	265768
GS energy	82960	80987	26226	3134	67249	62348

Table 7.4 Optimization Results of Optimal Model Using Forecasted Data

OT	**N_{pv}**	**N_B**	**PV_p^o (kW)**	**E_B (kWh)**	**BMG_p^o (kW)**	**BGG_p^o (kW)**	**NPC ($)**	**COE ($/kWh)**
TSA	999	10	234.76	24	88	63	493100.3	0.0627
CPA	995	48	233.82	115.2	67	28	533291.2	0.0763
AO	998	10	234.53	24	87	12	497713.7	0.0674

It became evident that TSA, when used in conjunction with forecasted data, yielded the most optimal results among the three OT. Moreover, the reduction in the COE of 0.22% is observed for the TSA model when forecasted data was utilized. The contribution of various RES in the yearly power production using TSA, CPA, and AO has been depicted in Fig.

7.3. The results indicate that the SPV generated the highest power output across all three optimization algorithms.

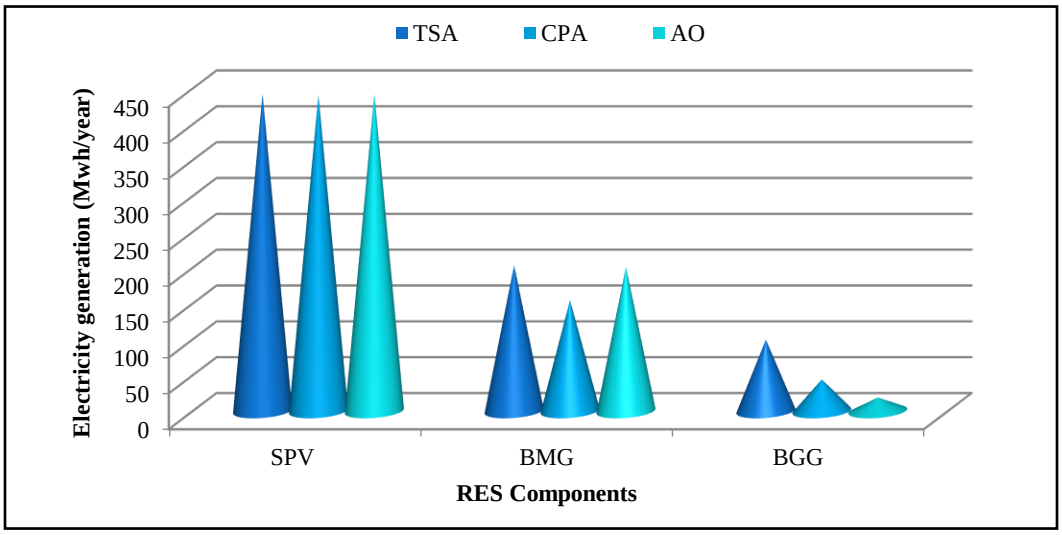

Fig. 7.3 Total Yearly Energy Generation for Various OT

Fig. 7.4 demonstrated the contribution of cost of different system elements to the NPC. The analysis revealed that, in the case of TSA, the cost of BGG was the highest among the system elements considered, followed by SPV, BMG, and the battery. However, when applying the CPA and AO algorithms, the highest cost share was attributed to the BMG, followed by SPV, battery, and BGG respectively.

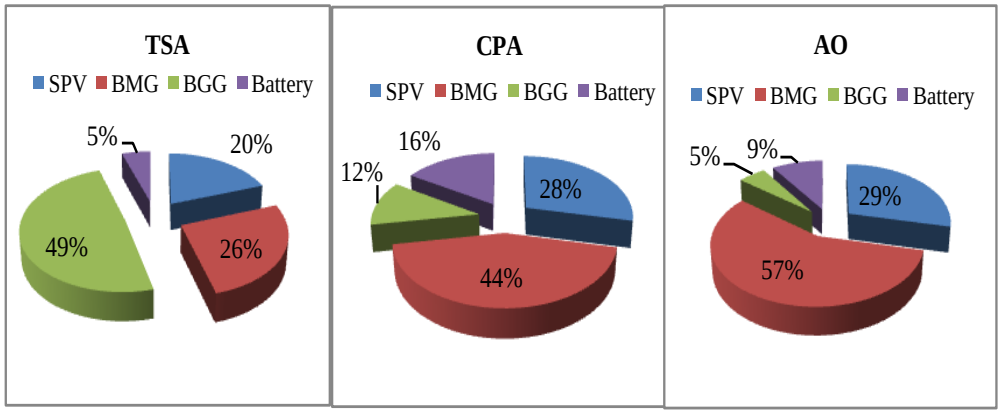

Fig. 7.4 Proportion of Various Components in the NPC

The findings highlight the varying cost contributions of different components within the system under different optimization algorithms. The results suggest that the optimization algorithm employed, can influence the cost distribution among the system elements. A comprehensive statistical analysis was conducted for all three proposed techniques: TSA, CPA, and AO in which the best and worst values of the cost function, as well as the mean, median, and SD for each technique has been provided. The statistical results are tabulated in Table 7.5, clearly demonstrating that TSA yields the most favorable outcomes in various metrics, such as SD, best value, median, and average.

Table 7.5 Performance Indicators for TSA, CPA, AO

OT	Best	Average	Worst	SD	Median
TSA	0.060884498	0.0609138	0.0609497	1.79E-05	0.060913578
CPA	0.076081546	0.0761696	0.0762298	4.95E-04	0.076201801
AO	0.07609432	0.0763138	0.0769903	1.70E-04	0.075201801

Furthermore, Fig.7.5. illustrates the convergence curves for the TSA, CPA, and AO algorithms of the proposed HRES model for study area I. From the figure, it is observed that the TSA algorithm and AO algorithm both converged and reached a fixed value at iterations 11 and 36, respectively. On the other hand, the CPA algorithm stabilized at a constant value at iteration seventy-one. This indicates that the TSA algorithm has a faster convergence rate compared to AO and CPA. The convergence curves provide insights into the optimization process and demonstrate how each algorithm progresses towards finding an optimal solution for the grid connected HRES model.

Fig. 7.5 Convergence Curve for TSA, CPA, and AO Algorithms

7.5 RESULTS AND DISCUSSION FOR STUDY AREA II

In the current work, the hourly forecasting of GHI, temperature, and wind speed is conducted for one year by utilizing ML techniques, specifically SVR, GPR, XGBT, and DT. The obtained results have been compared with the help of statistical indicators, and the best solution has been determined for GPR. Further, the forecasted data obtained through GPR is used for sizing HRES. The sizing of HRES is conducted using the recently developed OT: CPA, TSA and AO using forecasted data and without forecasted data. MATLAB was used for CPA, TSA, and AO algorithms to run hourly simulations over one year for a selected grid linked HRES. The obtained results are compared based on minimal NPC with the reliability of the power supply. In addition, in view of developing HRES, a comparative analysis of various parameters obtained after size optimization using forecasted data and without forecasted data is performed, and the results of TSA with forecasted data are found to be more optimal with a reduction of 0.42% in COE.

7.5.1. Training and Testing Phase

The different FM are trained using four years of data, i.e., 2016-2019 of wind, GHI and temperature. The training phase of FM offers a better understanding of the model's accuracy and is essential for selecting the best FM. Further, in the testing phase, also known as the real prediction stage, the GHI, temperature, and wind speed are forecasted using the model effectively trained in the previous phase. To evaluate the effectiveness of the FM, each model uses 2020 data for prediction. The performance indicators for GHI, temperature, and wind speed for the training and testing phases, respectively, have been determined and presented in Tables 7.6 - Table 7.8. respectively.

Table 7.6 Training and Testing Performance Comparison for GHI

ML Model	**Training Phase**			**Testing Phase**		
	RMSE	MAE	R^2	RMSE	MAE	R^2
DT	26.28087	20.10835	0.989453	30.149	23.3189	0.986104
SVR	33.83328	26.35761	0.982519	33.469	26.0625	0.982875
GPR	**23.70055**	**18.45589**	**0.991422**	**26.613**	**20.8928**	**0.989172**
XGBT	38.88621	30.73992	0.976908	43.199	34.0433	0.971471

Table 7.7 Training and Testing Performance Comparison for Temperature

ML Method	**Training Phase**			**Testing Phase**		
	RMSE	MAE	R^2	RMSE	MAE	R^2
DT	1.840803	1.358063	0.959016	2.261181	1.735343	0.939188
SVR	2.399271	1.794306	0.930376	2.566462	1.961314	0.921659
GPR	**1.775453**	**1.331063**	**0.961874**	**1.801434**	**1.404804**	**0.961403**
XGBT	2.705954	2.16118	0.91144	2.694554	2.22985	0.913644

Table 7.8 Training and Testing Performance Comparison for Wind Speed

ML Method	Training Phase			Testing Phase		
	RMSE	MAE	R^2	RMSE	MAE	R^2
DT	0.7351721	0.513848662	0.845943	1.1948515	0.88169812	0.836684
SVR	0.8769833	0.626250966	0.871789	1.1217303	0.81555375	0.882985
GPR	**0.6439014**	**0.452467609**	**0.891567**	**1.0579799**	**0.76115085**	**0.889172**
XGBT	0.8308530	0.605577454	0.876908	1.0551265	0.74767111	0.821514

From Table 7.6 -Table 7.8, it is apparent that the GPR method performs better for prediction out of all these ML techniques. The GPR method performs better because the generated statistical indicators have the lowest possible value, while the R^2 has the highest possible value. Since the GPR model has the lowest RMSE, MSE, and greatest R^2 for all training and testing phases, including GHI, temperature, and wind speed. Therefore, the forecasted GHI, temperature, and wind speed data obtained by the GPR approach have been used to develop HRES.

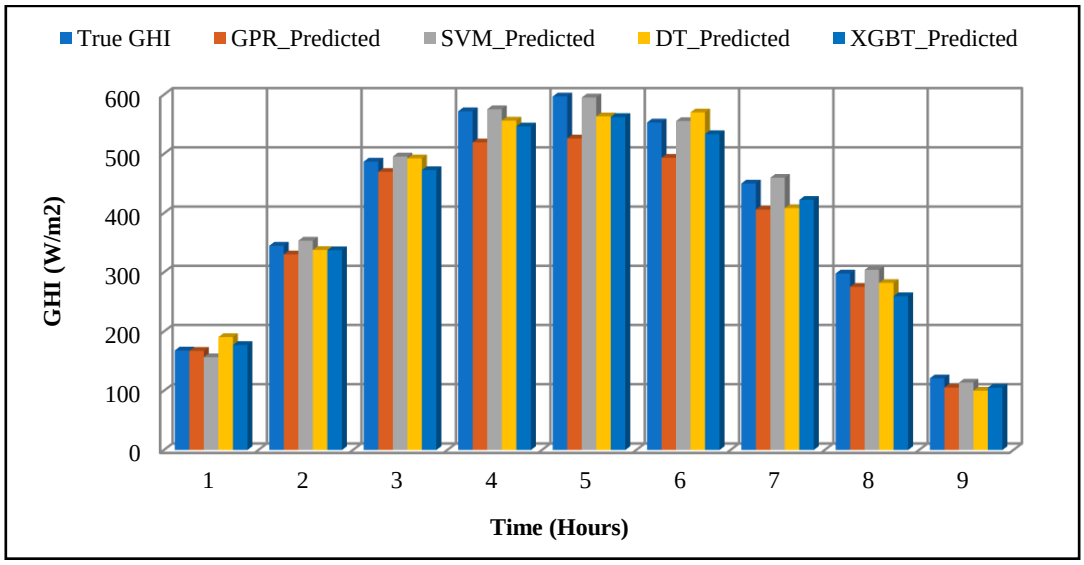

Fig. 7.6 Hourly Forecast Performance Comparisons of GHI

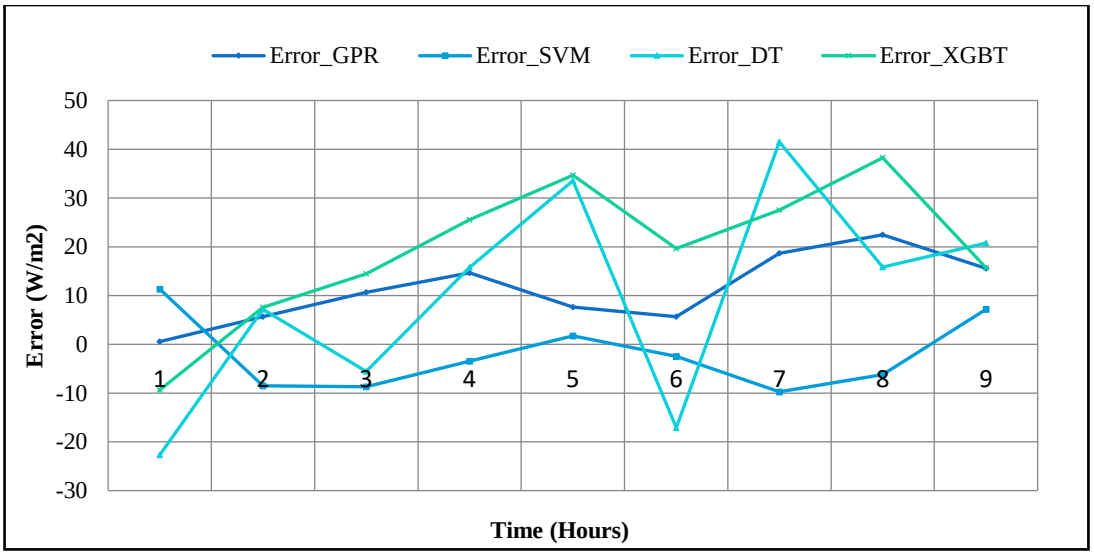

Fig. 7.7 Hourly Forecast Performance Comparisons of Error

Further, the prediction performance and prediction error of the proposed models along with meteorological data for GHI, temperature, wind speed is shown in Fig. 7.6 - Fig. 7.11 respectively.

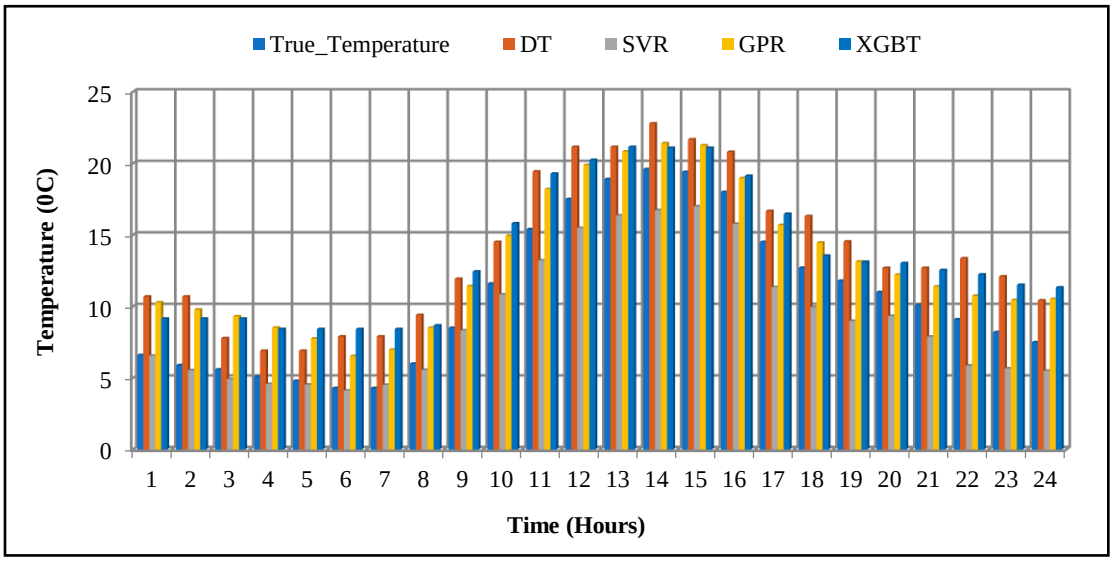

Fig. 7.8 Hourly Forecast Performance Comparison of Temperature

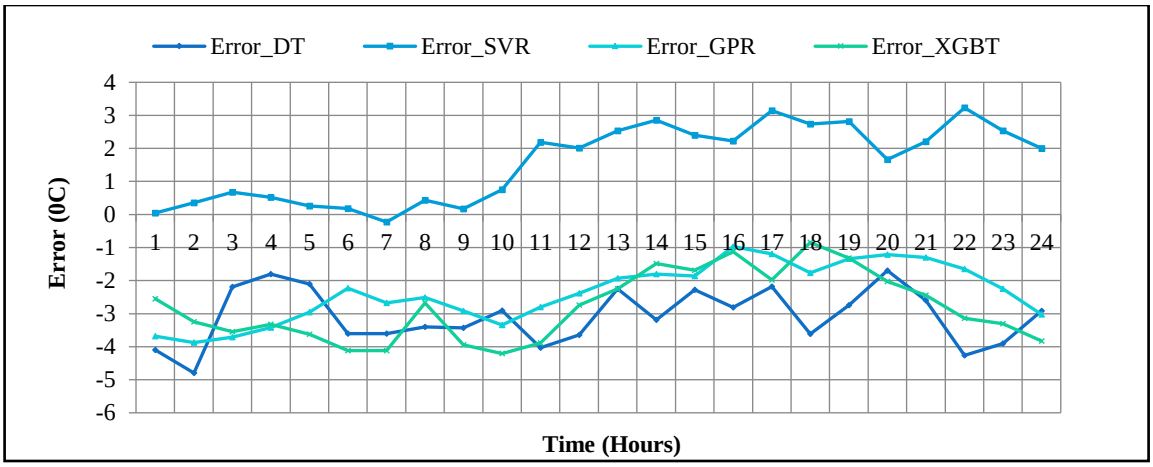

Fig. 7.9 Hourly Forecast Performance Comparison of Error

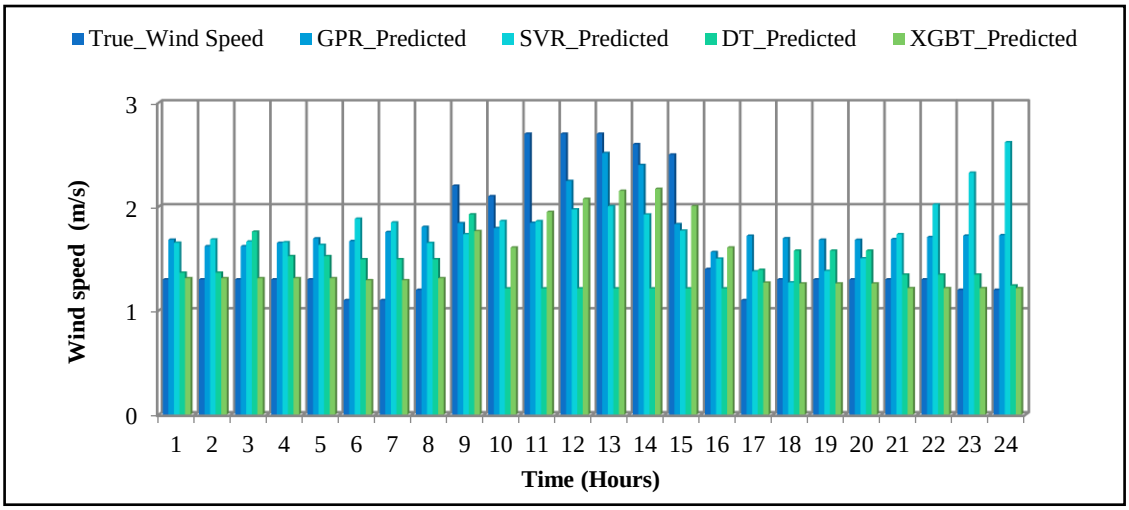

Fig. 7.10 Hourly Forecast Performance Comparison of Wind Speed

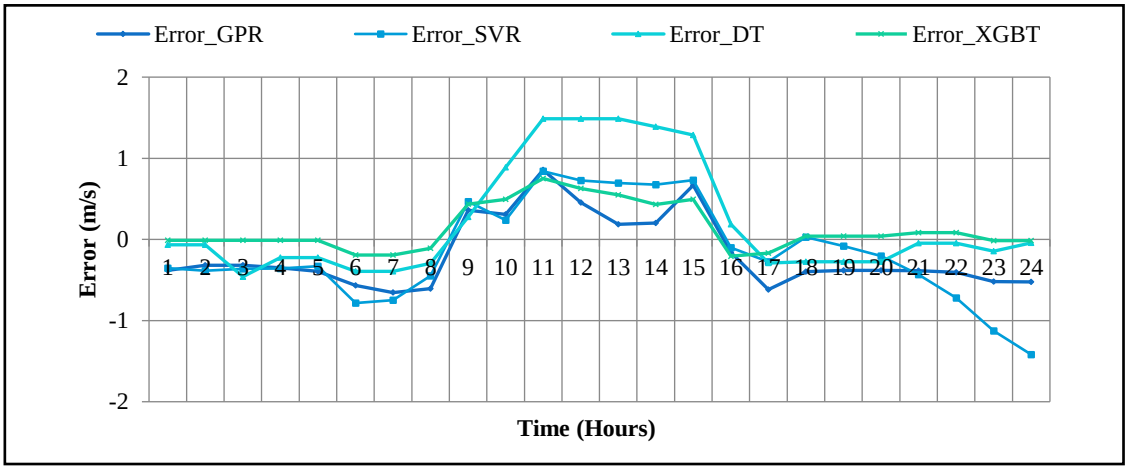

Fig. 7.11 Hourly Forecast Performance Comparison of Error

7.5.2. Optimization Results of Proposed HRES

After obtaining the forecasted data for GHI, wind speed and temperature, the size optimization of HRES has been conducted using recently developed algorithms: TSA, CPA, and AO. Various indices were obtained by applying these algorithms with forecasted and without forecasted data have been presented in Table 7.9. By analyzing and comparing the obtained result presented in Table 7.9, it has been evident that, out of three OTs, TSA with forecasted data gives the most optimal results. It is also found that there is a 0.42% reduction in COE for the TSA model with forecasted data. Further, the optimization result acquired for the selected grid linked HRES with their size using the forecasted data is shown in Table 7.10.

Table 7.9 Results of Optimization for Forecasted Data and Without Forecasted Data

Parameters	**TSA**		**CPA**		**AO**	
	With Forecasted data	**Without Forecasted data**	**With Forecasted data**	**Without Forecasted data**	**With Forecasted data**	**Without Forecasted data**
Energy generated by SPV (W)	4.670×10^5	4.438×10^5	4.483×10^5	4.354×10^5	4.46×10^5	4.321×10^5
Energy generated by WT (W)	1.80×10^5	1.651×10^5	1.293×10^5	1.182×10^5	1.40×10^5	1.20×10^5
NPC ($)	647800	659923	658120	664344	660831	669765
COE ($/kWh)	0.0701	0.0705	0.0709	0.0719	0.0728	0.0737
GP energy	4.324×10^4	6.798×10^4	5.120×10^4	6.828×10^4	5.420×10^4	6.992×10^4
GS energy	5.592×10^3	4.435×10^3	5.087×10^3	4.897×10^3	5.016×10^3	4.986×10^3

The contribution of various RES in yearly power production via TSA, CPA and AO has been obtained and illustrated in Fig. 7.12. The result demonstrates that the SPV array generated the highest power in all three algorithms.

Table 7.10 Optimum Configuration of Grid Linked HRES for Various Algorithms

OT	N_{pv}	N_W	N_B	PV_p^o (kW)	W_p^o (kW)	E_B (kWh)	BMG_p^o (kW)	BGG_p^o (kW)	NPC ($)	COE ($/kWh)
TSA	1200	35	15	282	115.5	36	25	10	647800	0.0701
CPA	1000	28	14	235	92.4	33.6	30	12	658120	0.0709
AO	1010	25	18	237.4	82.5	43.2	30	15	660831	0.0728

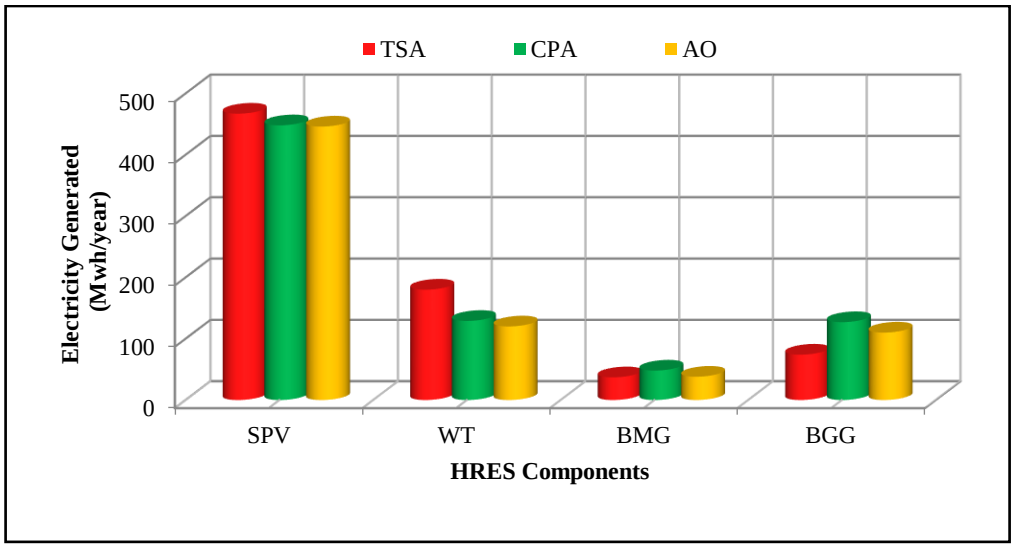

Fig. 7.12 Total Yearly Energy Generation for Various OT

Furthermore, the contribution of various system elements to the NPC is demonstrated in Fig. 7.13. It was found that, in the case of TSA, the cost of the WT system was the highest, followed by BGG, SPV, battery, and BMG. However, for the CPA and AO algorithms, the highest share was for BGG, followed by WT, SPV, BMG, and battery. In addition, Fig. 7.14. shows the energy generated by different HRES components for one day.

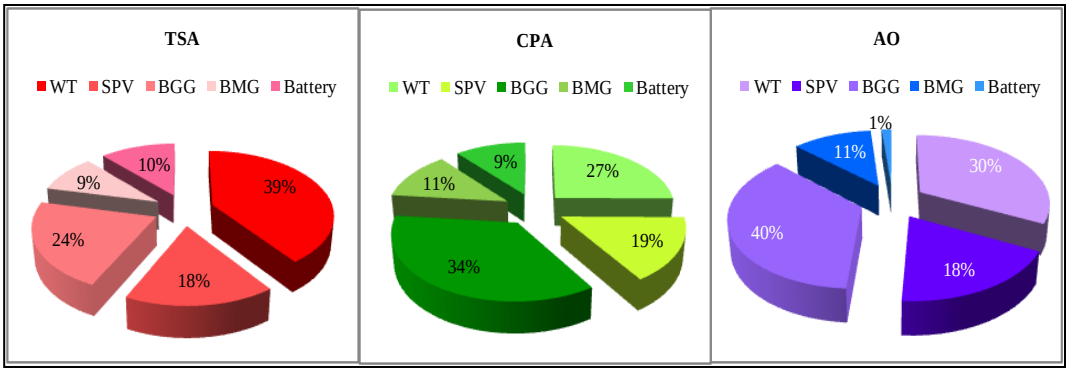

Fig. 7.13 Proportion of Various Components in the NPC

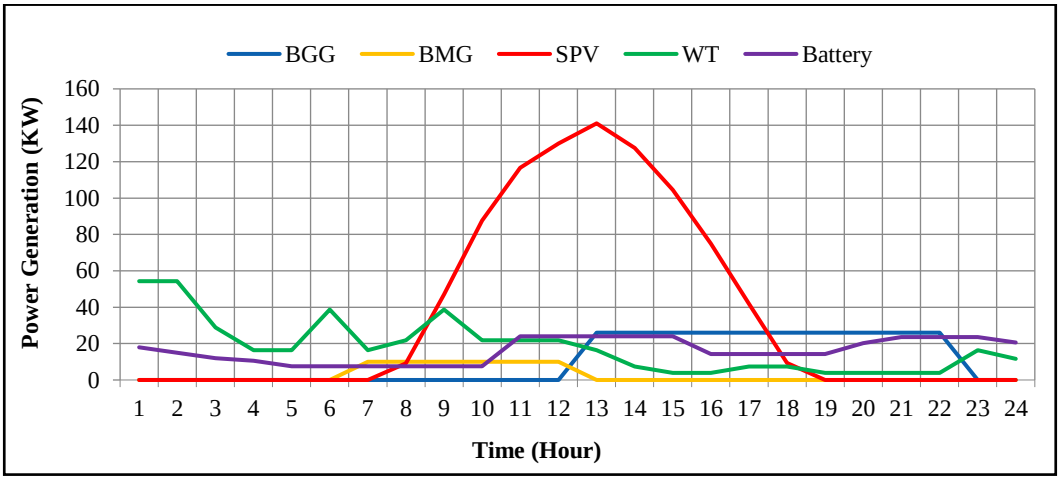

Fig. 7.14 Hourly Energy Generation for One Day by Various Sources

A comprehensive statistical analysis for all three proposed techniques is provided in the present work. The best and worst values of the cost function, mean, median, SD, relative error (RE), RMSE, MAE, and efficiency were obtained and presented in Table 7.11. for CPA, TSA, and AO. As it is evident from Table 7.11, that the statistical indicators, RMSE, SD, MAE, and average RE are all minimum for TSA, while efficiency is highest when contrasted with CPA and AO, demonstrating the TSA's superiority over other algorithms.

Table 7.11 Statistical Indicators for TSA, CPA, and AO Techniques

OT	Best	Average	Worst	SD	Median	Average RE	MAE	RMSE	Efficiency
TSA	649787.5	669837	689850	25	689852.41	0.00008	1.68416	12.0057	99.9927
CPA	659812.5	670850	690475	31.2	689854.71	0.00007	1.99563	24.8970	99.9913
AO	667850	673650	694237	100	690278.86	0.00115	26.5509	134.756	99.8849

Fig. 7.15 depicts the convergence curves for the TSA, CPA, and AO algorithms of the proposed grid connected HRES model. It can be seen that TSA and AO converged and produced a fixed value at iterations 16 and 32, respectively. However, at iteration sixty, CPA stabilized at a constant value. Consequently, TSA has a higher convergence rate than AO and CPA.

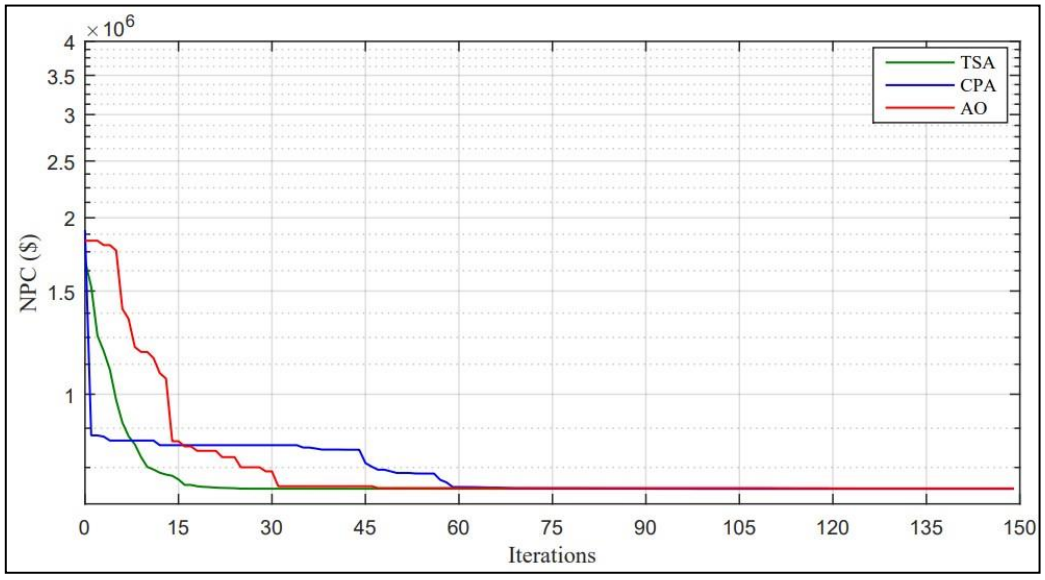

Fig. 7.15 Convergence Curve for TSA, CPA, and AO Algorithms

Furthermore, the findings of the present research are summarized as follows:

- The four recommended ML techniques: GPR, SVR, XGBT, and DT, were used to forecast temperature, wind speed and GHI.
- Based on the statistical indicators, the FM was contrasted, and GPR FM was identified as the best FM.

- The data obtained from GPR for GHI, wind speed and temperature was used as input data for the size optimization of HRES components.
- The recently developed optimization algorithms: TSA, CPA, and AO were initially used to find the optimal size of HRES components using historical meteorological data. The optimization results were also obtained by TSA, CPA, and AO techniques using the forecasted GHI, wind speed and temperature data obtained through the GPR approach.
- The findings of size optimization obtained through the forecasted data were compared with the results obtained for historical meteorological data. The size optimization results obtained using the forecasted data are more appealing due to low NPC and COE.
- Finally, the optimization results of TSA, CPA, and AO algorithms obtained using forecasted data are compared, and it was found that the TSA with forecasted data delivers an optimal solution with a reduction of 0.22% and 0.42% in COE for study area I and study area II respectively.
- The sizes obtained for the different components of the optimal HRES included a 234.77 kW SPV, a 10 kW BGG, an 88 kW BMG, and a 24 kWh BESS for study area I and 282 kW of SPV, 115.5 kW WT, 10 kW BGG, 25 kW BMG, and 36 kWh BESS for study area II.
- For the optimal design, the NPC and COE are estimated to be 0.0557$/kWh, $493100 for study area I and $647800, $ 0.0701/kWh for study area II.

7.6 CONCLUSION

In the present chapter, the size optimization of HRES has been conducted for the outlying region of Mewat, and Agra India. Grid-connected configurations were designed and presented using the forecasted data for GHI and temperature for study area I and GHI, temperature and wind speed for study area II. The four ML methods: SVR, DT, GPR, and XGBT, were used for forecasting, out of which GPR performs better. Therefore, data obtained from GPR FM was used for the sizing of HRES. Further, the HRES was optimized using recently developed CPA, TSA, and AO algorithms. All three algorithms performed well and were suitable for the size optimization of the HRES for both the study areas; however, the sizes of the HRES components for the grid-connected scenario have been found most optimal via the TSA algorithm in both the cases.

The optimal HRES obtained from TSA for study area I included a 234.77 kW SPV, a 10 kW BGG, an 88 kW BMG, and a 24 kWh battery bank. The COE and overall NPC costs were anticipated to be 0.0627 $/kWh and $493100, respectively. The optimal HRES obtained from TSA for study area II included a 282 kW SPV, a 115.5 kW WT, a 10 kW BGG, a 25 kW BMG, and a 36 kWh battery bank. The COE and overall NPC costs were anticipated to be 0.0701 $/kWh and $647,800, respectively. The findings of this study can be utilized to create HRES for locations with similar geographic characteristics, which can improve the lifestyle of people in rural areas by providing an uninterrupted power supply. This research can also help to some extent to fulfill the goal of the Indian government's "power to all" with its availability 24x 7.

CHAPTER 8

CONCLUSION AND FUTURE SCOPE OF WORK

8.1 GENERAL

The study presented in this thesis has made several salient and momentous contributions to the field of HRES. These contributions have advanced our understanding of HRES and have implications for their design, optimization, and overall performance. The significant original contributions of this study are outlined and discussed below:

- In this research, novel CPA, TSA, and AO algorithms were applied for the first time for tackling the problem of optimal sizing of HRES components. Consequently, a comprehensive comparison between these algorithms has been introduced in conjunction with a clear discussion and analysis.

- To improve the accuracy of size optimization of HRES components, the sizing of HRES is done using forecasted data which is rare in literature. In view of this, various ML models have been used for forecasting the solar irradiation, temperature, and wind speed.

- Although, being significant and potentially useful resources, particularly in rural regions, biogas and biomass-based power generation have not received much attention from researchers. Addressing this issue, the HRES developed in this work includes BMG and BGG with scheduling of their operation.

- Broadly speaking, to the best of the author's knowledge, this is the first attempt to apply the proposed OT, to optimize the system components, for solving a real problem of power shortage in Indian village located in Haryana and Uttar Pradesh based on a real-time load data and forecasted meteorological data of the site.

8.2. CONCLUSIONS OF THE PRESENT RESEARCH

The present research has demonstrated the potential of HRES to address the demand and generation mismatch issues, particularly in developing countries like India. Two study areas were identified for the development of HRES: a cluster of villages in the Agra district of Uttar Pradesh and a cluster of villages in the Mewat district of Haryana.

The estimation of RES potential in both study areas revealed significant availability of solar radiation, biomass, and biogas. Additionally, study area II showed the potential for wind energy, further diversifying the available resources for power generation.

Further, the feasibility analysis was conducted for the development of HRES at the selected sites to fulfill the energy needs of rural people. In this direction, various configurations of HRES models were considered, simulated and compared for selected sites and found the optimal one. The results based on NPC and COE indicated that a grid-connected SPV/BMG/BGG/BESS system was the most feasible solution for study area I, while a grid-connected SPV/WT/BMG/BGG/BESS system was the optimal solution for study area II. The development of hybrid models has been facilitated through the utilization of the HOMER Pro software. This work also delves into the understanding of the various advantages, obstacles, and challenges that may occur during the process of incorporating different RES into the grid. Furthermore, it examines potential alternative solutions to

address these issues. The novel AO technique was applied to optimize the size of HRES at specific locations, considering both off-grid and grid-connected scenarios. The study compared AO algorithm results with HS and PSO algorithms.

Furthermore, the research utilized intelligent algorithms TSA, CPA, and AO to optimize hybrid models for the selected sites using forecasted data. The proposed HRES obtained through TSA, consisting of SPV, biomass, and biogas with grid and battery storage, were identified as the least costly solution for study area I. In study area II, the combination of SPV, wind, biomass, and biogas with grid and battery storage proved to be the most economical.

Overall, the research findings demonstrate that HRES can be a viable solution for addressing the energy needs of rural areas in India. By utilizing the locally available RES and optimizing system configurations through advanced algorithms, it is possible to develop cost-effective and sustainable hybrid systems. These findings contribute to the field of renewable energy integration and provide valuable insights for policymakers, researchers, and practitioners in the pursuit of efficient and reliable energy solutions for rural electrification. Further, the results obtained by TSA, CPA, AO, HS and PSO algorithms for proposed hybrid power system for study area I and study area II has been demonstrated in Table 8.1 and Table 8.2.

Table 8.1 Results of TSA, CPA, AO, HS, and PSO Algorithms for Study Area I

Algorithm	PV_p^o (kW)	BMG_p^o (kW)	BGG_p^o (kW)	E_B (kWh)	NPC (10^5 $)	COE ($/kWh)
TSA	234.765	88	63	24	493100.3	0.0627
CPA	233.825	67	28	115.2	533291.2	0.0763
AO	235	64	10	50.40	547670	0.0765
HS	233.12	91	27	115.20	572490	0.082
PSO	149.93	118	58	280.8	759350	0.112

Table 8.2 Results of TSA, CPA, AO, HS and PSO Algorithms for Study Area II

Algorithm	PV_p^o (kW)	W_p^o (kW)	BMG_p^o (kW)	BGG_p^o (kW)	E_B (kWh)	NPC (10^5 $)	COE ($/kWh)
TSA	282	115.5	25	10	36	647800	0.0701
CPA	235	92.4	30	12	33.6	658120	0.0709
AO	237.4	82.5	30	15	43.2	6.61	0.0737
HS	232.65	95.7	20	31	89	8.01	0.0902
PSO	217.14	102.3	19	29	110	8.32	0.0950

In the context of the given problem, we have conducted a comprehensive assessment of the three algorithms based on several criteria, including net present cost (NPC), cost of energy (COE), root mean square error (RMSE), Mean absolute error (MAE), efficiency, and convergence rate which is tabulated in table. All the three techniques perform well but among these three techniques, TSA stands out for its notably swift convergence when compared to the proposed AO and CPA algorithms. TSA exhibits superior performance by achieving the highest efficiency, the lowest RMSE, and the lowest MAE values among the proposed algorithms. Moreover, TSA also demonstrates the least NPC and COE, which aligns with the primary objective of the problem. The comparative

analysis of the algorithms clearly indicates that TSA yields more promising results. the pros and cons of different optimization algorithms used in the current study are as follows:

Table 8.3 Comparision of proposed algorithms

Algorithm	MAE	RMSE	Efficiency	NPC (10^5 $)	COE ($/kWh)	Convergence iterations
TSA	1.68416	12.0057	99.9927	6.47	0.0701	16
CPA	1.99563	24.8970	99.9913	6.58	0.0709	60
AO	26.5509	134.756	99.8849	6.61	0.0737	32

AO demonstrates remarkable exploration capabilities, boasting superior robustness and resistance to fluctuations in population size. Changes in population size have minimal impact on its capacity to discover optimal solutions. This algorithm proves highly effective across a wide spectrum of optimization challenges, whether unconstrained or constrained, single-objective or multi-objective, and continuous or discrete. However, it can exhibit limitations in terms of exploitation for intricate engineering design problems and may suffer from sluggish convergence in more complex scenarios.

CPA, on the other hand, combines the virtues of global exploration and local exploitation. Its predator-prey mechanism inherently fosters population diversity, aiding in escaping local optima and conducting more effective searches through the solution space. Similar to numerous optimization algorithms, the effectiveness of CPA relies heavily on the precise adjustment of parameters.

TSA, designed with a primary focus on computational efficiency, commendable solutions with fewer function evaluations than its counterparts. TSA's commitment to maintaining diversity among potential solutions not only prevents premature convergence

but also fosters comprehensive exploration of the solution space, greatly enhancing its ability to discover global optima. Nonetheless, similar to many optimization methods, TSA necessitates careful tuning of parameters such as population size and convergence criteria.

SCOPE FOR FUTURE WORK

The current research could be extended in the future by including the following:

- The research can focus on optimizing HRES to satisfy different load demands, such as electric, hot water, space heating, cold water, and space cooling. This can involve integrating various hardware components, such as heat pumps, thermal storage systems, and heating, ventilation, and air conditioning units, into the system model. In addition, optimization algorithms can be developed to find the optimal configuration and operation strategy that meets the diverse load requirements while maximizing energy efficiency and minimizing costs.
- It is highly recommended to investigate the effects of advanced economical modelling techniques on the COE for HRES. This can involve incorporating factors such as inflation rates, carbon taxes, and hourly maintenance costs of hardware components into the cost analysis. By considering these economic factors, a more accurate and comprehensive evaluation of the financial viability and long-term economic performance of HRES can be achieved. This research can provide insights into the economic feasibility of HRES deployment and inform decision-making processes.
- The research can focus on the integration of emerging technologies, such as advanced energy storage systems like flow batteries, super capacitors, pumped hydro storage, smart grid technologies, and DR mechanisms, into HRES models and optimization frameworks.

- HRES can also undergo size optimization with a focus on accommodating electric vehicle charging loads.
- Recently developed intelligent hybrid OT can be explored for size optimization of HRES. These techniques can harness the strengths of multiple algorithms while compensating for their weaknesses resulting in improved problem solving capabilities.
- Investigating the impact of uncertainties, including load fluctuations, and component failures, on HRES performance can enhance the resilience and reliability of these systems. Research on risk analysis and mitigation strategies can also be valuable.
- Further, the present research can focus on assessing the life cycle environmental impacts of HRES, including their manufacturing, installation, operation, and decommissioning phases. Comparative studies with conventional energy systems can provide a comprehensive understanding of HRES's environmental benefits.

  By addressing these research areas, future studies can contribute to the practical implementation and economic viability of HRES and therefore will enhance the understanding of HRES's potential benefits and provide valuable insights for policymakers, investors, and stakeholders involved in the transition to RES.

LIST OF PUBLICATIONS

List of papers (s) published in Peer Reviewed Referred International Journals

1. B. Sharma, M. Rizwan, and P. Anand, "A new intelligent approach for size optimization of a renewable energy based grid connected hybrid energy system." **International Journal of Numerical Modelling: Electronic Networks, Devices and Fields,** vol. 36, no. 2 (Mar. 2023), doi.org/10.1002/jnm.3050 ISSN:1099-1204, Impact Factor: 1.6 (SCIE Journal)

2. B. Sharma, M. Rizwan, and P. Anand, "Optimal design of Renewable Energy based Hybrid system Considering Weather Forecasting using Machine Learning Techniques" **Electrical Engineering**, vol. 105, Dec. 2023, doi.org/10.1007/s00202-023-01945-w ISSN: 0948-7921, Impact factor: 1.8 (SCIE Journal)

List of Conferences

1. Sharma, Bandana, M. Rizwan, and P. Anand, "Optimal Sizing of a grid connected Biomass/Biogas/SPV system for Rural Electrification."Proceedings of 3rd International Conference on Machine Learning Advances in Computing Renewable Energy and Communication: MARC 2021. Singapore: Springer Nature Singapore, 2022 [Scopus Indexed Conference].

2. Sharma, Bandana M. Rizwan, and P. Anand, "Feasibility and Techno-Economic Analysis of Renewable Energy based Hybrid System for Rural Community of India", International Conference on "Advancements and Key Challenges in Green Energy and Computing (AKGEC 2023) at Ajay Kumar Garg Engineering College, Uttar Pradesh during 24-25 February 2023. [Scopus Indexed Conference].

3. Sharma, Bandana, M. Rizwan, "Techno-Economic Analysis of Renewable Energy based Hybrid System for Common Facilities of Rural Areas" (JTA 2020) at Jamia Milia Islamia, New Delhi. India during 16-18 Feb 2020

4. Sharma, Bandana, M. Rizwan, and P. Anand, "Techno-Economic Analysis of Renewable Energy based Hybrid System for Common Facilities of Remote Locations in India" (ICSGSM 2021) at KLEF Guntur Andhra Pradesh, India during 19-20 April 2021.

REFERENCES

[1] "World Energy Outlook 2022 – Analysis," *IEA*. https://www.iea.org/reports/world-energy-outlook-2022 (accessed Aug. 07, 2023).

[2] "Renewable capacity statistics 2023," Mar. 21, 2023. https://www.irena.org/Publications/2023/Mar/Renewable-capacity-statistics-2023 (accessed Aug. 07, 2023).

[3] B. Sharma, M. Rizwan, and P. Anand, "A new intelligent approach for size optimization of a renewable energy based grid connected hybrid energy system," *Int. J. Numer. Model. Electron. Netw. Devices Fields*, vol. 36, no. 2, p. e3050, 2023.

[4] "Statistical Review of World Energy | Energy economics | Home," *bp global*. https://www.bp.com/en/global/corporate/energy-economics/statistical-review-of-world-energy.html (accessed Aug. 07, 2023).

[5] N. US Department of Commerce, "Global Monitoring Laboratory - Carbon Cycle Greenhouse Gases." https://gml.noaa.gov/ccgg/trends/ (accessed Aug. 07, 2023).

[6] "Global Energy Outlook application | Long-term energy trends | Enerdata." https://www.enerdata.net/publications/energy-outlook-tool.html (accessed Aug. 07, 2023).

[7] "Executive Summary Report," *Central Electricity Authority*. https://cea.nic.in/executive-summary-report/?lang=en (accessed Aug. 07, 2023).

[8] "Koyla Darpan | Ministry of Coal." https://coaldashboard.cmpdi.co.in/dashboard.php (accessed Aug. 07, 2023).

[9] "Global Electricity Review 2023," *Ember*, Apr. 11, 2023. https://ember-climate.org/insights/research/global-electricity-review-2023/ (accessed Aug. 07, 2023).

[10] "DRAFT_NATIONAL_ELECTRICITY_PLAN_9_SEP_2022_2-1.pdf." Accessed: Aug. 07, 2023. [Online]. Available: https://cea.nic.in/wp-content/uploads/irp/2022/09/DRAFT_NATIONAL_ELECTRICITY_PLAN_9_SEP_2022_2-1.pdf

[11] "'National Electricity Plan (Generation) 2018'. Retrieved 25 March 2021.," *Bing*. https://www.bing.com/search?q="National+Electricity+Plan+(Generation)+2018". +Retrieved+25+March+2021.&cvid=bdd1e15fd3ac4e49af9f69f27fb1abb2&aqs=edge..69i57.2051j0j4&FORM=ANAB01&PC=DCTS (accessed Aug. 07, 2023).

[12] "Optimal_mix_report_2029-30_FINAL.pdf." Accessed: Aug. 07, 2023. [Online]. Available: https://cea.nic.in/old/reports/others/planning/irp/Optimal_mix_report_2029-30_FINAL.pdf

[13] "Growth of Electricity Sector in India (1947-2022)," *Central Electricity Authority*. https://cea.nic.in/notification/growth-of-electricity-sector-in-india-1947-2022/?lang=en (accessed Aug. 07, 2023).

[14] “file_s-1683099362708.pdf.” Accessed: Aug. 07, 2023. [Online]. Available: https://mnre.gov.in/img/documents/uploads/file_s-1683099362708.pdf

[15] “Installed Capacity Report - Central Electricity Authority.” https://cea.nic.in/installed-capacity-report/?lang=en (accessed Aug. 07, 2023).

[16] M. Sharafi, T. Y. ElMekkawy, and E. L. Bibeau, “Optimal design of hybrid renewable energy systems in buildings with low to high renewable energy ratio,” *Renew. Energy*, vol. 83, pp. 1026–1042, Nov. 2015, doi: 10.1016/j.renene.2015.05.022.

[17] “Optimal Sizing and Energy Management of a Microgrid Using Single and Multi-Objective Particle Swarm Optimization under Autonomous and Grid Connected Mode.” https://www.sae.org/publications/technical-papers/content/2019-28-0158/ (accessed Aug. 08, 2023).

[18] S. Das, A. Abraham, and A. Konar, “Particle Swarm Optimization and Differential Evolution Algorithms: Technical Analysis, Applications and Hybridization Perspectives,” in *Advances of Computational Intelligence in Industrial Systems*, Y. Liu, A. Sun, H. T. Loh, W. F. Lu, and E.-P. Lim, Eds., in Studies in Computational Intelligence. Berlin, Heidelberg: Springer, 2008, pp. 1–38. doi: 10.1007/978-3-540-78297-1_1.

[19] T. Bartz-Beielstein, “Designing particle swarm optimization with regression trees,” 2004.

[20] M. R. Elkadeem, S. Wang, S. W. Sharshir, and E. G. Atia, “Feasibility analysis and techno-economic design of grid-isolated hybrid renewable energy system for electrification of agriculture and irrigation area: A case study in Dongola, Sudan,” *Energy Convers. Manag.*, vol. 196, pp. 1453–1478, Sep. 2019, doi: 10.1016/j.enconman.2019.06.085.

[21] J. Ahmad *et al.*, “Techno economic analysis of a wind-photovoltaic-biomass hybrid renewable energy system for rural electrification: A case study of Kallar Kahar,” *Energy*, vol. 148, pp. 208–234, Apr. 2018, doi: 10.1016/j.energy.2018.01.133.

[22] J. Li, P. Liu, and Z. Li, “Optimal design and techno-economic analysis of a solar-wind-biomass off-grid hybrid power system for remote rural electrification: A case study of west China,” *Energy*, vol. 208, p. 118387, Oct. 2020, doi: 10.1016/j.energy.2020.118387.

[23] K. Gebrehiwot, Md. A. H. Mondal, C. Ringler, and A. G. Gebremeskel, “Optimization and cost-benefit assessment of hybrid power systems for off-grid rural electrification in Ethiopia,” *Energy*, vol. 177, pp. 234–246, Jun. 2019, doi: 10.1016/j.energy.2019.04.095.

[24] G. Zhang, C. Xiao, and N. Razmjooy, “Optimal operational strategy of hybrid PV/wind renewable energy system using homer: a case study,” *Int. J. Ambient Energy*, vol. 43, no. 1, pp. 3953–3966, Dec. 2022, doi: 10.1080/01430750.2020.1861087.

[25] O. D. T. Odou, R. Bhandari, and R. Adamou, “Hybrid off-grid renewable power system for sustainable rural electrification in Benin,” *Renew. Energy*, vol. 145, pp. 1266–1279, Jan. 2020, doi: 10.1016/j.renene.2019.06.032.

[26] M. M. A. Seedahmed, M. A. M. Ramli, H. R. E. H. Bouchekara, M. S. Shahriar, A. H. Milyani, and M. Rawa, “A techno-economic analysis of a hybrid energy system for the electrification of a remote cluster in western Saudi Arabia,” *Alex. Eng. J.*, vol. 61, no. 7, pp. 5183–5202, Jul. 2022, doi: 10.1016/j.aej.2021.10.041.

[27] P. Malik, M. Awasthi, and S. Sinha, “Techno-economic and environmental analysis of biomass-based hybrid energy systems: A case study of a Western Himalayan state in India,” *Sustain. Energy Technol. Assess.*, vol. 45, p. 101189, Jun. 2021, doi: 10.1016/j.seta.2021.101189.

[28] F. A. Khan, N. Pal, and Syed. H. Saeed, “Review of solar photovoltaic and wind hybrid energy systems for sizing strategies optimization techniques and cost analysis methodologies,” *Renew. Sustain. Energy Rev.*, vol. 92, pp. 937–947, Sep. 2018, doi: 10.1016/j.rser.2018.04.107.

[29] A. V. Anayochukwu, “Feasibility Assessment of a PV-Diesel Hybrid Power System for an Isolated Off-Grid Catholic Church,” *Electron. J. Energy Environ.*, vol. 1, no. 3, Dec. 2013, doi: 10.7770/ejee-V1N3-art684.

[30] S. Bhardwaj and S. K. Garg, “Rural electrification by effective mini hybrid PV solar, wind & biogas energy system for rural and remote areas of Uttar Pradesh,” *Int. J. Comput. Sci. Electron. Eng. IJCSEE*, vol. 2, no. 4, pp. 178–181, 2014.

[31] V. A. Ani and B. Abubakar, “Feasibility Analysis and Simulation of Integrated Renewable Energy System for Power Generation: A Hypothetical Study of Rural Health Clinic,” *J. Energy*, vol. 2015, pp. 1–7, 2015, doi: 10.1155/2015/802036.

[32] S. Goel and R. Sharma, “Feasibility study of hybrid energy system for off-grid rural water supply and sanitation system in Odisha, India,” *Int. J. Ambient Energy*, vol. 37, no. 3, pp. 314–320, May 2016, doi: 10.1080/01430750.2014.962089.

[33] A. Chauhan and R. P. Saini, “Techno-economic feasibility study on Integrated Renewable Energy System for an isolated community of India,” *Renew. Sustain. Energy Rev.*, vol. 59, pp. 388–405, Jun. 2016, doi: 10.1016/j.rser.2015.12.290.

[34] I. Padrón, D. Avila, G. N. Marichal, and J. A. Rodríguez, “Assessment of Hybrid Renewable Energy Systems to supplied energy to Autonomous Desalination Systems in two islands of the Canary Archipelago,” *Renew. Sustain. Energy Rev.*, vol. 101, pp. 221–230, Mar. 2019, doi: 10.1016/j.rser.2018.11.009.

[35] W. Ma, X. Xue, G. Liu, and R. Zhou, “Techno-economic evaluation of a community-based hybrid renewable energy system considering site-specific nature,” *Energy Convers. Manag.*, vol. 171, pp. 1737–1748, Sep. 2018, doi: 10.1016/j.enconman.2018.06.109.

[36] E. L. V. Eriksson and E. M. Gray, “Optimization and integration of hybrid renewable energy hydrogen fuel cell energy systems–A critical review,” *Appl. Energy*, vol. 202, pp. 348–364, 2017.

[37] A. S. R. Subramanian, T. Gundersen, and T. A. Adams, “Modeling and simulation of energy systems: A review,” *Processes*, vol. 6, no. 12, p. 238, 2018.

[38] M. Ghofrani and N. N. Hosseini, “Optimizing hybrid renewable energy systems: a review,” *Sustain. Energy-Technol. Issues Appl. Case Stud.*, pp. 161–176, 2016.

[39] G. Tina, S. Gagliano, and S. Raiti, “Hybrid solar/wind power system probabilistic modelling for long-term performance assessment,” *Sol. Energy*, vol. 80, no. 5, pp. 578–588, 2006.

[40] D. K. Khatod, V. Pant, and J. Sharma, “Analytical approach for well-being assessment of small autonomous power systems with solar and wind energy sources,” *IEEE Trans. Energy Convers.*, vol. 25, no. 2, pp. 535–545, 2009.

[41] S. Ashok, “Optimised model for community-based hybrid energy system,” *Renew. Energy*, vol. 32, no. 7, pp. 1155–1164, 2007.

[42] S. Singh, M. Singh, and S. C. Kaushik, “A review on optimization techniques for sizing of solar-wind hybrid energy systems,” *Int. J. Green Energy*, vol. 13, no. 15, pp. 1564–1578, 2016.

[43] J. Li, W. Wei, and J. Xiang, “A simple sizing algorithm for stand-alone PV/wind/battery hybrid microgrids,” *Energies*, vol. 5, no. 12, pp. 5307–5323, 2012.

[44] R. Chedid and S. Rahman, “Unit sizing and control of hybrid wind-solar power systems,” *IEEE Trans. Energy Convers.*, vol. 12, no. 1, pp. 79–85, 1997.

[45] F. Huneke, J. Henkel, J. A. Benavides González, and G. Erdmann, “Optimisation of hybrid off-grid energy systems by linear programming,” *Energy Sustain. Soc.*, vol. 2, no. 1, pp. 1–19, 2012.

[46] A. R. De and L. Musgrove, “The optimization of hybrid energy conversion systems using the dynamic programming model—Rapsody,” *Int. J. Energy Res.*, vol. 12, no. 3, pp. 447–457, 1988.

[47] A. G. Bakirtzis and E. S. Gavanidou, “Optimum operation of a small autonomous system with unconventional energy sources,” *Electr. Power Syst. Res.*, vol. 23, no. 2, pp. 93–102, 1992.

[48] A. R. Prasad and E. Natarajan, “Optimization of integrated photovoltaic–wind power generation systems with battery storage,” *Energy*, vol. 31, no. 12, pp. 1943–1954, 2006.

[49] G. Tina, S. Gagliano, and S. Raiti, “Hybrid solar/wind power system probabilistic modelling for long-term performance assessment,” *Sol. Energy*, vol. 80, no. 5, pp. 578–588, 2006.

[50] M. Hakimi, S. M. M. Tafreshi, and M. R. Rajati, “Unit sizing of a stand-alone hybrid power system using model-free optimization,” in *2007 IEEE International Conference on Granular Computing (GRC 2007)*, IEEE, 2007, pp. 751–751.

[51] J.-Y. Lee, C.-L. Chen, and H.-C. Chen, “A mathematical technique for hybrid power system design with energy loss considerations,” *Energy Convers. Manag.*, vol. 82, pp. 301–307, 2014.

[52] B. S. Borowy and Z. M. Salameh, “Methodology for optimally sizing the combination of a battery bank and PV array in a wind/PV hybrid system,” *IEEE Trans. Energy Convers.*, vol. 11, no. 2, pp. 367–375, 1996.

[53] T. Markvart, “Sizing of hybrid photovoltaic-wind energy systems,” *Sol. Energy*, vol. 57, no. 4, pp. 277–281, 1996.

[54] A. Askarzadeh and L. dos Santos Coelho, “A novel framework for optimization of a grid independent hybrid renewable energy system: A case study of Iran,” *Sol. Energy*, vol. 112, pp. 383–396, 2015.

[55] M. A. Mohamed, A. M. Eltamaly, and A. I. Alolah, “PSO-based smart grid application for sizing and optimization of hybrid renewable energy systems,” *PloS One*, vol. 11, no. 8, p. e0159702, 2016.

[56] M. J. Hadidian-Moghaddam, S. Arabi-Nowdeh, and M. Bigdeli, “Optimal sizing of a stand-alone hybrid photovoltaic/wind system using new grey wolf optimizer considering reliability,” *J. Renew. Sustain. Energy*, vol. 8, no. 3, p. 035903, 2016.

[57] S. S. Singh and E. Fernandez, “Modeling, size optimization and sensitivity analysis of a remote hybrid renewable energy system,” *Energy*, vol. 143, pp. 719–731, 2018.

[58] Z. Jing, J. Zhu, and R. Hu, “Sizing optimization for island microgrid with pumped storage system considering demand response,” *J. Mod. Power Syst. Clean Energy*, vol. 6, no. 4, pp. 791–801, 2018.

[59] A. Yahiaoui, F. Fodhil, K. Benmansour, M. Tadjine, and N. Cheggaga, “Grey wolf optimizer for optimal design of hybrid renewable energy system PV-Diesel Generator-Battery: Application to the case of Djanet city of Algeria,” *Sol. Energy*, vol. 158, pp. 941–951, 2017.

[60] M. K. Shahzad, A. Zahid, T. ur Rashid, M. A. Rehan, M. Ali, and M. Ahmad, “Techno-economic feasibility analysis of a solar-biomass off grid system for the electrification of remote rural areas in Pakistan using HOMER software,” *Renew. Energy*, vol. 106, pp. 264–273, 2017.

[61] A. Chauhan and R. P. Saini, “Size optimization and demand response of a stand-alone integrated renewable energy system,” *Energy*, vol. 124, pp. 59–73, 2017.

[62] Y. Sawle, S. C. Gupta, and A. K. Bohre, “Socio-techno-economic design of hybrid renewable energy system using optimization techniques,” *Renew. Energy*, vol. 119, pp. 459–472, 2018.

[63] S. Charfi, A. Atieh, and M. Chaabene, “Optimal sizing of a hybrid solar energy system using particle swarm optimization algorithm based on cost and pollution criteria,” *Environ. Prog. Sustain. Energy*, vol. 38, no. 3, p. e13055, 2019.

[64] P. Anand, S. K. Bath, and M. Rizwan, “Renewable energy-based hybrid model for rural electrification,” *Int. J. Energy Technol. Policy*, vol. 15, no. 1, pp. 86–113, 2019.

[65] P. Anand, S. K. Bath, and M. Rizwan, “Size optimisation of RES-based grid connected hybrid power system using harmony search algorithm,” *Int. J. Energy Technol. Policy*, vol. 16, no. 3, pp. 238–276, 2020.

[66] M. N. Ashtiani, A. Toopshekan, F. R. Astaraei, H. Yousefi, and A. Maleki, “Techno-economic analysis of a grid-connected PV/battery system using the teaching-learning-based optimization algorithm,” *Sol. Energy*, vol. 203, pp. 69–82, 2020.

[67] M. Das, M. A. K. Singh, and A. Biswas, “Techno-economic optimization of an off-grid hybrid renewable energy system using metaheuristic optimization approaches–case of a radio transmitter station in India,” *Energy Convers. Manag.*, vol. 185, pp. 339–352, 2019.

[68] S. Mishra, G. Saini, A. Chauhan, S. Upadhyay, and D. Balakrishnan, “Optimal sizing and assessment of grid-tied hybrid renewable energy system for electrification of rural site,” *Renew. Energy Focus*, vol. 44, pp. 259–276, 2023.

[69] A. Khare and S. Rangnekar, “A review of particle swarm optimization and its applications in solar photovoltaic system,” *Appl. Soft Comput.*, vol. 13, no. 5, pp. 2997–3006, 2013.

[70] S. A. Kalogirou, “Optimization of solar systems using artificial neural-networks and genetic algorithms,” *Appl. Energy*, vol. 77, no. 4, pp. 383–405, 2004.

[71] A. Mellit, S. A. Kalogirou, and M. Drif, “Application of neural networks and genetic algorithms for sizing of photovoltaic systems,” *Renew. Energy*, vol. 35, no. 12, pp. 2881–2893, 2010.

[72] T. Khatib, A. Mohamed, and K. Sopian, “Optimization of a PV/wind micro-grid for rural housing electrification using a hybrid iterative/genetic algorithm: Case study of Kuala Terengganu, Malaysia,” *Energy Build.*, vol. 47, pp. 321–331, 2012.

[73] A. Askarzadeh, “A discrete chaotic harmony search-based simulated annealing algorithm for optimum design of PV/wind hybrid system,” *Sol. Energy*, vol. 97, pp. 93–101, 2013.

[74] D. Xu, L. Kang, L. Chang, and B. Cao, “Optimal sizing of standalone hybrid wind/PV power systems using genetic algorithms,” in *Canadian Conference on Electrical and Computer Engineering, 2005.*, IEEE, 2005, pp. 1722–1725.

[75] Y. A. Katsigiannis, P. S. Georgilakis, and E. S. Karapidakis, “Hybrid simulated annealing–tabu search method for optimal sizing of autonomous power systems with renewables,” *IEEE Trans. Sustain. Energy*, vol. 3, no. 3, pp. 330–338, 2012.

[76] S. Ahmadi and S. Abdi, “Application of the Hybrid Big Bang–Big Crunch algorithm for optimal sizing of a stand-alone hybrid PV/wind/battery system,” *Sol. Energy*, vol. 134, pp. 366–374, Sep. 2016, doi: 10.1016/j.solener.2016.05.019.

[77] S. Kamel and C. Dahl, “The Economics of Hybrid Power Systems for Sustainable Desert Agriculture in Egypt”.

[78] R. Dufo-López and J. L. Bernal-Agustín, “Design and control strategies of PV-Diesel systems using genetic algorithms,” *Sol. Energy*, vol. 79, no. 1, pp. 33–46, Jul. 2005, doi: 10.1016/j.solener.2004.10.004.

[79] M. R. Nouni, S. C. Mullick, and T. C. Kandpal, “Providing electricity access to remote areas in India: Niche areas for decentralized electricity supply,” *Renew. Energy*, vol. 34, no. 2, pp. 430–434, Feb. 2009, doi: 10.1016/j.renene.2008.05.006.

[80] M. O. Abdullah, V. C. Yung, M. Anyi, A. K. Othman, K. B. Ab. Hamid, and J. Tarawe, “Review and comparison study of hybrid diesel/solar/hydro/fuel cell energy schemes for a rural ICT Telecenter,” *Energy*, vol. 35, no. 2, pp. 639–646, Feb. 2010, doi: 10.1016/j.energy.2009.10.035.

[81] S. Rehman and L. M. Al-Hadhrami, “Study of a solar PV–diesel–battery hybrid power system for a remotely located population near Rafha, Saudi Arabia,” *Energy*, vol. 35, no. 12, pp. 4986–4995, Dec. 2010, doi: 10.1016/j.energy.2010.08.025.

[82] S. Kumaravel and S. Ashok, “An Optimal Stand-Alone Biomass/Solar-PV/Pico-Hydel Hybrid Energy System for Remote Rural Area Electrification of Isolated Village in Western-Ghats Region of India,” *Int. J. Green Energy*, vol. 9, no. 5, pp. 398–408, Jul. 2012, doi: 10.1080/15435075.2011.621487.

[83] I. P. Panapakidis, D. N. Sarafianos, and M. C. Alexiadis, “Comparative analysis of different grid-independent hybrid power generation systems for a residential load,” *Renew. Sustain. Energy Rev.*, vol. 16, no. 1, pp. 551–563, Jan. 2012, doi: 10.1016/j.rser.2011.08.021.

[84] R. Sen and S. C. Bhattacharyya, “Off-grid electricity generation with renewable energy technologies in India: An application of HOMER,” *Renew. Energy*, vol. 62, pp. 388–398, Feb. 2014, doi: 10.1016/j.renene.2013.07.028.

[85] M. A. M. Ramli, A. Hiendro, and Y. A. Al-Turki, “Techno-economic energy analysis of wind/solar hybrid system: Case study for western coastal area of Saudi Arabia,” *Renew. Energy*, vol. 91, pp. 374–385, Jun. 2016, doi: 10.1016/j.renene.2016.01.071.

[86] N. Phuangpornpitak and S. Kumar, “PV hybrid systems for rural electrification in Thailand,” *Renew. Sustain. Energy Rev.*, vol. 11, no. 7, pp. 1530–1543, Sep. 2007, doi: 10.1016/j.rser.2005.11.008.

[87] D. Saheb-Koussa, M. Koussa, M. Belhamel, and M. Haddadi, “Economic and environmental analysis for grid-connected hybrid photovoltaic-wind power system in the arid region,” *Energy Procedia*, vol. 6, pp. 361–370, 2011, doi: 10.1016/j.egypro.2011.05.042.

[88] H. Garrido, V. Vendeirinho, and M. C. Brito, “Feasibility of KUDURA hybrid generation system in Mozambique: Sensitivity study of the small-scale PV-biomass and PV-diesel power generation hybrid system,” *Renew. Energy*, vol. 92, pp. 47–57, Jul. 2016, doi: 10.1016/j.renene.2016.01.085.

[89] M. K. Shahzad, A. Zahid, T. ur Rashid, M. A. Rehan, M. Ali, and M. Ahmad, “Techno-economic feasibility analysis of a solar-biomass off grid system for the

electrification of remote rural areas in Pakistan using HOMER software," *Renew. Energy*, vol. 106, pp. 264–273, Jun. 2017, doi: 10.1016/j.renene.2017.01.033.

[90] J. G. McGowan, J. F. Manwell, C. Avelar, and C. L. Warner, "Hybrid wind/PV/diesel hybrid power systems modeling and South American applications," *Renew. Energy*, vol. 9, no. 1–4, pp. 836–847, Sep. 1996, doi: 10.1016/0960-1481(96)88412-6.

[91] S. M. Shaahid and M. A. Elhadidy, "Technical and economic assessment of grid-independent hybrid photovoltaic–diesel–battery power systems for commercial loads in desert environments," *Renew. Sustain. Energy Rev.*, vol. 11, no. 8, pp. 1794–1810, Oct. 2007, doi: 10.1016/j.rser.2006.03.001.

[92] G. J. Dalton, D. A. Lockington, and T. E. Baldock, "Feasibility analysis of stand-alone renewable energy supply options for a large hotel," *Renew. Energy*, vol. 33, no. 7, pp. 1475–1490, Jul. 2008, doi: 10.1016/j.renene.2007.09.014.

[93] C.-H. Li, X.-J. Zhu, G.-Y. Cao, S. Sui, and M.-R. Hu, "Dynamic modeling and sizing optimization of stand-alone photovoltaic power systems using hybrid energy storage technology," *Renew. Energy*, vol. 34, no. 3, pp. 815–826, Mar. 2009, doi: 10.1016/j.renene.2008.04.018.

[94] J. Kenfack, F. P. Neirac, T. T. Tatietse, D. Mayer, M. Fogue, and A. Lejeune, "Microhydro-PV-hybrid system: Sizing a small hydro-PV-hybrid system for rural electrification in developing countries," *Renew. Energy*, vol. 34, no. 10, pp. 2259–2263, Oct. 2009, doi: 10.1016/j.renene.2008.12.038.

[95] P. Balamurugan, S. Ashok, and T. L. Jose, "Optimal Operation of Biomass/Wind/PV Hybrid Energy System for Rural Areas," *Int. J. Green Energy*, vol. 6, no. 1, pp. 104–116, Mar. 2009, doi: 10.1080/15435070802701892.

[96] A. V. Anayochukwu and E. A. Nnene, "Simulation and Optimization of Photovoltaic/ Diesel Hybrid Power Generation Systems for Health Service Facilities in Rural Environments," *Electron. J. Energy Environ.*, vol. 1, no. 1, May 2013, doi: 10.7770/ejee-V1N1-art521.

[97] M. Ismail, A. Alam, A. R. Masud, M. Hussain, and H. Rasheed, "Optimal configuration of Hybrid Renewable Energy System for remote areas of Balochistan," in *17th IEEE International Multi Topic Conference 2014*, Karachi: IEEE, Dec. 2014, pp. 539–544. doi: 10.1109/INMIC.2014.7097399.

[98] J. L. Bernal-Agustín, R. Dufo-López, and D. M. Rivas-Ascaso, "Design of isolated hybrid systems minimizing costs and pollutant emissions," *Renew. Energy*, vol. 31, no. 14, pp. 2227–2244, 2006.

[99] R. Dufo-López *et al.*, "Multi-objective optimization minimizing cost and life cycle emissions of stand-alone PV–wind–diesel systems with batteries storage," *Appl. Energy*, vol. 88, no. 11, pp. 4033–4041, 2011.

[100] H. Yang, W. Zhou, L. Lu, and Z. Fang, “Optimal sizing method for stand-alone hybrid solar–wind system with LPSP technology by using genetic algorithm,” *Sol. Energy*, vol. 82, no. 4, pp. 354–367, Apr. 2008, doi: 10.1016/j.solener.2007.08.005.

[101] B. O. Bilal, V. Sambou, P. A. Ndiaye, C. M. F. Kébé, and M. Ndongo, “Optimal design of a hybrid solar–wind-battery system using the minimization of the annualized cost system and the minimization of the loss of power supply probability (LPSP),” *Renew. Energy*, vol. 35, no. 10, pp. 2388–2390, 2010.

[102] S. M. M. Tafreshi, H. A. Zamani, S. M. Ezzati, M. Baghdadi, and H. Vahedi, “Optimal unit sizing of distributed energy resources in microgrid using genetic algorithm,” in *2010 18th Iranian Conference on Electrical Engineering*, IEEE, 2010, pp. 836–841.

[103] A. Navaeefard, S. M. Tafreshi, M. Barzegari, and A. J. Shahrood, “Optimal sizing of distributed energy resources in microgrid considering wind energy uncertainty with respect to reliability,” in *2010 IEEE International Energy Conference*, IEEE, 2010, pp. 820–825.

[104] M. Bashir and J. Sadeh, “Optimal sizing of hybrid wind/photovoltaic/battery considering the uncertainty of wind and photovoltaic power using Monte Carlo,” in *2012 11th International Conference on Environment and Electrical Engineering*, IEEE, 2012, pp. 1081–1086.

[105] M. Pirhaghshenasvali and B. Asaei, “Optimal modeling and sizing of a practical hybrid wind/PV/diesel generation system,” in *The 5th Annual International Power Electronics, Drive Systems and Technologies Conference (PEDSTC 2014)*, IEEE, 2014, pp. 506–511.

[106] A. Askarzadeh, “Developing a discrete harmony search algorithm for size optimization of wind–photovoltaic hybrid energy system,” *Sol. Energy*, vol. 98, pp. 190–195, 2013.

[107] M. S. Ismail, M. Moghavvemi, and T. M. I. Mahlia, “Genetic algorithm based optimization on modeling and design of hybrid renewable energy systems,” *Energy Convers. Manag.*, vol. 85, pp. 120–130, 2014.

[108] A. Maleki and A. Askarzadeh, “Optimal sizing of a PV/wind/diesel system with battery storage for electrification to an off-grid remote region: A case study of Rafsanjan, Iran,” *Sustain. Energy Technol. Assess.*, vol. 7, pp. 147–153, 2014.

[109] A. Heydari and A. Askarzadeh, “Optimization of a biomass-based photovoltaic power plant for an off-grid application subject to loss of power supply probability concept,” *Appl. Energy*, vol. 165, pp. 601–611, 2016.

[110] A. Tabak, E. Kayabasi, M. T. Guneser, and M. Ozkaymak, “Grey wolf optimization for optimum sizing and controlling of a PV/WT/BM hybrid energy system considering TNPC, LPSP, and LCOE concepts,” *Energy Sources Part Recovery Util. Environ. Eff.*, vol. 44, no. 1, pp. 1508–1528, 2022.

[111] A. A. Z. Diab, H. M. Sultan, I. S. Mohamed, O. N. Kuznetsov, and T. D. Do, "Application of different optimization algorithms for optimal sizing of PV/wind/diesel/battery storage stand-alone hybrid microgrid," *IEEE Access*, vol. 7, pp. 119223–119245, 2019.

[112] P. Anand, S. K. Bath, and M. Rizwan, "Renewable energy-based hybrid model for rural electrification," *Int. J. Energy Technol. Policy*, vol. 15, no. 1, pp. 86–113, 2019.

[113] I. J. Mwakitalima, M. Rizwan, and N. Kumar, "Standalone solar photovoltaic electricity supply to rural household in Tanzania," *IETE J. Res.*, pp. 1–16, 2021.

[114] P. Bakhshaei, A. Askarzadeh, and R. Arababadi, "Operation optimization of a grid-connected photovoltaic/pumped hydro storage considering demand response program by an improved crow search algorithm," *J. Energy Storage*, vol. 44, p. 103326, 2021.

[115] S. Jamshidi, K. Pourhossein, and M. Asadi, "Size estimation of wind/solar hybrid renewable energy systems without detailed wind and irradiation data: A feasibility study," *Energy Convers. Manag.*, vol. 234, p. 113905, 2021.

[116] M. Rezaei, U. Dampage, B. K. Das, O. Nasif, P. F. Borowski, and M. A. Mohamed, "Investigating the impact of economic uncertainty on optimal sizing of grid-independent hybrid renewable energy systems," *Processes*, vol. 9, no. 8, p. 1468, 2021.

[117] S. Acharya, G. Sivarajan, D. V. Kumar, and S. Srikrishna, "A hybridized approach for design and optimization of combined economic emission dispatch," *Energy Sources Part B Econ. Plan. Policy*, vol. 16, no. 10, pp. 903–928, 2021.

[118] B. K. Das, M. S. H. Tushar, and R. Hassan, "Techno-economic optimisation of stand-alone hybrid renewable energy systems for concurrently meeting electric and heating demand," *Sustain. Cities Soc.*, vol. 68, p. 102763, 2021.

[119] M. Lei, L. Shiyan, J. Chuanwen, L. Hongling, and Z. Yan, "A review on the forecasting of wind speed and generated power," *Renew. Sustain. Energy Rev.*, vol. 13, no. 4, pp. 915–920, May 2009, doi: 10.1016/j.rser.2008.02.002.

[120] J. P. S. Catalao, H. M. I. Pousinho, and V. M. F. Mendes, "Hybrid Wavelet-PSO-ANFIS Approach for Short-Term Wind Power Forecasting in Portugal," *IEEE Trans. Sustain. Energy*, p. 5571038, Jan. 2010, doi: 10.1109/TSTE.2010.2076359.

[121] M. Khalid and A. V. Savkin, "A model predictive control approach to the problem of wind power smoothing with controlled battery storage," *Renew. Energy*, vol. 35, no. 7, pp. 1520–1526, Jul. 2010, doi: 10.1016/j.renene.2009.11.030.

[122] A. Tascikaraoglu, M. Uzunoglu, and B. Vural, "The assessment of the contribution of short-term wind power predictions to the efficiency of stand-alone hybrid systems," *Appl. Energy*, vol. 94, pp. 156–165, Jun. 2012, doi: 10.1016/j.apenergy.2012.01.017.

[123] F. O. Hocaoglu, O. N. Gerek, and M. Kurban, “The effect of model generated solar radiation data usage in hybrid (wind–PV) sizing studies,” *Energy Convers. Manag.*, vol. 50, no. 12, pp. 2956–2963, Dec. 2009, doi: 10.1016/j.enconman.2009.07.011.

[124] W. Zhang, A. Maleki, M. A. Rosen, and J. Liu, “Sizing a stand-alone solar-wind-hydrogen energy system using weather forecasting and a hybrid search optimization algorithm,” *Energy Convers. Manag.*, vol. 180, pp. 609–621, Jan. 2019, doi: 10.1016/j.enconman.2018.08.102.

[125] R. A. Gupta, R. Kumar, and A. K. Bansal, “BBO-based small autonomous hybrid power system optimization incorporating wind speed and solar radiation forecasting,” *Renew. Sustain. Energy Rev.*, vol. 41, pp. 1366–1375, Jan. 2015, doi: 10.1016/j.rser.2014.09.017.

[126] A. Maleki, M. G. Khajeh, and M. A. Rosen, “Weather forecasting for optimization of a hybrid solar-wind–powered reverse osmosis water desalination system using a novel optimizer approach,” *Energy*, vol. 114, pp. 1120–1134, Nov. 2016, doi: 10.1016/j.energy.2016.06.134.

[127] A. A. Medina-Santana and L. E. Cárdenas-Barrón, “Optimal Design of Hybrid Renewable Energy Systems Considering Weather Forecasting Using Recurrent Neural Networks,” *Energies*, vol. 15, no. 23, p. 9045, Nov. 2022, doi: 10.3390/en15239045.

[128] M. Bilgili, A. Ozbek, B. Sahin, and A. Kahraman, “An overview of renewable electric power capacity and progress in new technologies in the world,” *Renew. Sustain. Energy Rev.*, vol. 49, pp. 323–334, Sep. 2015, doi: 10.1016/j.rser.2015.04.148.

[129] A. Alshahrani, S. Omer, Y. Su, E. Mohamed, and S. Alotaibi, “The Technical Challenges Facing the Integration of Small-Scale and Large-scale PV Systems into the Grid: A Critical Review,” *Electronics*, vol. 8, no. 12, p. 1443, Dec. 2019, doi: 10.3390/electronics8121443.

[130] Kulkarni, Sonali N and Prashant Shingare, “A review on power quality challenges in renewable Energy grid integration,” *Int. J. Curr. Eng. Technol.*, Jan. 2011, doi: 10.14741/Ijcet/22774106/6.5.2016.14.

[131] J. Oyekale, M. Petrollese, V. Tola, and G. Cau, “Impacts of Renewable Energy Resources on Effectiveness of Grid-Integrated Systems: Succinct Review of Current Challenges and Potential Solution Strategies,” *Energies*, vol. 13, no. 18, p. 4856, Sep. 2020, doi: 10.3390/en13184856.

[132] E. M. Sandhu and D. T. Thakur, “Issues, Challenges, Causes, Impacts and Utilization of Renewable Energy Sources - Grid Integration,” vol. 4, no. 3, 2014.

[133] M. Al Talaq and C. A. Belhaj, “Optimal PV Penetration for Power Losses Subject to Transient Stability and Harmonics,” *Procedia Comput. Sci.*, vol. 175, pp. 508–516, 2020, doi: 10.1016/j.procs.2020.07.072.

[134] A. Zahedi, "A review of drivers, benefits, and challenges in integrating renewable energy sources into electricity grid," *Renew. Sustain. Energy Rev.*, vol. 15, no. 9, pp. 4775–4779, Dec. 2011, doi: 10.1016/j.rser.2011.07.074.

[135] A. Soroudi, M. Ehsan, R. Caire, and N. Hadjsaid, "Possibilistic Evaluation of Distributed Generations Impacts on Distribution Networks," *IEEE Trans. Power Syst.*, vol. 26, no. 4, pp. 2293–2301, Nov. 2011, doi: 10.1109/TPWRS.2011.2116810.

[136] V. S. Lopes and C. L. T. Borges, "Impact of the Combined Integration of Wind Generation and Small Hydropower Plants on the System Reliability," *IEEE Trans. Sustain. Energy*, vol. 6, no. 3, pp. 1169–1177, Jul. 2015, doi: 10.1109/TSTE.2014.2335895.

[137] A. Colmenar-Santos, C. Reino-Rio, D. Borge-Diez, and E. Collado-Fernández, "Distributed generation: A review of factors that can contribute most to achieve a scenario of DG units embedded in the new distribution networks," *Renew. Sustain. Energy Rev.*, vol. 59, pp. 1130–1148, Jun. 2016, doi: 10.1016/j.rser.2016.01.023.

[138] C. D. Iweh, S. Gyamfi, E. Tanyi, and E. Effah-Donyina, "Distributed Generation and Renewable Energy Integration into the Grid: Prerequisites, Push Factors, Practical Options, Issues and Merits," *Energies*, vol. 14, no. 17, p. 5375, Aug. 2021, doi: 10.3390/en14175375.

[139] B. Sharma, M. Rizwan, and P. Anand, "Optimal design of renewable energy based hybrid system considering weather forecasting using machine learning techniques," *Electr. Eng.*, Jul. 2023, doi: 10.1007/s00202-023-01945-w.

[140] P. Anand, S. K. Bath, and M. Rizwan, "Size optimisation of RES-based grid connected hybrid power system using harmony search algorithm," *Int. J. Energy Technol. Policy*, vol. 16, no. 3, pp. 238–276, 2020.

[141] "About UP | State Profile | Official Website of NRI Department, Government of Uttar Pradesh, India | UPNRI." https://nri.up.gov.in/en/page/state-profile (accessed Aug. 08, 2023).

[142] "file_s-1683779844352.pdf." Accessed: Aug. 08, 2023. [Online]. Available: https://mnre.gov.in/img/documents/uploads/file_s-1683779844352.pdf

[143] "Agra Tehsil Map." https://www.mapsofindia.com/maps/uttarpradesh/tehsil/agra.html (accessed Aug. 08, 2023).

[144] "About Haryana | Haryana Government | India." https://haryana.gov.in/about-haryana/ (accessed Aug. 08, 2023).

[145] A. Bhatt, M. P. Sharma, and R. P. Saini, "Feasibility and sensitivity analysis of an off-grid micro hydro–photovoltaic–biomass and biogas–diesel–battery hybrid energy system for a remote area in Uttarakhand state, India," *Renew. Sustain. Energy Rev.*, vol. 61, pp. 53–69, 2016.

[146] A. Chauhan and R. P. Saini, “Techno-economic feasibility study on Integrated Renewable Energy System for an isolated community of India,” *Renew. Sustain. Energy Rev.*, vol. 59, pp. 388–405, 2016.
[147] “ASDC | Projects | SSE.” https://asdc.larc.nasa.gov/project/SSE (accessed Aug. 09, 2023).
[148] “Wind Data and Tools | Wind Research | NREL.” https://www.nrel.gov/wind/data-tools.html (accessed Aug. 09, 2023).
[149] “Uttar Pradesh - Agriculture Department,Government of Uttar Pradesh.” https://upagripardarshi.gov.in/StaticPages/UttarPradesh.aspx (accessed Aug. 08, 2023).
[150] “Home | Animal Husbandry Department, Government of Uttar Pradesh.” http://www.animalhusb.upsdc.gov.in/en (accessed Aug. 09, 2023).
[151] “Livestock Census | Department of Animal Husbandry & Dairying, Government of Haryana.” http://www.pashudhanharyana.gov.in/livestock-census-0 (accessed Aug. 08, 2023).
[152] “Description of HOMER Software - An Optimal Analysis Tool | PDF | Photovoltaics | Wind Power.” https://www.scribd.com/document/189587779/Homer-Report (accessed Aug. 09, 2023).
[153] A. H. Mamaghani, S. A. A. Escandon, B. Najafi, A. Shirazi, and F. Rinaldi, “Techno-economic feasibility of photovoltaic, wind, diesel and hybrid electrification systems for off-grid rural electrification in Colombia,” *Renew. Energy*, vol. 97, pp. 293–305, 2016.
[154] H. S. Das, C. W. Tan, A. H. M. Yatim, and K. Y. Lau, “Feasibility analysis of hybrid photovoltaic/battery/fuel cell energy system for an indigenous residence in East Malaysia,” *Renew. Sustain. Energy Rev.*, vol. 76, pp. 1332–1347, 2017.
[155] A. Chauhan and R. P. Saini, “Techno-economic optimization based approach for energy management of a stand-alone integrated renewable energy system for remote areas of India,” *Energy*, vol. 94, pp. 138–156, 2016.
[156] F. R. Yu, P. Zhang, W. Xiao, and P. Choudhury, “Communication systems for grid integration of renewable energy resources,” *IEEE Netw.*, vol. 25, no. 5, pp. 22–29, 2011.
[157] P. Paliwal, N. P. Patidar, and R. K. Nema, “Planning of grid integrated distributed generators: A review of technology, objectives and techniques,” *Renew. Sustain. Energy Rev.*, vol. 40, pp. 557–570, 2014.
[158] K. S. Manoj, *Smart Grid: Concepts To Design*. Notion Press, 2019.
[159] G. M. Shafiullah, A. M. Oo, D. Jarvis, A. S. Ali, and P. Wolfs, “Potential challenges: Integrating renewable energy with the smart grid,” in *2010 20th australasian universities power engineering conference*, IEEE, 2010, pp. 1–6.
[160] K. V. Vidyanandan and B. Kamath, “Grid integration of renewables: challenges and solutions,” *Emerg. Energy Scenar. India-Issues Chall. Way Forw.*, 2018.

[161] C. D. Iweh, S. Gyamfi, E. Tanyi, and E. Effah-Donyina, “Distributed generation and renewable energy integration into the grid: Prerequisites, push factors, practical options, issues and merits,” *Energies*, vol. 14, no. 17, p. 5375, 2021.

[162] S. Singh, M. Singh, and S. C. Kaushik, “A review on optimization techniques for sizing of solar-wind hybrid energy systems,” *Int. J. Green Energy*, vol. 13, no. 15, pp. 1564–1578, 2016.

[163] L. Abualigah, D. Yousri, M. Abd Elaziz, A. A. Ewees, M. A. A. Al-qaness, and A. H. Gandomi, “Aquila Optimizer: A novel meta-heuristic optimization algorithm,” *Comput. Ind. Eng.*, vol. 157, p. 107250, Jul. 2021, doi: 10.1016/j.cie.2021.107250.

[164] S. Wang, H. Jia, L. Abualigah, Q. Liu, and R. Zheng, “An improved hybrid aquila optimizer and harris hawks algorithm for solving industrial engineering optimization problems,” *Processes*, vol. 9, no. 9, p. 1551, 2021.

[165] A. Mahesh and K. S. Sandhu, “Optimal sizing of a grid-connected PV/wind/battery system using particle swarm optimization,” *Iran. J. Sci. Technol. Trans. Electr. Eng.*, vol. 43, pp. 107–121, 2019.

[166] P. Anand, S. K. Bath, and M. Rizwan, “Renewable energy-based hybrid model for rural electrification,” *Int. J. Energy Technol. Policy*, vol. 15, no. 1, pp. 86–113, 2019.

[167] F. O. Hocaoglu, O. N. Gerek, and M. Kurban, “The effect of model generated solar radiation data usage in hybrid (wind–PV) sizing studies,” *Energy Convers. Manag.*, vol. 50, no. 12, pp. 2956–2963, 2009.

[168] J. Tu, H. Chen, M. Wang, and A. H. Gandomi, “The Colony Predation Algorithm,” *J. Bionic Eng.*, vol. 18, no. 3, pp. 674–710, May 2021, doi: 10.1007/s42235-021-0050-y.

[169] S. Kaur, L. K. Awasthi, A. L. Sangal, and G. Dhiman, “Tunicate Swarm Algorithm: A new bio-inspired based metaheuristic paradigm for global optimization,” *Eng. Appl. Artif. Intell.*, vol. 90, p. 103541, 2020.